

AD-A198 709

January 1988

Report No. STAN-CS-88-1191
Thesis

(2)

DTIC FILE COPY

**Instantaneous Robot Motion
with Contact between Surfaces**

by

Chunsheng Cai



Department of Computer Science

**Stanford University
Stanford, California 94305**

DISTRIBUTION STATEMENT A

**Approved for public release
Distribution Unlimited**

UNCLASSIFIED

SECURITY CLASSIFICATION OF THIS PAGE

REPORT DOCUMENTATION PAGE				Form Approved OMB No 0704-0188 Exp Date Jun 30, 1986	
1a. REPORT SECURITY CLASSIFICATION UNCLASSIFIED			1b. RESTRICTIVE MARKINGS		
2a. SECURITY CLASSIFICATION AUTHORITY			3. DISTRIBUTION / AVAILABILITY OF REPORT		
2b. DECLASSIFICATION / DOWNGRADING SCHEDULE					
4. PERFORMING ORGANIZATION REPORT NUMBER(S)			5. MONITORING ORGANIZATION REPORT NUMBER(S)		
6a. NAME OF PERFORMING ORGANIZATION Computer Science Department Stanford University		6b. OFFICE SYMBOL (if applicable)	7a. NAME OF MONITORING ORGANIZATION DARPA		
6c. ADDRESS (City, State, and ZIP Code) Stanford, CA 94305			7b. ADDRESS (City, State, and ZIP Code) 1400 Wilson boulevard Arlington, Virginia 22209		
8a. NAME OF FUNDING / SPONSORING ORGANIZATION		8b. OFFICE SYMBOL (if applicable)	9. PROCUREMENT INSTRUMENT IDENTIFICATION NUMBER		
8c. ADDRESS (City, State, and ZIP Code)			10. SOURCE OF FUNDING NUMBERS N00039-84-C-0211		
			PROGRAM ELEMENT NO	PROJECT NO	TASK NO
11. TITLE (Include Security Classification) INSTANTANEOUS ROBOT MOTION WITH CONTACT BETWEEN SURFACES					
12. PERSONAL AUTHOR(S) Chunsheng Cai					
13a. TYPE OF REPORT Technical Report		13b. TIME COVERED FROM _____ TO _____		14. DATE OF REPORT (Year, Month, Day) December 1987	
15. PAGE COUNT 183					
16. SUPPLEMENTARY NOTATION None.					
17. COSATI CODES			18. SUBJECT TERMS (Continue on reverse if necessary and identify by block number) Contact Kinematics Force Control Motion Planning AL Robot Language Motion Sensing Impact Impulse		
FIELD	GROUP	SUB-GROUP			
19. ABSTRACT (Continue on reverse if necessary and identify by block number) In this work, we analyze the motion constraints needed to maintain direct contact between two rigid bodies, when one or both bodies are being moved under computer control. We first study the time-based instantaneous contact kinematics, then develop a control formulation and specifications within the AL robot language for moving so as to maintain the desired contact. Finally we study the impact which results when bodies are moved into direct contact. These studies on robot motion with direct contact between bodies are useful for robot motion planning and control.					
20. DISTRIBUTION / AVAILABILITY OF ABSTRACT <input checked="" type="checkbox"/> UNCLASSIFIED / UNLIMITED <input type="checkbox"/> SAME AS RPT <input type="checkbox"/> DTIC USERS				21. ABSTRACT SECURITY CLASSIFICATION UNCLASSIFIED	
22a. NAME OF RESPONSIBLE INDIVIDUAL				22b. TELEPHONE (Include Area Code)	
				22c. OFFICE SYMBOL	

INSTANTANEOUS ROBOT MOTION WITH CONTACT BETWEEN SURFACES

A DISSERTATION

SUBMITTED TO THE DEPARTMENT OF MECHANICAL ENGINEERING

AND THE COMMITTEE ON GRADUATE STUDIES

OF STANFORD UNIVERSITY

IN PARTIAL FULFILLMENT OF THE REQUIREMENTS

FOR THE DEGREE OF

DOCTOR OF PHILOSOPHY



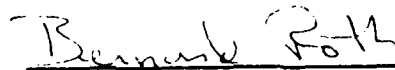
By

Chunsheng Cai

December 1987

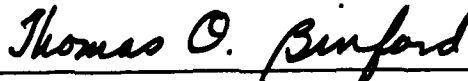
Acquisition For	
DTIC (DAAG)	<input checked="" type="checkbox"/>
DTIC (DAAG)	<input type="checkbox"/>
DTIC (DAAG)	<input type="checkbox"/>
By <i>per NP</i>	
Date <i>12/1/87</i>	
DTIC (DAAG)	
DTIC (DAAG)	
<i>A-1</i>	

I certify that I have read this thesis and that in my opinion it is fully adequate, in scope and in quality, as a dissertation for the degree of Doctor of Philosophy.



Bernard Roth

I certify that I have read this thesis and that in my opinion it is fully adequate, in scope and in quality, as a dissertation for the degree of Doctor of Philosophy.




Thomas O. Binford

I certify that I have read this thesis and that in my opinion it is fully adequate, in scope and in quality, as a dissertation for the degree of Doctor of Philosophy.



Mark R. Cutkosky

Approved for the University Committee
on Graduate Studies:


Dean of Graduate Studies

Abstract

In this work, we analyze the motion constraints needed to maintain direct contact between two rigid bodies, when one or both bodies are being moved under computer control. We first study the time-based instantaneous contact kinematics, then develop a control formulation and specifications within the AL robot language for moving so as to maintain the desired contact. Finally we study the impact which results when bodies are moved into direct contact. These studies on robot motion with direct contact between bodies are useful for robot motion planning and control.

We have studied the instantaneous contact kinematics, under planar and spatial motion, of a moving object with point or line contact between surfaces. In particular, the velocity, acceleration and jerk of the instantaneous contact point, and the constraints on the angular velocity and angular acceleration for line contact have been obtained as functions of surface geometries and the rigid body motions under contact. These results have been specialized for the study of the special motions of pure rolling and pure sliding, and for the contact geometries where contact occurs on a sharp vertex, a sharp edge or a plane. They have also been used to study bodies moving with multiple contacts.

Body trajectories to maintain the contact can be preplanned using the equations developed in this thesis. In addition these results can be used in real time control in conjunction with tactile sensing. The equations for the trajectory of an instantaneous contact point are useful in position and force control. We have shown that the availability of a proper force sensor can replace the need for knowledge of the contact surfaces' geometry in determining the normal acceleration at contact.

As an implementation of the instantaneous contact kinematics, we have formulated a controller to maintain the direct contact motion, and extended the AL

robot language to facilitate direct contact motion specification. The control can be formulated directly in contact-task variables, and include the inertia force corresponding to acceleration along the contact normal. The language extensions allow for the specification of contact surface geometry, contact trajectories, and the motion parameters such as error tolerance and directional wobble.

Concerning the instant of making contact, we have studied the sensitivity of the impact impulse to the link-mass distribution of a revolute-jointed planar manipulator. In this connection, link-space representations, optimal pivot location, influence of the mass and orientation of each link on the impact impulse at the end-effector have been considered.

ACKNOWLEDGMENTS

First of all, I am very grateful to Professor Bernard Roth, for his invaluable guidance and encouragement during the course of this research, and his great effort in improving the writing in this manuscript.

I am very grateful to Professor Thomas O. Binford, for his guidance relative to the extensions of the AL robot language, and his many insightful comments and support for this research.

I would like to thank Professor Mark R. Cutkosky for his critical review of this manuscript.

In addition, I would like to thank my friends Brian Armstrong, Joel Burdick, Ronald Fearing, Zhiming Ji, Ossum Khatib, Madhusudan Raghavan, Shashank Shekhar, and many others for their encouragement and help.

Last but not least, I would like to express my gratitude to my motherland for giving me the opportunity to study in the United States, and to my family for their constant support.

My financial support during this research was provided by DARPA (grant No. MDA903-86-K-0002).

Contents

Abstract	iii
Acknowledgements	v
List of Illustrations	ix
Chapter 1. Introduction	1
1.1 Contact between surfaces	1
1.2 Relevant literature	5
1.3 Preview	7
Chapter 2. Planar Motion with Point Contact	9
2.1 Several results from classical kinematics	10
2.2 Constraints on point contact between curves	11
2.3 Motion properties for point contact between curves	16
2.3.1 Motion properties expressed in the contact frame	16
2.3.2 Motion properties expressed in arc-length coordinates	22
2.3.3 Calculation of contact position	24
2.4 Special geometry of contacting curves	26
2.5 Planning planar motion with point contact	30
2.6 Two point contacts between curves	34
Chapter 3. Spatial Motion with Point Contact	41
3.1 Constraints on point contact between surfaces	42
3.2 Motion properties for point contact between surfaces	48
3.3 Spatial motion with point contact between two spheres	55
3.4 Special geometry of contacting surfaces	59
3.5 Planning spatial motion with point contact	67
3.6 Two or three point contacts between surfaces	71
Chapter 4. Spatial Motion with Line Contact	77
4.1 Constraints on line contact	78

4.2 Motion properties for line contact	85
4.3 Line contact between two circular cones	90
4.4 Special geometries of ruled surfaces	94
4.5 Two line contacts between surfaces	100
Chapter 5. A Control Formulation for Contact	104
5.1 Operational coordinates and task variables	105
5.2 Control in task variable space	109
5.3 Motion compatibility filter	111
5.4 Transformation of dynamics parameters	114
5.5 An efficient inverse of the Jacobian matrix	115
5.6 On extension to grasping	117
5.7 Number of force unknowns at one contact	120
5.8 Contact force manipulability	121
Chapter 6. AL Language Specification for Contact	124
6.1 Geometry of a moving object	125
6.2 Cartesian trajectory of a moving object	126
6.3 Calculation of contact-task frames	133
6.4 Motion constraints with respect to task frames	136
Chapter 7. Impact Impulse and Link-mass Distribution	141
7.1 Representation in link space	142
7.2 Impact impulse at point of contact	145
7.3 Effect on S_N of the last link's mass distribution	146
7.4 Mass proportions of links for reducing S_N	148
7.5 Dominant influence of last link on S_N	150
7.6 Influence of other links on S_N	151
7.7 Change of angular velocity and reaction impulse at joint	154
7.8 On the extension to spatial linkages	156
Chapter 8. Conclusions	158
Appendix A - Curvatures of the Contacting Curves	162
Appendix B - Compound Planar Motion at a Point of Contact	163

Appendix C – Derivatives of $h(x, y)$ from a General Surface Representation	165
Appendix D – Curvature Expressions from $h(x, y)$	167
Appendix E – Compound Spatial Motion at a Point of Contact	168
Appendix F – Finding an Orthogonal Curve on a Ruled Surface	169
Bibliography	170

List of Illustrations

Figure 1.1	Instantaneous trajectories defined at a point contact	2
Figure 2.1	Arbitrary position of a moving curve in point contact	9
Figure 2.2	Initial position of a moving curve in point contact	11
Figure 2.3	Contact trajectories	14
Figure 2.4	Limiting cases of equation 3.17	20
Figure 2.5	Distance and sense of arc length	22
Figure 2.6	Relationship among rotation angles	26
Figure 2.7	Special geometries for point contact between curves	26
Figure 2.8	Two point contact between curves	34
Figure 3.1	Arbitrary position of a moving surface in point contact	41
Figure 3.2	Initial position of a moving surface in point contact	42
Figure 3.3	Contact trajectories on surfaces	45
Figure 3.4	A relative surface	49
Figure 3.5	Moving point's acceleration under pure rolling	52
Figure 3.6	Moving point's acceleration under pure sliding	54
Figure 3.7	Special geometries for point contact between surfaces	60
Figure 3.8	Two point contact between surfaces	71
Figure 3.9	Motion variables for multiple contacts	71
Figure 4.1	Arbitrary position of a moving surface in line contact	78
Figure 4.2	Contact trajectories on ruled surfaces	82
Figure 4.3	Projectional curves	85
Figure 4.4	Two reference frames on a fixed surface	89
Figure 4.5	Two circular cones under line contact	90
Figure 4.6	Special geometries for line contact	94
Figure 4.7	Reference lines of a moving body	95
Figure 4.8	Two line contacts	100
Figure 5.1	Original reference frame and task frame	106

Figure 5.2	Moving body with force and position sensors	107
Figure 5.3	Free body diagram for single mass contact	112
Figure 5.4	Wrist frame and a reference frame	116
Figure 5.5	Multiple fingers in grasping	117
Figure 6.1	Position-error correction trajectory	127
Figure 6.2	Rotation with a line trajectory specified	128
Figure 6.3	Types of reference-line trajectories	129
Figure 6.4	Rotation-error correction trajectory	131
Figure 6.5	Condition-monitored motions	132
Figure 6.6	Spatial motion with point contact	135
Figure 6.7	A corresponding control gain for an error tolerance	137
Figure 6.8	Examples of directional wobble	138
Figure 6.9	A peg rotation	139
Figure 7.1	A planar manipulator	142
Figure 7.2	Configuration of the last link	147
Figure 7.3	Influence on S_N of mass proportions of 2- or 3-link chains	149
Figure 7.4	influence on S_N of the first link of 2- or 3-link chains	152
Figure B.1	Two moving curves	163

Chapter 1

INTRODUCTION

1.1 Contact between surfaces

System and assumptions

Industrial robots operating under computer control are often required to move so as to make and maintain contact between bodies which are, except for this contact, capable of completely independent relative motions. Examples of single and multiple contacts are found in the use of industrial robots for grinding, polishing, cleaning, parts sliding, peg insertion, and object re-positioning within a dextrous hand. Motion with direct contact sometimes provides a way to reach a goal position, sometimes it is the task itself. In this work we study the motion of a manipulator (or a finger) with direct contact between rigid surfaces.

From a kinematic point of view the direct contact temporarily forms a higher kinematic pair between the contacting bodies. One body can be the end-effector or one link of a manipulator, and the other body can be a work-piece or the environmental support. A grasped object and a contacting link of a finger of a robot hand also form such a kinematic pair. Although both bodies being in motion could be considered as the general case, the essence of the kinematics is in the relative motion between the contacting bodies. Therefore, we can, for the most part, assume only one body is moving and that its motion is its relative motion with respect to the other body. We will therefore refer to the bodies of

contact as, respectively, the moving and the fixed bodies, and label the contacting moving surface as m and the contacting fixed surface as f .

The actual contact characteristics depend heavily on the elasticity of the surface materials. We limit ourselves to the study of rigid body motions, and assume both contact surfaces are rigid. In many applications the elastic deformation of the contacting surfaces is negligible. An artificial surface which is constructed mathematically to facilitate manipulation tasks such as arc welding, painting, etc., can also be considered as a rigid surface in our study. When two rigid surfaces are in relative motion, in practice there are three possibilities of practical interest: point contact, line contact, and planar contact.

For the most part, in this work, we also assume that the geometries of both surfaces are given at the contact. This is the case when a robot is in contact with an object of simple geometry, such as a sphere, a plane, a circular cylinder, or when complete geometric models of the contacting surfaces exist. Later on we will show that this restriction can be relaxed, in calculating a contact point's acceleration, if there exist force sensors which can determine the position of the contact point or contact line.

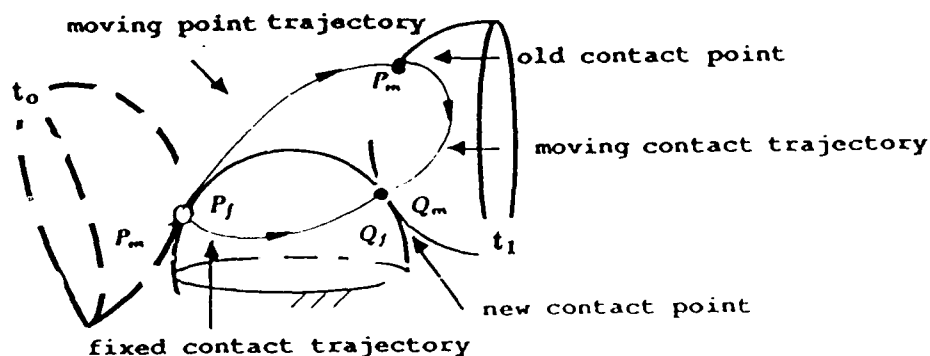


Figure 1.1 Instantaneous trajectories defined at a point contact

Motion compatibility for maintaining contact

In studying the instantaneous kinematics of direct contact, it is useful to distin-

guish between the several associated trajectories. For rigid body motion with point contact we label the point of contact as P , and distinguish between the point on the fixed body P_f and point on the moving body P_m . We refer to the trajectory of P_m as the **moving point trajectory** (Fig. 1.1.). For rigid body motion with line contact it will also be useful to define a moving point trajectory; this will be done by relocating P_m as one of the points on the contact line fixed in the moving body.

It is a well known result that the basic kinematic constraint of the direct contact is that the velocity of the contact point must be zero in the direction of the common normal of the contacting surfaces. If this condition is violated the direct contact constraint is broken. In this thesis we are also interested in higher order instantaneous restrictions on the the moving point's trajectory. For example, we know that the normal acceleration for a particle moving with velocity V on a circle of radius R is V^2/R , and that this information gives the second order motion compatibility for keeping the particle in circular orbit. We need to know the analogous relationships when direct contact occurs between two smooth curves or two smooth surfaces.

Motion planning and sensing for contact

We have referred to the trajectory of P_m as the moving point trajectory: this is the trajectory of an actual point. We now introduce two other trajectories that will be of equal importance, but do not represent the motion of any single physical point. For rigid body motion with point contact, we imagine a pair of points, Q_m and Q_f , which do not belong to either body and move along the moving and fixed surfaces, respectively, so that they are always at the instantaneous contact point. We call the trajectories generated by these points the moving and fixed **contact trajectories**, respectively (Fig. 1.1). Their first and second order time derivatives are called the moving and fixed **contact velocities** and **contact accelerations**, respectively. For rigid body motion with line contact, the trajectories of the contact lines with respect to each surface are of importance, these trajectories are ruled surfaces. However, a line trajectory can be partitioned

into a point trajectory tracing a reference curve on the ruled surface, and a spherical image curve* tracing the direction of each ruling in contact. We will see that the line contact trajectories can be studied as point trajectories, these capture enough motion information since the line's orientation can be determined from the geometries of the contacting surface.

We are interested in the instantaneous relationships between the contact trajectories and the motion of the moving body since such relationships are useful in trajectory planning. The contact relationships can help us to determine the required motion of the moving body. On the other hand, these relationships are also useful in the calculation of the actual motion of the moving body: with a force sensor we can measure the contact positions, velocities, etc. on one surface, and use this information in the instantaneous kinematics relationships to calculate contact trajectories.

Force is sensed using either remote force sensors or direct tactile sensors. Remote force sensors, such as a force wrist, a spherical force cell on a finger [Brock and Chiu, '85], or pair of force cells on a gripper, can sense a force wrench at the contact, and determine the contact point of the force. When the inertial forces between the contact point and sensor are not negligible, we can compensate for them if we have two force sensors in cascade (a force wrist and a gripper with force cells), and know precisely the inertia parameters between the two sensors. A direct tactile sensor consists of an array of deformation or force sensing elements. Since there is usually an elastic skin cover on a tactile sensor, many of its elements will be affected when there is a single point contact. By signal analysis, contact position can be estimated. Taking time derivatives to the contact position obtained from either a remote force sensor or a tactile sensor, we can calculate the contact velocity, or even the contact acceleration although the latter will be very noisy. In the following we use the term tactile sensor to

* A spherical image curve, also known as the Gaussian image, is a spherical curve on which each point represents a unit vector parallel to the direction of a spatial line corresponding to a given time [Bottema and Roth, '79].

refer to either a force sensor (or a combination of force sensors) or a tactile sensor which can sense the contact position.

Control formulation and language specification for contact

The instantaneous relationships we develop for calculating the moving point's trajectory can be used for the trajectory control of direct contact motions. For a robot under both position and force control, the methods developed in this thesis allow for the use of the acceleration or even the jerk of the moving point's path, and this should improve the smoothness of contact. We present one such control formulation directly in terms of the contact variables.

Considering robot motion, there is a need for the development of robot language capabilities for contact specifications. Particularly, we need to determine how to describe a direct contact with sufficient generality, and at the same time with simplicity and efficiency. In this regard we present an extension of the AL robot language, which specifically adds to the language high level, direct contact programming capabilities.

Impact impulse reduction in making contact

Most of this thesis focuses on maintaining a contact. Another problem deals with how to reduce the impact impulse which usually occurs in first making contact. In most robot operations, it is desired that the initial contact be as soft as possible. Even for a task like hammering a nail into a board, we don't want the impulse to be felt by the hand; the hammer's center of percussion or a nearby point will be used. We therefore investigate how to design parallel revolute-jointed manipulators or plan their postures to reduce such impact impulses under a given approach velocity.

1.2 Relevant literature

There have been many studies on contact kinematics. From classic kinematics theory, it is well known that general planar motion can be represented by two

centrodes rolling on each other, and that general spatial motion can be represented by two axodes raccording with each other (for example, see [Bottema and Roth, '79]). However, except for planar pure rolling, there are no previous detailed derivations on the general higher order instantaneous kinematics of direct contact. There have been many studies of gear contact, these address issues of both line and point contact between two surfaces, but the relative motions considered there are usually of special types (under the constraints of gear axes), and the emphasis is on gear analysis and design. In robotics some researchers have considered motions constrained to maintain a single point contact on a surface [Vukobratović and Potkonjak, '85], and first order pure rolling in grasping [Kerr, 1984; Cutkosky, 1985; Ji, 1987]. In terms of combined rolling and sliding, and motion relationships in connection with surface curvature, however, the only study we know of that approximately parallels ours, is Montana's recent thesis [Montana, '86]. He derived the first order relationships between the contact velocities, the sliding velocity and the angular velocity of the moving body. We used a different approach to independently derive essentially the same first order results at approximately the same time [Cai and Roth, '86, '87]. In addition we derive the kinematics of second and higher order contact constraints, these topics are completely new.

Hybrid position and force control schemes have been extensively developed. Mason [Mason, 81] proposed the Configuration space, Raibert and Craig [Raibert and Craig, '81] provided an implementation of the hybrid position and force control formulation. The hybrid position and force control scheme was then generalized to an arbitrary frame, [West and Asada, '85; Lipkin and Duffy, '86]. A dynamics model based control formulation on operational space has been developed by [Khatib, '80; Khatib and Burdick, '86]. We use these results to show that the acceleration of the moving point at the contact is important to force control. Since joint torques change non-linearly with the motor's control voltages or currents, which unfortunately are usually the lowest level input commands, some researchers have included third order motion derivatives into control formulations [Goor, '85]. These provide the motivation for the development of third

order properties in this thesis. The development of AL was due to Goldman [Goldman, '82]. His work is the point of departure for our extension.

Finally, as related to our study on impact impulse, the previous works are mainly restricted to motion or simulation analyses [Vukobratović and Potkonjak, '85; Wang and Mason, '87] and control strategies for dealing with the effects of impact [Khatib and Burdick, '86]. The virtual mass [Asada and Ogawa, '87] is a useful concept particularly relevant to our study.

1.3 Preview

Chapter 2 through Chapter 4 are dedicated to the development of the instantaneous contact kinematics. Besides point contact between planar curves, we study point contact between two surfaces and line contact between two ruled surfaces.

In Chapter 2 we study the so-called planar roll-slide motions between curves with point contact. The velocity, acceleration and jerk of the moving point, and the contact velocity and contact acceleration have been expressed as functions of curve curvatures and motion variables. The special geometries where either the moving or the fixed curve is a point or a line are treated. Finally, planar motion planning and sensing for moving bodies with multiple point contacts has also been treated.

In Chapter 3 we study spatial roll-slide motions between two surfaces with point contact, and derive the instantaneous relationships for the contact trajectories and moving point's trajectory. The special geometries when either surface is a point, a line or a plane are treated. Spatial motion planning and sensing for moving bodies under single and multiple point contacts have also been treated.

In Chapter 4 we study spatial roll-slide motions between two developable ruled surfaces with line contact. Besides the moving point's trajectory and the contact trajectories, we also consider the constraints on the moving body's angular velocity and angular acceleration for maintaining line contact. The special geometries where either surface is a line or a plane are treated. Spatial motion planning and sensing for moving bodies under multiple line contacts have been treated.

The moving point's higher order properties can be useful for the position and force control of a manipulator; the moving contact point can be either on the end-effector or on any other link. In Chapter 5, we consider the case where the contact point varies with respect to the moving surface and modify the "operational space control" formulation. This study addresses the choice of task variables for contact, expressing the control law directly in terms of task variables, designing motion compatibility filters, and calculating parameters of dynamics model for the task space from those for a reference system. We have shown that given the moving surface's geometry, and a force sensor which can determine the moving contact velocity, we can measure the moving point's acceleration along the contact normal, and hence compensate for the corresponding inertia force of the moving body. We have also derived the number of unknowns associated with force sensing and static force manipulability.

As a counterpart to the control formulation for contact, Chapter 6 describes the new specifications for the AL robot language. This chapter discusses the specifications of a moving object's geometry, and a Cartesian trajectory. The kinematic and force conditions for calculating task frames, and motion constraints with respect to the task frames are treated.

As an initial study to consider the reduction of impact impulse, in Chapter 7 we study the impulse's sensitivity to link-mass distribution for revolute-jointed planar manipulators. Based on a link-space coordinate representation, we analyze how to reduce the impact impulse by optimum pivot location and choice of mass proportions. The influences of the number of links on the impact response, and the reaction impulse at the joints, are also developed. These results are useful for designing parallel revolute-joint manipulators which are exposed to impact loads and for planning their trajectories.

Chapter 8 gives a summary and indicates areas of possible further work along these lines.

Chapter 2

PLANAR MOTION WITH POINT CONTACT

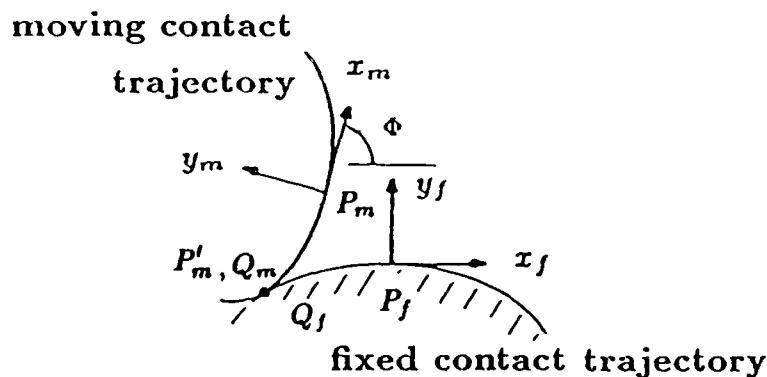


Figure 2.1 *Arbitrary position of a moving curve in point contact*

For planar motion of a rigid body, the direct contact can often be modeled as point contact between two curves, as shown in Fig. 2.1. Here, the moving point P_m is a contact point on the moving curve, and the fixed point P_f is a contact point on the fixed curve. The fictitious points Q_m and Q_f move along the moving and fixed contact curves so as to always be at the contact point. We define P'_m as a new contact point on the moving body corresponding to a given Φ . P'_m will be coincident with P_m as Φ approaches zero.

In the following, we collect several important results from classic kinematics. Based on these we consider the contact constraints, and obtain the basic kinematic relationships for contact trajectories and moving point trajectories. We

then consider how to preplan the motion variables involved in these relationships, and extend the relationships for single point contact to cases where there exist simultaneous multiple point contacts.

2.1 Several results from classical kinematics

The velocity of P'_m as measured in a fixed frame, V_m , is in general not zero. We call V_m the sliding velocity at the contact or simply the **sliding velocity**. The moving body also has some rotation, and because of this its motion is often referred to in German as a "Rollgleit", i.e., roll-slide. We will refer to roll-slide motions as **general motions** since neither pure sliding or pure rolling occurs relative to the contact. These latter two special motions are also interesting: pure sliding, in which every point in the moving body has velocity V_m , and pure rolling, in which the moving curve is rolling on the fixed curve. Under pure rolling, the contact curves are the moving and fixed centrodes, respectively. In each such position the contact point is obviously the instantaneous center of rotation.

It is well known that the velocity of Q_m and Q_f , with respect to a fixed frame, are equal, i.e.,

$$V_{Q_m} = V_{Q_f}. \quad (1.1)$$

Let us define the velocity difference or the so-called relative velocity of Q_m to P_m , $V_{Q/P'}$. From this one of the basic relations used in the study of the direct contact follows:

$$V_{Q_f} = V_{Q_m} = V'_P + V_{Q/P'}. \quad (1.2)$$

The other important property that is well known deals with the curvatures of the contacting curves: the centers of curvatures for the contacting curves are conjugate points, i.e., at the instant of contact, the trajectory of the moving point which is the center of curvature of the moving curve, C_m , has the same center of curvature as the fixed curve, C_f (see Fig. 2.2). Most important is the fact that the instantaneous radii of curvature, ρ_m and ρ_f , of the curves satisfy

the general Euler-Savary equation, which has the form

$$\left(\frac{1}{\rho_m} - \frac{1}{\rho_f}\right) \sin \theta = \frac{1}{b_2}, \quad (1.3)$$

where θ is the ray angle and b_2 the second order instantaneous invariant – see p. 278 of [Bottema and Roth, '79]. The ratio $V_{Q/P}/V_{Q_f}$ is a scalar called the roll-slide number, this number is known to be a projective invariant [Müller, '63], since it equals the cross ratio of the points (I, P, C_f, C_m) , where I is the instantaneous center of rotation.

Equations (1.1), (1.2) and (1.3) embody the known results which are relevant to our study, it is from these that we take our point of departure.

2.2 Constraints on point contact between curves

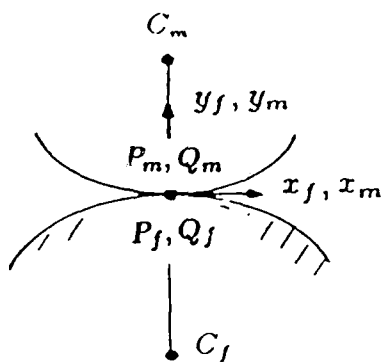


Figure 2.2 Initial position of a moving curve in point contact

Motion constraints for maintaining point contact are due to restrictions on the contact normal, contact trajectories, and the moving point trajectory.

Consider an instantaneous contact at points P_m and P_f as shown in Fig. 2.2. We call this configuration the reference or zero position, and use P_m and P_f as the origins for fixed and moving coordinate systems. In the reference, or zero position, P_m and P_f are coincident; the x axes, x_m and x_f , are along the common tangent to the two curves; the y axes, y_m and y_f , are along the common normals

and point in toward the moving curve (Fig. 2.2). As the motion proceeds the moving body rotates by an angle Φ (counter clockwise sense is positive) and the geometry is as shown in Fig 2.1.

The moving curve with respect to the moving frame is represented by *

$$y_m = h_m(x_m). \quad (2.1)$$

The fixed curve is represented by,

$$y_f = -h_f(x_f). \quad (2.2)$$

By definition, at the reference or zero position,

$$x_m = x_f = 0, \quad h_m = h_f = 0, \quad h_{m,1} = h_{f,1} = 0. \quad (2.3)$$

We have adopted the following convention, $h_{m,j} \equiv d^j h_m / dx_m^j$ and $h_{f,j} \equiv d^j h_f / dx_f^j$.

Constraints on the curve normal at contact

The slopes of the tangents to the curves are given by $h_{m,1}$ and $h_{f,1}$ respectively. Thus, using a column matrix form, at every point on the moving curve the inward pointing unit normal is

$$N_m = \frac{1}{\sqrt{1 + h_{m,1}^2}} \begin{pmatrix} -h_{m,1} \\ 1 \end{pmatrix}, \quad (2.4)$$

* We have assumed the explicit forms of the equations of the moving and fixed curves. If, instead we used the implicit forms $g(x, y) = 0$, then we would have an analogous development but instead of (A1) in Appendix A we would use

$$k = \frac{g_x g_{yy} - g_y g_{xx}}{(g_x^2 + g_y^2)^{\frac{3}{2}}},$$

and all the other results would follow. Here the subscripts denote derivatives with respect to the subscripted variables.

and at every point on the fixed curve the outward pointing unit normal is

$$N_f = \frac{1}{\sqrt{1 + h_{f,1}^2}} \begin{pmatrix} h_{f,1} \\ 1 \end{pmatrix}. \quad (2.5)$$

Taking t to be a time variable, we can consider $x_m(t)$ as the x coordinate of a point, Q_m , which generates the curve $h_m(t)$ and moves at such a rate that the point is always at the contact. For this curve $N_m(t)$ corresponds to the inward pointing normal. Similarly, we can consider the coordinate x_f of Q_f as a function of time, and the function $N_f(t)$ gives the outward pointing normals of the fixed curve. At each instant the inward pointing normal of the moving curve and the outward pointing normal of the fixed curve, at the current point of contact, must coincide. This property holds true for any motion regardless of the amount of rotation and sliding, so long as the contact is not broken. Thus we require that

$$N_f(t) = R(t) N_m(t), \quad (2.6)$$

where $R(t)$ is the 2×2 matrix which transforms the coordinates of the moving system to their values in the fixed system. Using the rotation angle Φ in Fig. 2.1,

$$R(t) = \begin{pmatrix} \cos \Phi(t) & -\sin \Phi(t) \\ \sin \Phi(t) & \cos \Phi(t) \end{pmatrix}. \quad (2.7)$$

Since (6) is valid for entire motion trajectory, its n^{th} order time derivatives can be written as

$$\frac{d^n}{dt^n} N_f(t) = \frac{d^n}{dt^n} [R(t) N_m(t)]. \quad (2.8)$$

If we define $\omega = d\Phi/dt$ and $\epsilon = d^2\Phi/dt^2$, and substitute from Appendix A (A2) and (A3) into the first two derivatives of (8), their first rows yield in the initial position

$$k_m \dot{x}_m + k_f \dot{x}_f = -\omega, \quad (2.9)$$

$$k'_m \dot{x}_m^2 + k'_f \dot{x}_f^2 + k_m \ddot{x}_m + k_f \ddot{x}_f = -\epsilon. \quad (2.10)$$

The second two rows of (8) are not independent, since we have the constraints $N_m(t)^T N_m(t) \equiv 1$ and $N_f(t)^T N_f(t) \equiv 1$. (The superscript T denotes the transpose.)

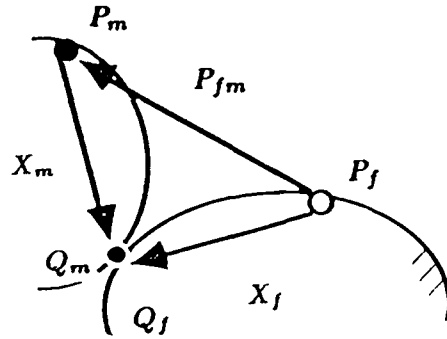


Figure 2.3 Contact trajectories

Constraints on contact trajectories

The position vector for Q_f with respect to the fixed frame (see Fig 2.1) can be represented by

$$\mathbf{r}_{Q_f} = \mathbf{X}_f = \begin{pmatrix} x_f \\ y_f \end{pmatrix}. \quad (2.11)$$

If we define the position vector for P_m , with respect to the fixed frame as P_{fm} , then the position vector for Q_m , with respect to the fixed frame, can be represented by

$$\mathbf{r}_{Q_m} = P_{fm} + R\mathbf{X}_m, \quad (2.12)$$

where \mathbf{X}_m a position vector for Q_m with respect to the moving frame.

$$\mathbf{X}_m = \begin{pmatrix} x_m \\ y_m \end{pmatrix}. \quad (2.13)$$

Considering x_m and x_f as parameters tracing the locus of the contact points, equations (11) and (12) are expressions for the same trajectory (as viewed from the fixed space – Fig. 2.3). Equating them yields

$$\mathbf{X}_f = P_{fm} + R\mathbf{X}_m. \quad (2.14)$$

Taking the first-order time derivative of (14) and making use of (1.1) yields

$$\mathbf{V}_{Q_f} = \mathbf{V}_{Q_m} = \dot{\mathbf{X}}_m = (\dot{P}_{fm} + \dot{R}\mathbf{X}_m) + (R\dot{\mathbf{X}}_m). \quad (2.15)$$

Comparing this with (1.2) we have $\dot{P}_{fm} + \dot{R}X_m = V'_p$ and $R\dot{X}_m = V_{Q/P'}$. For simplicity we drop the subscript P' from the sliding velocity and denote it simply as V . The first parenthesis in (15) is the general expression for the sliding velocity at every point of the fixed curve. Taking higher derivatives of V (i.e. V_p) yields

$$\frac{d^n}{dt^n}(\dot{P}_{fm} + \dot{R}X_m) \equiv V^{(n)}, \quad (2.16)$$

where

$$V = \begin{pmatrix} v_x \\ v_y \end{pmatrix} \text{ and } V^{(n)} = \begin{pmatrix} v_x^{(n)} \\ v_y^{(n)} \end{pmatrix}. \quad (2.17)$$

We have used the notation, $d^n v_x / dt^n = v_x^{(n)}$ and $d^n v_y / dt^n = v_y^{(n)}$. \dot{V} is the rate of change of the sliding velocity, it depends on both the change in sliding speed and change in sliding vector orientation, we call it the **sliding acceleration**. Null sliding acceleration corresponds exactly to the condition for second order pure rolling of the contacting curves, provided of course we have null sliding velocity. In other words for null sliding velocity and acceleration, the contacting curves are, to second order, identical with the centrodes of the motion. Similar statements are true for the higher order terms, that is, for pure rolling up to the n^{th} order, $V = \dot{V} = V^{(n-1)} = 0$. We will refer to this in (4.8).

We take the first three derivatives of (14) at the initial position and use (16), (A2) and (A3), the first row of each derivative can be written as:

$$\dot{x}_f = v_x + \dot{x}_m, \quad (2.18)$$

$$\ddot{x}_f = \dot{v}_x + \ddot{x}_m, \quad (2.19)$$

$$x_f^{(3)} = \ddot{v}_x + x_m^{(3)} - \dot{x}_m \omega^2 - 2k_m \dot{x}_m^2 \omega; \quad (2.20)$$

the second rows yield

$$v_y = 0, \quad (2.21)$$

$$\dot{v}_y = -k_f \dot{x}_f^2 - \dot{x}_m \omega - k_m \dot{x}_m^2, \quad (2.22)$$

$$\ddot{v}_y = -k'_f \dot{x}_f^3 - 3k_f \dot{x}_f \ddot{x}_f - 2\ddot{x}_m \omega - \dot{x}_m \epsilon - k'_m \dot{x}_m^3 - 3k_m \dot{x}_m \ddot{x}_m. \quad (2.23)$$

Constraints on the moving point

Let the position vector for the moving point

$$P_{fm} = \begin{pmatrix} p_x \\ p_y \end{pmatrix}.$$

Substituting $n = 0, 1$ and 2 into (16), and using (A2) and (A3), the first rows of the resulting matrix equations yield

$$\dot{p}_x = v_x, \quad (2.24)$$

$$\ddot{p}_x = \dot{v}_x, \quad (2.25)$$

$$p_x^{(3)} = \ddot{v}_x + 2\dot{x}_m\omega^2 + k_m\dot{x}_m^2\omega; \quad (2.26)$$

the second rows yield

$$\dot{p}_y = 0, \quad (2.27)$$

$$\ddot{p}_y = -k_f\dot{x}_f^2 - 2\dot{x}_m\omega - k_m\dot{x}_m^2, \quad (2.28)$$

$$p_y^{(3)} = -k'_f\dot{x}_f^3 - 3k_f\dot{x}_f\ddot{x}_f - k'_m\dot{x}_m^3 - 3k_m\dot{x}_m\ddot{x}_m - 3\ddot{x}_m\omega - 3\dot{x}_m\epsilon. \quad (2.29)$$

2.3 Motion properties for point contact between curves

It will be useful to express the motion relationships in both the contact frame (the x_f, y_f frame) and the arc length coordinates. The position constraints are also useful in determining the actual contact point.

2.3.1 Motion properties expressed in the contact frame

The first and second order properties for contact trajectories, and the first order through third order properties for the moving point have been considered.

First order properties

From (2.9) and (2.18), the tangential components of the moving and fixed contact velocities are

$$\dot{x}_m = -\frac{\omega + k_f v_x}{(k_m + k_f)}, \quad (3.1)$$

$$\dot{x}_f = \frac{-\omega + k_m v_x}{(k_m + k_f)}. \quad (3.2)$$

If the moving body is, to the first order, undergoing a pure rolling, by definition $v_x = 0$. Therefore

$$\dot{x}_m = \dot{x}_f = -\frac{\omega}{(k_m + k_f)}. \quad (3.3)$$

On the other hand, if, to the first order, the body is undergoing pure sliding, by definition $\omega = 0$. Therefore

$$\dot{x}_m = -\frac{k_f v_x}{(k_m + k_f)}, \quad (3.4)$$

$$\dot{x}_f = \frac{k_m v_x}{(k_m + k_f)}. \quad (3.5)$$

If we know the curve curvatures k_m, k_f , the angular velocity ω and the sliding velocity v_x (for a robot hand the sliding velocity is computed from the joint position or velocity sensor readings), then equations (1) and (2) determine the contact velocities.

If we know the geometry k_m, k_f , and there is a tactile sensor mounted on the moving body (such as on a finger of a robot hand), we can calculate \dot{x}_m from the sensor, and then we can compute the angular velocity ω needed for the body to move under pure rolling from equation (3), or we can compute the sliding velocity v_x for the body to move under pure sliding from equation (4). For a general motion we are not able to infer both ω and v_x if there is only one contact point and one tactile sensor, but we can if both the moving and fixed curves have tactile sensors. This follows from equations (1) and (2).

Alternatively if we know the moving body's motion ω, v_x and its geometry k_m , we are able to calculate the fixed body's curvature k_f from equation (1) if we have the tactile sensor reading \dot{x}_m . This property can be useful in connection with tactile search algorithms.

From (2.24) and (2.27), the moving point making the contact has velocity v_x along its direction of motion, its normal velocity is zero, which is as expected.

Second order properties

From (2.10), (2.19), (1) and (2), the tangential component of the moving contact accelerations is

$$\ddot{x}_m = \frac{-k_f \dot{v}_x (k_m + k_f)^2 - [(k'_m (\omega + k_f v_x)^2 + k'_f (-\omega + k_m v_x)^2)]}{(k_m + k_f)^3} - \frac{\epsilon}{k_m + k_f}, \quad (3.6)$$

and that of the fixed contact acceleration is

$$\ddot{x}_f = \frac{k_m \dot{v}_x (k_m + k_f)^2 - [(k'_m (\omega + k_f v_x)^2 + k'_f (-\omega + k_m v_x)^2)]}{(k_m + k_f)^3} - \frac{\epsilon}{k_m + k_f}. \quad (3.7)$$

The analysis of (6) and (7) is similar to that of (1) and (2): knowing k_m, k_f, k'_m, k'_f and having a single tactile sensor at one contact does not give enough information to uniquely determine both the sliding and angular acceleration, unless both curves contain tactile sensors, which allows us to know both \ddot{x}_m and \ddot{x}_f .

If a motion is a pure rolling to second order, by definition, $v_x = v_y = 0, \dot{v}_x = \dot{v}_y = 0$, and hence from (6) and (7)

$$\ddot{x}_m = \ddot{x}_f = -\frac{(k'_m + k'_f)\omega^2}{(k_m + k_f)^3} - \frac{\epsilon}{k_m + k_f}. \quad (3.8)$$

Not only the contact velocities, but also the contact accelerations with respect to both the fixed and moving curves are the same.

If we know the geometry (i.e., k_m, k_f, k'_m, k'_f) and ω , \ddot{x}_m or \ddot{x}_f , (8) can be used to determine the angular acceleration ϵ .

For pure sliding to second order, by definition $\omega = \epsilon = 0$, and therefore from (6) and (7)

$$\ddot{x}_m = \frac{-k_f \dot{v}_x (k_m + k_f)^2 - (k'_m k_f^2 + k'_f k_m^2) v_x^2}{(k_m + k_f)^3}, \quad (3.9)$$

$$\ddot{x}_f = \frac{k_m \dot{v}_x (k_m + k_f)^2 - (k'_m k_f^2 + k'_f k_m^2) v_x^2}{(k_m + k_f)^3}. \quad (3.10)$$

Once we know the geometry (k_m, k_f, k'_m, k'_f), from \ddot{x}_m or \ddot{x}_f , we can compute the sliding acceleration \dot{v}_x from (9) or (10).

Now we look at the acceleration of the moving point. We substitute (1) and (2) into (2.25) and (2.28), and obtain

$$\ddot{p}_x = \dot{v}_x, \quad (3.11)$$

$$\ddot{p}_y = \frac{\omega^2 \rho_m \rho_f}{\rho_m + \rho_f} - \frac{1}{\rho_m + \rho_f} v_x^2 + \frac{2\omega v_x \rho_m}{\rho_m + \rho_f}, \quad (3.12)$$

where ρ_m and ρ_f are, respectively, the radii of curvature for the moving and fixed curves. Alternatively, (12) can be written in terms of the curvatures as

$$\ddot{p}_y = \frac{\omega^2}{k_m + k_f} - \frac{k_m k_f}{k_m + k_f} v_x^2 + \frac{2\omega v_x k_f}{k_m + k_f}. \quad (3.13)$$

For pure rolling up to second order, we have $v_x = 0$ and $\dot{v}_x = 0$, so from (11) and (13)

$$\ddot{p}_x = 0, \quad (3.14)$$

$$\ddot{p}_y = \frac{\omega^2}{k_m + k_f}. \quad (3.15)$$

This result is well known in kinematics. (In its usual form the fixed normal is taken pointing in toward the center of curvature and therefore k_f appears with a minus sign.)

For pure sliding to first order $\omega = 0$, (11) and (12) yield

$$\ddot{p}_x = \dot{v}_x, \quad (3.16)$$

$$\ddot{p}_y = -\frac{v_x^2}{\rho_m + \rho_f}. \quad (3.17)$$

The acceleration along the normal is proportional to the product of the sliding velocity, and inversely proportional to the sum of the radii of curvature, the smaller the sum, the larger the normal acceleration required to maintain the contact at the given sliding velocity.

Equation (17) has three interesting limiting cases as illustrated in Fig. 2.4. In the first case the moving curve becomes a point, ρ_m shrinks to zero (Fig 2.4a), and (17) takes its classically familiar form. (If instead ρ_f shrinks to zero, the result is

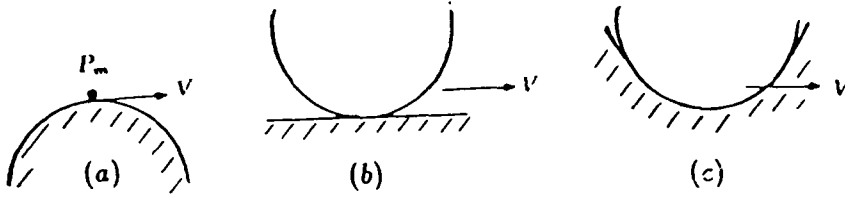


Figure 2.4 Limiting cases of equation (17)

similar, although less familiar.) In the second case the fixed curve becomes a line, ρ_f approaches infinity (Fig 2.4b). Obviously, when a curve is sliding on a line, the acceleration in the normal direction must be zero (If instead ρ_m approaches infinity, the same situation will result). In the third case, ρ_m, ρ_f are of equal value but of different sign (Fig. 2.4c), the acceleration along the normal must be infinite if there is any sliding velocity, but it is physically impossible for this to occur.

We now consider the sliding velocity's effect on the y_m component of the velocity center's acceleration, a_y . The velocity pole is along y_m at a distance $d = v_x/\omega$ from the contact, hence subtracting $(v_x/\omega)\omega^2$ from (13) it follows that a_y is zero if

$$d = \frac{(k_f - k_m) \pm \sqrt{(k_m - k_f)^2 + 4k_mk_f}}{2k_mk_f}.$$

This happens when d takes either of two values, $d = 1/k_m$ or $d = -1/k_f$. When $-\rho_f < d < \rho_m$, a_y is pointing away from the contact point, otherwise it is pointing toward the contact point. When $d = \rho_m$ or $d = -\rho_f$, a_y becomes zero. In general a_y is only one component of the velocity pole's acceleration. However, if $\epsilon = \dot{v}_x = 0$ then a_y is the total acceleration, which is known to equal $\omega^2/(k_{mp} + k_{fp})$ (or $b_2\omega^2$ if we use b_2 from (1.3)), where k_{mp} and k_{fp} are the curvatures of the moving and fixed centrodes at the velocity pole.

Third and higher order properties

From (2.26), (2.29), (1), (2), (6) and (7), the jerk of the moving point becomes

$$p_x^{(3)} = \ddot{v}_x + \frac{\omega(\omega + k_f v_x)[-(k_m + 2k_f)\omega + k_m k_f v_x]}{(k_m + k_f)^2}, \quad (3.18)$$

$$p_y^{(3)} = \frac{3}{k_m + k_f}[(\omega + k_f v_x)\epsilon - k_f(-\omega + k_m v_x)\dot{v}_x] - \frac{1}{(k_m + k_f)^3}[-k'_m(\omega + k_f v_x)^3 + k'_f(-\omega + k_m v_x)^3]. \quad (3.19)$$

For pure rolling to the third order, by definition $v_x = v_y = 0$, $\dot{v}_x = \dot{v}_y = 0$, $\ddot{v}_x = \ddot{v}_y = 0$. From (18) and (19), the third order time derivatives of the moving point's coordinates become

$$p_x^{(3)} = \frac{-\omega^3(k_m + 2k_f)}{(k_m + k_f)^2}, \quad (3.20)$$

$$p_y^{(3)} = \frac{3}{k_m + k_f}\omega\epsilon + \frac{1}{(k_m + k_f)^3}(k'_m + k'_f)\omega^3. \quad (3.21)$$

Let us take a simple example of two circles contacting each other, and let $\omega = 1$, $\epsilon = 0$. If the circle radii are ρ_m and ρ_f , (20) and (21) yield

$$p_x^{(3)} = -\frac{\rho_f \rho_m (\rho_f + 2\rho_m)}{(\rho_m + \rho_f)^2}, \quad (3.22)$$

$$p_y^{(3)} = 0. \quad (3.23)$$

This agrees with the directly calculated results in [Roth and Yang, '77].

For second order pure sliding, $\omega = \epsilon = 0$. Hence, equations (18) and (19) reduce to

$$p_x^{(3)} = \ddot{v}_x, \quad (3.24)$$

$$p_y^{(3)} = \frac{-3k_f k_m v_x \dot{v}_x}{k_m + k_f} - \frac{v_x^3}{(k_m + k_f)^3}(-k'_m k_f^3 + k'_f k_m^3) \quad (3.25).$$

Following the same procedure as in the foregoing section, and taking the higher derivatives of (2.8) and (2.14), we can calculate the contact relations to any arbitrary order. For pure sliding of the moving body up to n^{th} order, we set

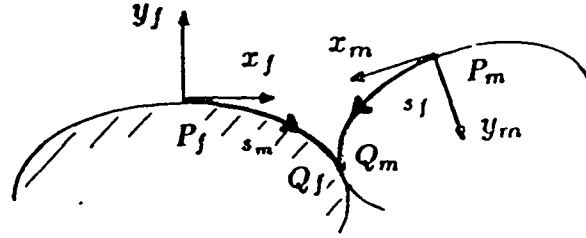


Figure 2.5 Distance and sense of arc length

$d^k \Phi / dt^n = 0$ for $k = 1$ to n . For pure rolling of the moving body up to n^{th} order, we have $V^{(k)} = 0$ for $k = 0$ to $n - 1$. In the context of this thesis, properties higher than third order do not currently have practical uses.

2.3.2 Motion properties expressed in arc-length coordinates

We define s_m and s_f as arc lengths measured from P_m and P_f , respectively, with the positive senses given by the positive \dot{x}_m, \dot{x}_f directions near the origin (as shown in Fig. 2.5). The sliding distance is $s_v = s_f - s_m$. The sliding speed in arc length coordinates is

$$v = \dot{s}_v = \dot{s}_f - \dot{s}_m. \quad (3.26)$$

The rate of change of sliding speed in arc length coordinate is $\dot{v} = \ddot{s}_f - \ddot{s}_m$. By taking derivatives, higher orders terms can be similarly defined.

A scalar λ is referred to as the roll-slide number in the literature, and is defined by $\dot{s}_m = \lambda \dot{s}_f$. Hence, $v = (1 - \lambda) \dot{s}_f$. λ (or its equivalent) is a useful index that has been basic to several studies [Blaschke and Müller, '56; Bottema, '55, '75; Bottema and Roth, '79; Müller, '53, '63] that have considered motions with constant λ . In our case λ is generally a motion variable. If $\lambda = 1$, the contact point must be the velocity pole of the moving body. We will in places also refer to λ in our study.

At the zero position, contact velocity is zero in the normal direction (2.21). Obviously then, the contact speed along the moving and fixed curves, \dot{s}_m and \dot{s}_f , must be the same as the contact velocity components in the tangential direction,

i.e.,

$$\dot{s}_m = \dot{x}_m, \quad \dot{s}_f = \dot{x}_f. \quad (3.27)$$

Combining (27) with (1) and (2), the contact speeds in terms of the arc length coordinates are

$$\dot{s}_m = -\frac{\omega + k_f v}{(k_m + k_f)}, \quad (3.28)$$

$$\dot{s}_f = \frac{-\omega + k_m v}{(k_m + k_f)}. \quad (3.29)$$

Although (1) and (2) are only associated with the zero position, in terms of the arc length coordinates (28) and (29) are general expressions for \dot{s}_m and \dot{s}_f . Hence we can directly take derivatives of (28) and (29) to get the rates of change of the contact speeds.

$$\ddot{s}_m = \frac{-k_f \dot{v}(k_m + k_f)^2 - [(k'_m(\omega + k_f v)^2 + k'_f(-\omega + k_m v)^2)]}{(k_m + k_f)^3} - \frac{\epsilon}{k_m + k_f}, \quad (3.30)$$

$$\ddot{s}_f = \frac{k_m \dot{v}(k_m + k_f)^2 - [(k'_m(\omega + k_f v)^2 + k'_f(-\omega + k_m v)^2)]}{(k_m + k_f)^3} - \frac{\epsilon}{k_m + k_f}. \quad (3.31)$$

In (4.4), we will see that $\dot{v}_x = \dot{v}$. Combined with (6) and (7), equations (30) and (31) give

$$\ddot{s}_m = \ddot{x}_m, \quad \ddot{s}_f = \ddot{x}_f. \quad (3.32)$$

In real-time control calculations, we may need to know the rates of change of the magnitudes for the tangential and the normal acceleration component. We denote them as a'_t and a'_n . (These are different from $p_x^{(3)}$ and $p_y^{(3)}$ which refer to the moving point, a'_t and a'_n refer to Q_m , i.e., the continuously varying contact points on the moving body.) In the equation for the tangential acceleration (11), we replace \dot{v}_x by \dot{v} , and in the equation for the normal acceleration (13), we replace v_x by v . Taking the derivative with respect to time, we have

$$a'_t = \ddot{v}, \quad (3.33)$$

$$\begin{aligned} a'_n = & -\frac{(\omega^2 + 2\omega v k_f + k_f^2 v^2) k'_m \dot{s}_m}{(k_m + k_f)^2} - \frac{(\omega^2 + k_m^2 v^2 - 2\omega v k_m) k'_f \dot{s}_f}{(k_m + k_f)^2} \\ & + \frac{2}{k_m + k_f} [\omega \epsilon - k_m k_f v \dot{v} + k_f (\epsilon v + \omega \dot{v})]. \end{aligned} \quad (3.34)$$

For pure rolling up to second order,

$$a'_t = 0, \quad (3.35)$$

$$a'_n = \frac{\omega^3(k'_m + k'_f)}{(k_m + k_f)^3} + \frac{2\omega\epsilon}{k_m + k_f}. \quad (3.36)$$

For pure sliding up to second order,

$$a'_t = \ddot{v}, \quad (3.37)$$

$$a'_n = \frac{(k_f^3 k'_m - k_m^3 k'_f) v^3}{(k_m + k_f)^3} - \frac{2}{k_m + k_f} k_m k_f v \dot{v}. \quad (3.38)$$

2.3.3 Calculation of contact position

Given the first order contact speed equations (28) and (29), we can theoretically get the contact position by integration. In real-time control, since the integration is performed on discrete time sampled data, error will accumulate. An alternative way is to use global constraints to get the desired contact position. Arc lengths and rotation angles provide useful information for accurately locating the contact position.

Arc length constraints

In (28) and (29) when k_m and k_f are invariant, i.e., we have two circular curves (one can be a line) in contact, the equations can actually be integrated: $s_m = [-\Phi - k_f s_v]/(k_m + k_f)$, $s_f = [-\Phi + k_m s_v]/(k_m + k_f)$, where s_v is the sliding distance, and Φ is the angle the moving object rotates through. Usually we know Φ from position sensors in the joints of the moving system, and if there is a tactile sensor mounted on the moving body we also know the moving contact distance s_m , then from the expression for s_m we know s_v the sliding distance. From the s_f expression we know s_f , which gives the contact position on the fixed body.

In general for other than circular curves, (28) and (29) can not be explicitly integrated. However, for pure rolling contact, since $s_m = s_f$, if we have a tactile

sensor which gives arc length s_m , we can infer the exact position. For pure sliding, when $k_m = k_f$ we have $s_m = -(1/2)s_v$ and $s_f = (1/2)s_v$. This happens when two anti-symmetric curves are in contact and there is no rotation. For the general cases of pure sliding, from (2.9) and (27)

$$s_m = - \int \frac{k_f}{k_m} ds_f. \quad (3.39)$$

If we know s_f , by integration we know the exact arc length of s_m . The integration limit is determined by s_f , and at each position the corresponding k_m can be determined from the condition that the contact normals must be coincident.

When k_f is proportional to k_m (i.e., their ratio is constant), s_m is linearly proportional to s_f by the same constant factor. From (2.9) and (27) we can show that the constant is the roll-slide number λ .

Rotation angle constraint

There is a global constraint for the rotation angle, which is required of any motion. Substituting (27) into (2.9) and integrating, we have, $\int k_f ds_f + \int k_m ds_m = - \int \omega dt$. Here, we have used the relations $ds_m = \dot{s}_m dt$ and $ds_f = \dot{s}_f dt$. From the definition of curvature (we take the sign convention such that the positive sense of N_m or N_f 's rotation angle with respect to its frame corresponds to a decrease in the arc length), $k_f ds_f = -d\Phi_f$, and $k_m ds_m = -d\Phi_m$. Substituting this into the above integral equation, we have,

$$\Phi_m + \Phi_f = \Phi. \quad (3.40)$$

Equation (40) tells us that the rotation angle of the moving curve with respect to the fixed space is the sum of the rotation angles of the inward pointing normal with respect to the moving frame and that of the outward pointing normal of the fixed curve with respect to the fixed frame (Fig. 2.6). This equation appears to be very useful. If a tactile sensor has been mounted on a moving body, since we always know the rotation angle of the moving body and we can use the sensor to obtain the rotation of the moving normal, we can use (40) to calculate the

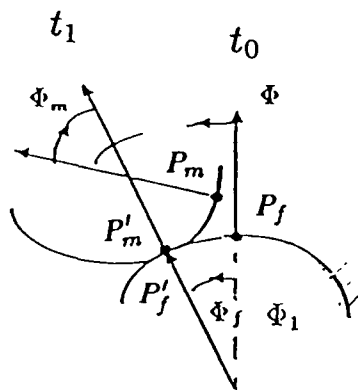


Figure 2.6 Relationship among rotation angles

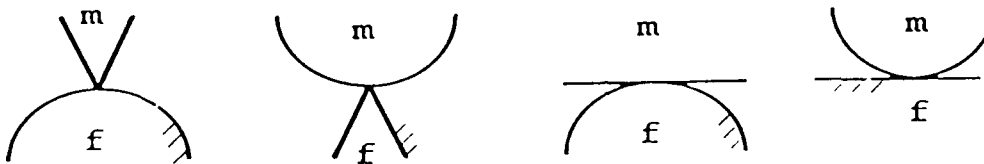


Figure 2.7 Special geometries for point contact between curves

rotation angle of the fixed curve's normal. Knowing the normal, we can search out the exact contact position on the fixed curve.

2.4 Special geometry of contacting curves

There are several special cases that require additional discussion (Fig. 2.7): 1) the moving curve is a point (for example, the moving contact is a sharp point of a tool), 2) the fixed curve is a point (a workpiece has a sharp point), 3) the moving curve is a line , and 4) the fixed curve is a line.

Moving curve is a point

We can model the contact point as the limiting case of a circular curve, i.e., k_m approaches ∞ and $k'_m = 0$. From (3.1) and (3.27) for \dot{x}_m , and from (3.6) and (3.32) for \ddot{x}_m , the contact velocity and acceleration with respect to the moving

frame are, respectively,

$$\dot{x}_m = \dot{s}_m = 0, \quad \ddot{x}_m = \ddot{s}_m = 0. \quad (4.1)$$

In fact, $x_m^{(n)} = 0$, hence $y_m^{(n)} = 0$, and the contact point is stationary in the moving system.

From (3.2) and (3.27) for \dot{x}_f , and from (3.7) and (3.32) for \ddot{x}_f , the contact velocity and acceleration with respect to the fixed frame are, respectively,

$$\dot{x}_f = \dot{s}_f = v_x, \quad \ddot{x}_f = \ddot{s}_f = \dot{v}_x. \quad (4.2)$$

The contact velocity along the fixed curve and its derivatives are determined from the sliding velocity and its derivatives. This can be seen clearly from (2.15) and (2.16). (If a single tactile sensor is mounted on the fixed curve, no rotational information can be inferred from the sensor reading.)

Considering the roll-slide number λ , from (1) and (2) we see that in this case $\lambda = 0$.

From (3.13), (3.19) and (3.34), the normal acceleration of the moving point and its rates of change are, respectively,

$$\ddot{p}_y = -k_f v_x^2, \quad (4.3)$$

$$p_y^{(3)} = -3k_f v_x \dot{v}_x - k'_f v_x^3, \quad (4.4)$$

$$a'_n = -k'_f v^3 - 2k_f v \dot{v}. \quad (4.5)$$

Notice that these quantities are the same as the sliding velocity and its higher order derivatives, and also the contact velocity and its higher order derivatives on the fixed curve. This can be seen from (2.15) and (2.16), since from (1) \dot{X}_m and \ddot{X}_m vanish. For pure sliding, equations (3)-(5) show that the normal acceleration and its rates of change are larger than when the contacting curves are convex.

Fixed curve is a point

To study the fixed curve as a point, let k_f approach ∞ and $k'_f = 0$. The contact velocity and acceleration with respect to the fixed frame are, respectively,

$$\dot{x}_f = \dot{s}_f = 0, \quad \ddot{x}_f = \ddot{s}_f = 0. \quad (4.6)$$

The contact velocity and its higher order derivatives on the fixed curve all vanish.

The contact velocity and its derivative with respect to the moving frame are, respectively,

$$\dot{x}_m = \dot{s}_m = -v_x, \quad \ddot{x}_m = \ddot{s}_m = -\dot{v}_x. \quad (4.7)$$

These are in the negative sense to the sliding velocity and its derivative.

Considering the roll-slide number λ , from (6) and (7) we see $\lambda = \infty$ in this case.

From (3.13), (3.19) and (3.34), the moving point's normal acceleration and its rates of change are, respectively,

$$\ddot{p}_y = -k_m v_x^2 + 2\omega v_x, \quad (4.8)$$

$$p_y^{(3)} = 3v_x \epsilon - 3(-\omega + k_m v_r) \dot{v}_x + k'_m v_x^3, \quad (4.9)$$

$$a'_n = k'_m v^3 - 2(k_m v \dot{v} - \epsilon v - \omega \dot{v}). \quad (4.10)$$

The sliding velocity is the dominant term.

Moving curve is a line

We take k_m and k'_m to be zero. From (3.1) and (3.27) for \dot{x}_m , and from (3.6) and (3.32) for \ddot{x}_m , the contact velocity and acceleration with respect to the moving frame are, respectively,

$$\dot{x}_m = \dot{s}_m = -\frac{\omega}{k_f} - v_x, \quad \ddot{x}_m = \ddot{s}_m = -\dot{v}_x - \frac{k'_f \omega^2}{k_f^3} - \frac{\epsilon}{k_f}. \quad (4.11)$$

From (3.2) and (3.27) for \dot{x}_f , and from (3.7) and (3.32) for \ddot{x}_f , the contact velocity and acceleration with respect to the fixed frame are, respectively,

$$\dot{x}_f = \dot{s}_f = -\frac{\omega}{k_f}, \quad \ddot{x}_f = \ddot{s}_f = -\frac{k'_f \omega^2}{k_f^3} - \frac{\epsilon}{k_f}. \quad (4.12)$$

These depend only on the angular velocity and angular acceleration. Hence, if we can determine the fixed contact velocity and contact acceleration, these can be used to determine the angular velocity and angular acceleration.

Considering the roll-slide number λ , from (11) and (12) we see that $\lambda = 1 + v_x k_f / \omega$; for pure sliding, $\lambda = \infty$.

From (3.13), (3.19) and (3.34), the moving point's normal acceleration and its rates of change are, respectively,

$$\ddot{p}_y = \frac{\omega^2}{k_f} + 2\omega v_x, \quad (4.13)$$

$$p_y^{(3)} = \frac{3}{k_f}[(\omega + k_f v_x)\epsilon + k_f \omega \dot{v}_x] + \frac{k'_f \omega^3}{k_f^3}, \quad (4.14)$$

$$a'_n = \frac{k'_f \omega^3}{k_f^3} + \frac{2}{k_f}(\omega \epsilon + k_f \epsilon v + \omega \dot{v}). \quad (4.15)$$

In expressions (13)-(15), the rolling is the dominant part.

Fixed curve is a line

If the fixed curve is a line, then k_f, k'_f are zero. The contact velocity and acceleration with respect to the moving frame are, respectively,

$$\dot{x}_m = \dot{s}_m = -\frac{\omega}{k_f}, \quad \ddot{x}_m = \ddot{s}_m = -\frac{k'_m \omega^2}{k_m^3} - \frac{\epsilon}{k_m}. \quad (4.16)$$

Hence, the contact velocity and acceleration are only functions of rolling of the moving body.

Similarly, the contact velocity and acceleration with respect to the fixed frame are, respectively,

$$\dot{x}_f = \dot{s}_f = -\frac{\omega}{k_m} + v_x, \quad \ddot{x}_f = \ddot{s}_f = -\frac{k'_m \omega^2}{k_m^3} + \dot{v}_x - \frac{\epsilon}{k_m}. \quad (4.17)$$

Considering the roll-slide number λ , from (16) and (17) we see $\lambda = 1/(1 - v_x k_m / \omega)$; for pure sliding $\lambda = 0$.

From (3.13), (3.19) and (3.34), the moving point's normal acceleration and its rates of change are, respectively,

$$\ddot{p}_y = \frac{\omega^2}{k_m}, \quad (4.18)$$

$$\dot{p}_y^{(3)} = \frac{3}{k_m} \omega \epsilon + \frac{k'_m \omega^3}{k_m^3}, \quad (4.19)$$

$$a'_n = \frac{k'_m \omega^3}{k_m^3} + \frac{2\omega \epsilon}{k_m}. \quad (4.20)$$

With regard to the normal acceleration, the rolling is the dominant aspect.

2.5 Planning planar motion with point contact

In preceding sections, we have derived analytic expressions for the moving point's trajectory and contact trajectories in terms of the motion parameters (i.e., which are related to the sliding velocity and sliding acceleration, as well as the body's angular velocity and angular acceleration). We now discuss how one can determine the motion parameters from path planning.

Sliding speed planning

Assume first that we know the desired sliding speed for the direct contact: the Taylor expansion of the sliding velocity, which is defined in (2.16), is

$$V(t) = V(0) + \dot{V}(0)t + \frac{\ddot{V}(0)}{2!}t^2 + \dots, \quad (5.1)$$

The Taylor expansion of the sliding speed, which is defined in (3.26), is

$$v(t) = v(0) + \dot{v}(0)t + \frac{\ddot{v}(0)}{2!}t^2 + \dots \quad (5.2)$$

If the desired $v(0)$, $\dot{v}(0)$, $\ddot{v}(0)$, ... have already been defined, then we can calculate $V(0)$, $\dot{V}(0)$, $\ddot{V}(0)$, We notice from (2.21) that for all time the sliding velocity must be parallel to T_f the unit tangent vector of the fixed curve. Thus

$$V(0) = v(0)T_f, \quad (5.3)$$

$$\dot{V}(0) = \dot{v}(0)T_f + v(0)\dot{T}_f, \quad (5.4)$$

$$\ddot{V}(0) = \ddot{v}(0)T_f + 2\dot{v}(0)\dot{T}_f + v(0)\ddot{T}_f. \quad (5.5)$$

T_f can be expressed as

$$T_f(t) = \begin{pmatrix} T_{f,x} \\ T_{f,y} \end{pmatrix} = \frac{1}{\sqrt{1 + h_{f,1}^2}} \begin{pmatrix} 1 \\ -h_{f,1} \end{pmatrix}. \quad (5.6)$$

By definition, for the outward pointing unit normal of the fixed curve, from (2.5) we have $T_{f,x}^{(n)} = N_{f,y}^{(n)}$, $T_{f,y}^{(n)} = -N_{f,x}^{(n)}$.

One interesting case is for pure rolling up to n^{th} order. We have

$$v(0) = \dot{v}(0) = \ddot{v}(0) = \dots = v^{(n-1)}(0) = 0. \quad (5.7)$$

From the above we see immediately that

$$V(0) = \dot{V}(0) = \ddot{V}(0) = \dots = V^{(n-1)}(0) = 0. \quad (5.8)$$

This shows that for pure rolling, up to n^{th} order, defining the derivatives of the sliding velocity vector, $V^{(k)}$, to be zero (for k from 0 to $n-1$) is the same as setting the derivatives of the sliding speed scalar, $v^{(k)}$, to zero (for k from 0 to $n-1$).

Another interesting case is constant sliding speed. This is considered desirable for minimizing frictional heat generation and improving the quality of machining and other operations which are sensitive to the sliding speed. The required conditions are of course

$$v(t) = v(0), \quad \dot{v}(0) = \ddot{v}(0) = \dots = v^{(n)}(0) = 0. \quad (5.9)$$

By substituting the expressions for \dot{T}_f , \ddot{T}_f , and equation (9) into (4) and (5), we have

$$\dot{v}_x(0) = 0, \quad (5.10)$$

$$\ddot{v}_x(0) = -\frac{\dot{v}_y^2}{v_x(0)} = -k_f^2 \dot{x}_f^2 v_x(0). \quad (5.11)$$

Contact speed planning

Next, we assume we know the contact speed along the fixed curve: we notice that the contact velocity with respect to the fixed curve as defined by the derivative of (2.11) must be parallel to the unit tangent vector of the fixed curve for all time. Hence the contact velocity and the contact speed with respect to the fixed curve are related to each other by relationships similar to those we have obtained for sliding velocity and sliding speed. When $\dot{s}_f(0), \ddot{s}_f(0), \dots$ are specified, we can calculate the contact velocity and its rates of change $\dot{X}_f, \ddot{X}_f, \dots$

One interesting case is that of constant contact speed, by definition

$$\dot{s}_f(t) = \dot{s}_f(0), \quad \ddot{s}_f(0) = s_f^{(3)} = \dots = s_f^{(n)} = 0. \quad (5.12)$$

By calculation, we have

$$\dot{x}_f(0) = \dot{s}_f(0), \quad (5.13)$$

$$\ddot{x}_f(0) = \ddot{s}_f(0) = 0, \quad (5.14)$$

$$x_f^{(3)}(0) = -\frac{\ddot{y}_f^2}{\dot{x}_f(0)} = -k_f^2 \dot{x}_f(0)^3. \quad (5.15)$$

For constant contact speed equations (13) and (14) impose a constraint on equations (3.2) and (3.7), respectively.

Planning the contact speed with respect to the moving curve will essentially follow the same procedure as with respect to the fixed curve, except that s_f should be replaced by s_m and T_f by T_m .

Orientation path planning

Finally, we assume we know the desired orientation of the moving system as it moves under point contact: to plan the rotation with respect to the fixed space, ω and ϵ need to be specified. A special case is pure sliding. When considering the roll-slide number λ , from (2.9) and (3.27) we see that for pure sliding $\lambda = -k_f/k_m$. From (2.10) and (3.32) we see that $\dot{\lambda} = -(k'_m k_f^2 + k'_f k_m^2) \dot{s}_f / k_m^3$, where $\dot{\lambda}$ is the time derivative of λ . For two circular curves undergoing pure sliding, $\dot{\lambda} = 0$.

Another way is to plan the moving curve's orientation with respect to the fixed curve's contact normal. If we let the the moving body's orientation be always coincident with the fixed curve's current normal

$$\Phi = \Phi_f. \quad (5.16)$$

From (2.9) and (3.27), since the contact trajectory with respect to the moving frame becomes a point, we have

$$\omega = -k_f \dot{s}_f. \quad (5.17)$$

Taking a derivative, and maintaining constant contact speed,

$$\epsilon = -k'_f \dot{s}_f^2. \quad (5.18)$$

The fixed contact trajectory is the same as the moving point trajectory in this case.

In terms of the roll-slide number λ , for this special motion we have $\lambda = \dot{\lambda} = \dots = \lambda^{(n)} = 0$.

Determining the planar finger motions

Now we give an example of finger path planning to illustrate the path planning process. Given the desired motion of the moving body with respect to the fixed space (for the moving body the contact point's velocity \mathbf{v}_m and acceleration \mathbf{a}_m can always be calculated), we can determine $\bar{\mathbf{v}}$ (the velocity at the contact point of the moving body with respect to the finger) or $\bar{\omega}$ (the angular velocity of the moving body with respect to the finger) or both by planning the relative contact position and orientation, as explained earlier in this section. From (B2) and (B3) we can calculate the finger tip velocity \mathbf{v}_f , from which we can determine the joint rates $\dot{\Theta}$ by using the inverse Jacobian of the finger [Salisbury and Roth, '83]

$$\dot{\Theta} = J^{-1} \mathbf{v}_f. \quad (5.19)$$

Having the joint rates, we can calculate the angular velocity of the finger. For a two-degree-of-freedom finger $\Theta = [\theta_1, \theta_2]^T$ and hence $\omega_f = \dot{\theta}_1 + \dot{\theta}_2$. From the relative motion planning, we can further select \bar{a} (the acceleration of the moving body at the contact point with respect to the finger), then from (B4) and (B5) we can calculate the finger tip acceleration a_f , from which the desired joint accelerations can be determined:

$$\ddot{\Theta} = J^{-1}(a_f - \dot{J}\dot{\Theta}). \quad (5.20)$$

For a two-degree-of-freedom finger, the angular acceleration of the finger tip is $\epsilon = \ddot{\theta}_1 + \ddot{\theta}_2$. Thus we have determined the required joint velocities and accelerations in terms of the motion variables given by the planning considerations outlined in the foregoing paragraphs.

2.6 Two point contacts between curves

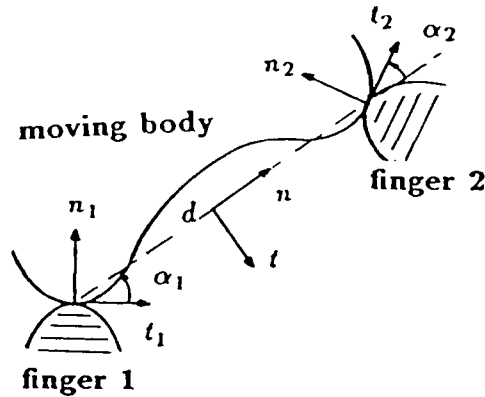


Figure 2.8 Two points contact between curves

As is well known and as we reaffirmed in section 3, the angular velocity and angular acceleration of a moving body are generally not uniquely determined by one point contact. It is well known that the geometric aspects of a planar motion are uniquely determined by two point contacts. In this section we will

derive relationships for the motion variables when there are two point contacts. We consider a moving planar body represented by a planar curve, which may be a compound curve made up of several different segments which all move together as one rigid body. We will refer to this as "the moving body". This body will be required to move so as to maintain point contact along its curve with two separate curves - which we will call fingers. Each of the fingers is capable of independent motion relative to a fixed space.

Fig. 2.8 shows the two fingers and the moving body. We refer to one of the fingers as finger 1 and the other as finger 2, and we refer to their contact points as, respectively, contact points 1 and 2. If we connect the contact points with a straight line of length d and give this line direction \mathbf{n} and transverse direction \mathbf{t} , then from Fig. 2.8 it follows that,

$$\mathbf{t}_1 \cdot \mathbf{n}_2 = -\sin(\alpha_1 + \alpha_2), \quad \mathbf{n}_1 \cdot \mathbf{n}_2 = \cos(\alpha_1 + \alpha_2), \quad \mathbf{t} \cdot \mathbf{n}_2 = -\cos \alpha_2, \quad \mathbf{n} \cdot \mathbf{n}_2 = -\sin \alpha_2 \quad (6.1)$$

We adopt the following notations: we use the subscript j to denote the j^{th} finger and also the j^{th} contact point; j can be either 1 or 2. If we start at an arbitrary configuration and a motion occurs, then in any subsequent position, Φ_{mj} is the contact normal's rotation angle with respect to the moving body at the finger contact j , Φ_{fj} is the contact normal's rotation angle with respect to finger j ; ω_m and ϵ_m are the moving body's angular velocity and angular acceleration with respect to the fixed space; ω_j and ϵ_j are the angular velocity and angular acceleration of finger j ; $\bar{\omega}_j$ and $\bar{\epsilon}_j$ are the moving body's angular velocity and angular acceleration with respect to finger j ; \mathbf{v}_{mj} , \mathbf{a}_{mj} are the moving body's velocity and acceleration at contact position j ; \mathbf{v}_{fj} and \mathbf{a}_{fj} are the j^{th} finger's velocity and the acceleration at its contact point; $\bar{\mathbf{v}}_j$ and $\bar{\mathbf{a}}_j$ are the moving body's velocity and acceleration at the j^{th} contact point with respect to finger j ; \dot{s}_{fj} and \ddot{s}_{fj} are the contact velocity and acceleration (in arc length coordinates) for finger j ; k_{mj} is the moving body's curvature at contact point j ; k_{fj} is the j^{th} finger's curvature at the contact point. For our current study we need to consider all the contacting bodies as being in motion. To study these motions it becomes useful to introduce a stationary, or absolute, frame. In Fig. B.1

of Appendix B we show the basic geometry at one contact, and list the basic kinematic equations for the case where both bodies f and m are in motion.

Calculating the contact position from two contacts

From (2.9), (3.27) and Appendix B (B1), for the configuration in Fig 2.8 we have

$$k_{f1}\dot{s}_{f1} + k_{m1}\dot{s}_{m1} = -\omega_m + \omega_1, \quad k_{f2}\dot{s}_{f2} + k_{m2}\dot{s}_{m2} = -\omega_m + \omega_2 \quad (6.2)$$

If we integrate these, we obtain

$$\Phi_{f1} + \Phi_{m1} = \Phi - \Phi_1, \quad (6.3)$$

$$\Phi_{f2} + \Phi_{m2} = \Phi - \Phi_2. \quad (6.4)$$

where the positive senses of Φ_{fj} and Φ_{mj} are consistent with those defined in (3.40). If we know the finger motions and we know the finger contact points, then we know Φ_{f1} , Φ_{f2} , Φ_1 and Φ_2 , so there are three unknowns, Φ , Φ_{m1} , Φ_{m2} , in the two equations. However if there are contact sensors in the fingers, we have an additional constraint due to the contact positions determined from the contact sensor readings. This provides a simple iterative algorithmic way to determine Φ : If we assume an arbitrary Φ , then from (3) we can determine Φ_{m1} , thus the first contact on the moving body (after rotation) is temporarily determined. This point is coincident with the contact point on the first finger. From (4) we can solve for Φ_{m2} using the previously assumed Φ , hence the second contact point on the moving body is determined. This contact on the moving body will be coincident with the second finger's contact point if Φ is correct, otherwise it indicates that our assumed Φ is incorrect. If Φ is incorrect, we choose a new value for it based on any of the well known one-dimensional search techniques, and repeat this procedure until it converges to a correct Φ .

Calculating the angular velocity from two contacts

To calculate the angular velocity from two contacts, from (3.29), (B1) and (B2), we have,

$$\dot{s}_{f1} = \frac{-\omega_m + \omega_1 + k_{m1}(\mathbf{v}_{m1} - \mathbf{v}_{f1}) \cdot \mathbf{t}_1}{k_{m1} + k_{f1}}. \quad (6.5)$$

Since the contact points on the moving body, $m1$ and $m2$, are both points on the same rigid body under planar motion,

$$\mathbf{v}_{m2} = (\mathbf{v}_{m1} \cdot \mathbf{t}_1)\mathbf{t}_1 + (\mathbf{v}_{m1} \cdot \mathbf{n}_1)\mathbf{n}_1 - \omega_m d\mathbf{t}. \quad (6.6)$$

If we take the \mathbf{n}_2 component of (6) and substitute from (1), we get

$$\mathbf{v}_{m2} \cdot \mathbf{n}_2 = -(\mathbf{v}_{m1} \cdot \mathbf{t}_1) \sin(\alpha_1 + \alpha_2) + (\mathbf{v}_{m1} \cdot \mathbf{n}_1) \cos(\alpha_1 + \alpha_2) + \omega_m d \cos \alpha_2. \quad (6.7)$$

$\mathbf{v}_{m1} \cdot \mathbf{t}_1$, $\mathbf{v}_{m1} \cdot \mathbf{n}_1$ and $\mathbf{v}_{m2} \cdot \mathbf{n}_2$ can be obtained from (5) and (B3). By substituting these into (7), we get a formula for ω_m ,

$$\begin{aligned} \omega_m = & \frac{-1}{[d \cos \alpha_2 - (\sin(\alpha_1 + \alpha_2)/k_{m1})]} \left\{ -\sin(\alpha_1 + \alpha_2) \left[\frac{(k_{m1} + k_{f1})}{k_{m1}} \dot{s}_{f1} \right. \right. \\ & \left. \left. - \frac{\omega_1}{k_{m1}} + \mathbf{v}_{f1} \cdot \mathbf{t}_1 \right] + \mathbf{v}_{f1} \cdot \mathbf{n}_1 \cos(\alpha_1 + \alpha_2) - \mathbf{v}_{f2} \cdot \mathbf{n}_2 \right\}. \end{aligned} \quad (6.8)$$

Equation (8) can be used to determine the moving body's angular velocity if the fingers' motions are known and one finger's contact speed is available from the tactile sensors. From (3.29), we can calculate the sliding speed at the contacts, hence the motion of the moving body to first order is completely known.

Calculating the angular acceleration from two contacts

To calculate the angular acceleration from two contacts, from (3.31),

$$\begin{aligned} \ddot{s}_{f1} = & \frac{k_{m1}(\mathbf{a}_{m1} - \mathbf{a}_{f1}) \cdot \mathbf{t}_1}{(k_{m1} + k_{f1})} + \frac{-\epsilon_m + \epsilon_1}{k_{m1} + k_{f1}} \\ & - \frac{[k'_{m1}(\bar{\omega}_1 + k_{f1}\bar{\mathbf{v}}_1 \cdot \mathbf{t}_1)^2 + k'_{f1}(-\bar{\omega}_1 + k_{m1}\bar{\mathbf{v}}_1 \cdot \mathbf{t}_1)^2]}{(k_{m1} + k_{f1})^3}. \end{aligned} \quad (6.9)$$

We know that since $m1$ and $m2$ are two points on the same rigid body,

$$\mathbf{a}_{m2} = \mathbf{a}_{m1} - \epsilon_m d\mathbf{t} - \omega_m^2 d\mathbf{n}. \quad (6.10)$$

Taking the \mathbf{n}_2 component of (10) and substituting from (1) yields,

$$\mathbf{a}_{m2} \cdot \mathbf{n}_2 = -(\mathbf{a}_{m1} \cdot \mathbf{t}_1) \sin(\alpha_1 + \alpha_2) + (\mathbf{a}_{m1} \cdot \mathbf{n}_1) \cos(\alpha_1 + \alpha_2) + \omega_m^2 d \sin \alpha_2 + \epsilon_m d \cos \alpha_2 \quad (6.11)$$

$\mathbf{a}_{m1} \cdot \mathbf{t}_1$ can be obtained from (9), and from (B5) we can obtain an expression for $\mathbf{a}_{m1} \cdot \mathbf{n}_1$ and $\mathbf{a}_{m2} \cdot \mathbf{n}_2$, in which we use $\bar{\mathbf{a}}_1 \cdot \mathbf{n}_1$ and $\bar{\mathbf{a}}_2 \cdot \mathbf{n}_2$ as obtained from (3.13). By substituting these into (11), we obtain a formula for ϵ_m ,

$$\begin{aligned} \epsilon_m = & \frac{-1}{[d \cos \alpha_2 - (\sin(\alpha_1 + \alpha_2)/k_{m1})]} \left\{ -\sin(\alpha_1 + \alpha_2) [\mathbf{a}_{f1} \cdot \mathbf{t}_1 + \frac{(k_{m1} + k_{f1})}{k_{m1}} \ddot{s}_{f1} \right. \\ & - \frac{\epsilon_1}{k_{m1}} + \frac{1}{k_{m1}(k_{m1} + k_{f1})^2} (k'_{m1}(\bar{\omega}_1 + k_{f1} \bar{\mathbf{v}}_1 \cdot \mathbf{t}_1)^2 + k'_{f1}(-\bar{\omega}_1 + k_{m1} \bar{\mathbf{v}}_1 \cdot \mathbf{t}_1)^2) \\ & + \omega_m^2 d \sin \alpha_2 + \cos(\alpha_1 + \alpha_2) + [\mathbf{a}_{f1} \cdot \mathbf{n}_1 + 2\omega_1 \bar{\mathbf{v}}_1 \cdot \mathbf{t}_1 \\ & + \cos(\alpha_1 + \alpha_2) \left[\frac{\bar{\omega}_1^2}{k_{m1} + k_{f1}} - \frac{k_{m1} k_{f1}}{k_{m1} + k_{f1}} \bar{\mathbf{v}}_1^2 + \frac{2\bar{\omega}_1 \bar{\mathbf{v}}_1 \cdot \mathbf{t}_1 k_{f1}}{k_{m1} + k_{f1}} \right] \\ & \left. - (\mathbf{a}_{f2} \cdot \mathbf{n}_2 + 2\omega_2 \bar{\mathbf{v}}_2 \cdot \mathbf{t}_2 + \frac{\bar{\omega}_2^2}{k_{m2} + k_{f2}} - \frac{k_{m2} k_{f2}}{k_{m2} + k_{f2}} \bar{\mathbf{v}}_2^2 + \frac{2\bar{\omega}_2 \bar{\mathbf{v}}_2 \cdot \mathbf{t}_2 k_{f2}}{k_{m2} + k_{f2}}) \right\}. \end{aligned} \quad (6.12)$$

Equation (12) can be used to determine the moving body's angular acceleration if the fingers' motions are known and one contact velocity and acceleration are available. From (3.31) we can calculate the sliding acceleration at the contact points. Hence the motion of the moving body to second order is completely known.

Special geometry

From equations (8) and (12) we obtain simplified expressions for the angular velocity and acceleration for the following three special cases: the moving curve reduces to two lines, the finger curves reduce to lines, the moving curve reduces to two points.

When the moving curve is reduced to two lines, k_{m1}, k_{m2}, k'_{m1} and k'_{m2} are all zero, and $k_{m1}/k_{m2} = 1$. From (8),

$$\omega_m = -k_{f1} \dot{s}_{f1} + \omega_1.$$

This is essentially the same expression as for ω in (4.12) when combined with (B1). For angular acceleration, from (12),

$$\epsilon_m = -k_{f1} \ddot{s}_{f1} + \epsilon_1 - \frac{k'_{f1} \bar{\omega}_1^2}{k_{f1}^2}.$$

This is essentially the same expression as for ϵ in (4.12) when combined with (B1).

The next case we consider is when the moving curve is general but both finger curves are lines. We let $k_{f1} = k'_{f1} = 0$ and $k_{f2} = k'_{f2} = 0$ in (8),

$$\omega_m = \frac{-1}{[d \cos \alpha_2 - \sin(\alpha_1 + \alpha_2)/k_{m1}]} \left\{ -\sin(\alpha_1 + \alpha_2) \left[\dot{s}_{f1} - \frac{\omega_1}{k_{m1}} + \mathbf{v}_{f1} \cdot \mathbf{t}_1 \right] + \mathbf{v}_{f1} \cdot \mathbf{n}_1 \cos(\alpha_1 + \alpha_2) - \mathbf{v}_{f2} \cdot \mathbf{n}_2 \right\}. \quad (6.13)$$

For angular acceleration from (12),

$$\epsilon_m = \frac{-1}{[d \cos \alpha_2 - \sin(\alpha_1 + \alpha_2)/k_{m1}]} \left\{ -\sin(\alpha_1 + \alpha_2) \left[\mathbf{a}_{f1} \cdot \mathbf{t}_1 + \ddot{s}_{f1} - \frac{\epsilon_1}{k_{m1}} + \frac{k'_{m1} \bar{\omega}_1^2}{k_{m1}^3} \right] + \cos(\alpha_1 + \alpha_2) \left[\mathbf{a}_{f1} \cdot \mathbf{n}_1 + 2\omega_1 \bar{\mathbf{v}}_1 \cdot \mathbf{t}_1 + \frac{\bar{\omega}_1^2}{k_{m1}} \right] + \omega_m^2 d \sin \alpha_2 - (\mathbf{a}_{f2} \cdot \mathbf{n}_2 + 2\omega_2 \bar{\mathbf{v}}_2 \cdot \mathbf{t}_2 + \frac{\bar{\omega}_2^2}{k_{m2}}) \right\}. \quad (6.14)$$

The third case we consider is when the curve of the moving body is reduced to two points. For this case from (4.2) we notice that with one contact we can only sense the sliding velocity, however with two contacts we can also sense the rotation of the object. We let k_{m1} and k_{m2} approach ∞ , but $k_{m1}/k_{m2} = 1$ and $k'_{m1} = k'_{m2} = 0$, then from (8)

$$\omega_m = \frac{-1}{d \cos \alpha_2} \left\{ -\sin(\alpha_1 + \alpha_2) [\dot{s}_{f1} + \mathbf{v}_{f1} \cdot \mathbf{t}_1] + \mathbf{v}_{f1} \cdot \mathbf{n}_1 \cos(\alpha_1 + \alpha_2) - \mathbf{v}_{f2} \cdot \mathbf{n}_2 \right\} \quad (6.15)$$

The angular acceleration can be obtained from (12)

$$\epsilon_m = \frac{-1}{d \cos \alpha_2} \left\{ -\sin(\alpha_1 + \alpha_2) [\mathbf{a}_{f1} \cdot \mathbf{t}_1 + \ddot{s}_{f1}] - (\mathbf{a}_{f2} \cdot \mathbf{n}_2 + 2\omega_2 \bar{\mathbf{v}}_2 \cdot \mathbf{t}_2 - k_{f2} \bar{\mathbf{v}}_2^2) + \cos(\alpha_1 + \alpha_2) [\mathbf{a}_{f1} \cdot \mathbf{n}_1 + 2\omega_1 \bar{\mathbf{v}}_1 \cdot \mathbf{t}_1 - k_{f1} \bar{\mathbf{v}}_1^2] + \omega_m^2 d \sin \alpha_2 \right\}. \quad (6.16)$$

Equations (8) and (12), as well as their special cases, can be used for path planning with two contacts. An unconstrained planar motion involves three degrees of freedom. The two contacts remove two of these freedoms, and the

one remaining degree-of-freedom can be used to plan the contact velocity and acceleration (at one contact), or the sliding velocity and acceleration (at one contact). Once the motion at one contact is specified the orientation is completely determined by equations (8) and (12).

We notice that in equations (8) and (12), when both segments of the moving curve form a portion of one circle, the denominators of these equations will be zero, and hence the rotation motion is indeterminate. This is obvious since a circle can always rotate about its center at an arbitrary rate without being affected by the contacting supports.

This completes our study of planar motions, in the next chapters we consider spatial motions.

Chapter 3

SPATIAL MOTION WITH POINT CONTACT

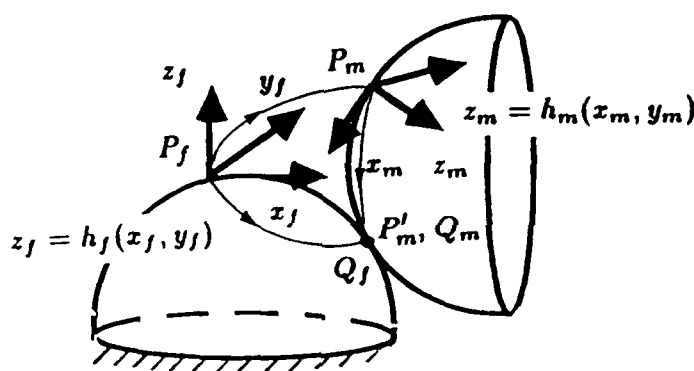


Figure 3.1 *Arbitrary position of a moving surface in point contact*

In this chapter, we study the instantaneous spatial motion of a rigid body with point contact between two surfaces. The moving point P_m is a contact point on the moving surface, and the contact trajectories of Q_m and Q_f are the loci of the contact points on the moving and fixed surfaces, respectively. In general, the moving body is rolling and sliding on the fixed body. We also define P'_m as a new contact point on the moving body after a given time interval. P'_m will be coincident with P_m when the time interval approaches zero. The basic relationships between the roll-sliding motion of the moving object and the moving point's trajectory and contact trajectories are our main focus. We are also interested in two special motions, pure rolling and pure sliding.

Following a similar route as in the last chapter, we start with the basic contact constraints, then obtain from them the motion properties at the point of contact. An example of spatial motion with point contact between two spheres is included to illustrate these properties. The variations in these properties for special geometries where either surface becomes a point, a line and a plane are listed. We also consider trajectory planning for the roll-sliding variables and for motions with multiple contacts.

3.1 Constraints on point contact between surfaces

The essential motion constraints are due to restrictions on the contact normal, contact trajectories, and the moving point trajectory.

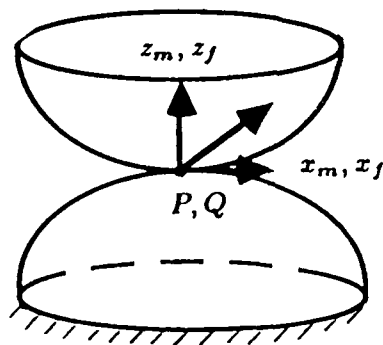


Figure 3.2 Initial position of a moving surface in point contact

Consider an instantaneous contact at points P_m and P_f as shown in Fig. 3.2. We call this configuration the reference (or zero) position, and use P_m and P_f as the origins of moving and fixed coordinate systems. In the reference (or zero) position, the x_m and y_m axes are coincident with the x_f and y_f axes respectively and they are in the common tangent plane to the two surfaces. The z_m and z_f axes are along the common normals and point in toward the moving surface (Fig. 3.2). As the motion proceeds the moving body rotates to a general orientation where the geometry is as shown in Fig. 3.1.

The moving surface with respect to the moving frame is represented by *

$$z_m = h_m(x_m, y_m). \quad (1.1)$$

The fixed surface with respect to the fixed frame is represented by

$$z_f = -h_f(x_f, y_f). \quad (1.2)$$

By definition, at the reference (or zero) position,

$$\begin{aligned} x_m = y_m = h_m = h_{m,x} = h_{m,y} = 0, \\ x_f = y_f = h_f = h_{f,x} = h_{f,y} = 0. \end{aligned} \quad (1.3)$$

We have adopted the following convention

$$h_{m,x} \equiv \frac{\partial h_m}{\partial x_m}, \quad h_{m,xy} \equiv \frac{\partial^2 h_m}{\partial x_m \partial y_m}.$$

$h_{m,xx}, h_{m,yy}$ and higher order derivatives are similarly defined. The same notations extend to h_f when we substitute m for f in the above expressions. To simplify the matter, we shall use h_i, x_i and y_i , where the subscript i indicates that either m or f can be substituted for i . (However, the same meaning of i must be used throughout the entire equation.) Also, if i is used as a superscript we use the convention $(-1)^i = -1$ when $i = m$ and $(-1)^i = 1$ when $i = f$.

We imagine that the surface i has two families of curves which are parallel to the x_i - z , plane and y_i - z , plane respectively. Let $\bar{k}_{i,x}$ and $\bar{k}_{i,y}$ denote the planar curvatures at a general point of the two families of curves, respectively, these are written as $k_{i,x}$ and $k_{i,y}$ at P_m and P_f . Let $g_i = h_{i,xy}$ so that g_i is a measure of the parallelism of tangents to one family of curves at the reference position. For a surface, $k_{i,x}$ and $k_{i,y}$ characterize its symmetric bending and the g_i characterize

* We have assumed explicit analytic forms of the moving and fixed surfaces with respect to the corresponding reference frames. In the following development, however, only the partial derivatives of these forms are used, and in Appendix C we have shown that these partial derivatives can always be explicitly obtained from any analytic representation of a surface.

its anti-symmetric bending about the tangential axes. We define $k_{i,xx}$ to be the rate of change with respect to x_i for $\bar{k}_{i,x}$ and $k_{i,xy}$ to be the rate of change with respect to y_i for $\bar{k}_{i,x}$ at the reference points. Similarly, we define $k_{i,yx}$ to be the rate of change with respect to x_i of $\bar{k}_{i,y}$ and $k_{i,yy}$ to be the rate of change with respect to y_i of $\bar{k}_{i,y}$ at the reference points. All these quantities are simply related to the partial derivatives of h_i (see Appendix D), and will be used throughout this chapter.

Constraints on the surface normal at contact

At every point on the moving surface the inwardly directed unit normal is

$$N_m = \frac{1}{\sqrt{1 + h_{m,x}^2 + h_{m,y}^2}} \begin{pmatrix} -h_{m,x} \\ -h_{m,y} \\ 1 \end{pmatrix}, \quad (1.4)$$

and at every point on the fixed surface the outwardly directed unit normal is

$$N_f = \frac{1}{\sqrt{1 + h_{f,x}^2 + h_{f,y}^2}} \begin{pmatrix} h_{f,x} \\ h_{f,y} \\ 1 \end{pmatrix}. \quad (1.5)$$

Let x_m and y_m in h_m be the time varying coordinates of Q_m , and x_f and y_f in h_f be the time varying coordinates of Q_f . At each instant the inwardly directed normal of the moving surface and the outwardly directed normal of the fixed surface, at the current point of contact, must coincide. Thus

$$N_f(t) = R(t)N_m(t), \quad (1.6)$$

where $R(t)$ is the 3×3 matrix which transforms the coordinates of the moving system to their values in the fixed system.

Since (6) is valid for the entire motion, its n^{th} order time derivatives can be written as

$$\frac{d^n}{dt^n} N_f(t) = \frac{d^n}{dt^n} [R(t)N_m(t)]. \quad (1.7)$$

We define $\Omega = [\omega_1, \omega_2, \omega_3]^T$, the angular velocity vector, and $\mathcal{E} = d\Omega/dt = [\epsilon_1, \epsilon_2, \epsilon_3]^T$, the angular acceleration vector. The derivatives of R have been

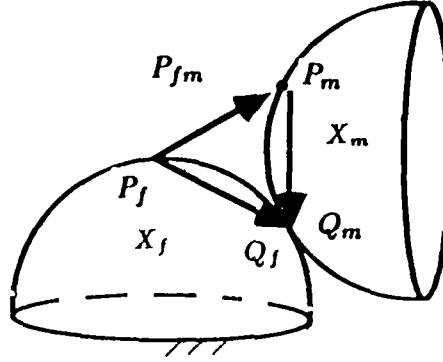


Figure 3.3 Contact trajectories on surfaces

analyzed by many authors, for example see p. 22 of [Bottema and Roth, '79]. At our reference position, $\dot{R}(0)$ is an anti-symmetric angular velocity matrix and $\ddot{R}(0)$ is the sum of an anti-symmetric angular acceleration matrix and a symmetric matrix. Using Appendix D (D1)-(D3), the first row of (7) yields in the initial position, for $n = 1$

$$k_{f,x}\dot{x}_f + g_f\dot{y}_f = -k_{m,x}\dot{x}_m - g_m\dot{y}_m + \omega_2, \quad (1.8)$$

and for $n = 2$

$$\sum_i [k_{i,xx}\dot{x}_i^2 + 2k_{i,xy}\dot{x}_i\dot{y}_i + k_{i,yx}\dot{y}_i^2 + k_{i,x}\ddot{x}_i + g_i\ddot{y}_i] = 2\omega_3(g_m\dot{x}_m + k_{m,y}\dot{y}_m) + \omega_1\omega_3 + \epsilon_2 \quad (1.9)$$

While the second row yields in the initial position, for $n = 1$

$$g_f\dot{x}_f + k_{f,y}\dot{y}_f = -g_m\dot{x}_m - k_{m,y}\dot{y}_m - \omega_1, \quad (1.10)$$

and for $n = 2$

$$\begin{aligned} \sum_i [k_{i,xy}(\dot{x}_i)^2 + 2k_{i,yx}\dot{x}_i\dot{y}_i + k_{i,yy}\dot{y}_i^2 + g_i\ddot{x}_i + k_{i,y}\ddot{y}_i] = \\ -2\omega_3(k_{m,x}\dot{x}_m + g_m\dot{y}_m) + \omega_2\omega_3 - \epsilon_1. \end{aligned} \quad (1.11)$$

The third row of (7) is dependent on (8) and (10) for $n = 1$, and (9) and (11) for $n = 2$.

Constraints on the contact trajectories

The position vector for Q_f (see Fig. 3.3) with respect to the fixed frame, can be represented by

$$\mathbf{r}_{Q_f} = X_f = \begin{pmatrix} x_f \\ y_f \\ z_f \end{pmatrix}. \quad (1.12)$$

Defining P_{fm} as the position vector for P_m with respect to fixed frame, the position vector for Q_m with respect to fixed frame can be represented as

$$\mathbf{r}_{Q_m} = P_{fm} + R(t)X_m, \quad (1.13)$$

where

$$X_m = \begin{pmatrix} x_m \\ y_m \\ z_m \end{pmatrix}. \quad (1.14)$$

Let us consider the pair (x_m, y_m) as the time-varying coordinates of Q_m with respect to the moving frame, and the pair (x_f, y_f) as the time-varying coordinates of Q_f with respect to the fixed frame, equations (12) and (13) are expressions for the same trajectory (as viewed from the fixed space). Equating these we find

$$X_f = P_{fm} + R(t)X_m. \quad (1.15)$$

Taking the first-order time derivative of (15) yields

$$V_{Q_f} = \dot{X}_f = [\dot{P}_{fm} + \dot{R}(t)X_m] + [R(t)\dot{X}_m]. \quad (1.16)$$

By the same argument as in Section 2.2, the first parenthesis in (16) is the general expression for the sliding velocity, V , at any contact point of the fixed surface. Taking higher derivatives of V (i.e. V_p) yields

$$\frac{d^n}{dt^n}(\dot{P}_{fm} + \dot{R}(t)X_m) \equiv V^{(n)}, \quad (1.17)$$

where

$$V = \begin{pmatrix} v_1 \\ v_2 \\ v_3 \end{pmatrix} \text{ and } V^{(n)} = \begin{pmatrix} v_1^{(n)} \\ v_2^{(n)} \\ v_3^{(n)} \end{pmatrix} \quad (1.18)$$

We have used the notation, $d^n v_1/dt^n = v_1^{(n)}$, $d^n v_2/dt^n = v_2^{(n)}$ and $d^n v_3/dt^n = v_3^{(n)}$. \dot{V} is the rate of change of both the sliding speed and its orientation, we call it the **sliding acceleration**. For pure rolling, up to the n^{th} order, $V = \dot{V} = \dots = V^{(n-1)} = 0$.

To simplify the expressions in the following we explicitly express (from the derivatives of (1.1) and (1.2))

$$\ddot{z}_i = (-1)^{i+1} (k_{i,x} \dot{x}_i^2 + 2g_i \dot{x}_i \dot{y}_i + k_{i,y} \dot{y}_i^2), \quad (1.19)$$

$$\begin{aligned} z_i^{(3)} = & (-1)^{i+1} [k_{i,xx} \dot{x}_i^3 + 3(k_{i,xy} \dot{x}_i + k_{i,yx} \dot{y}_i) \dot{x}_i \dot{y}_i + k_{i,yy} \dot{y}_i^3 \\ & + 3(k_{i,x} \dot{x}_i \ddot{x}_i + k_{i,y} \dot{y}_i \ddot{y}_i + g_i (\dot{x}_i \ddot{y}_i + \dot{y}_i \ddot{x}_i))]. \end{aligned} \quad (1.20)$$

We take the first three derivatives of (15) and substitute (17), the first row of each derivative can be written as, respectively,

$$\dot{x}_f = v_1 + \dot{x}_m, \quad (1.21)$$

$$\ddot{x}_f = \dot{v}_1 + \ddot{x}_m - \dot{y}_m \omega_3, \quad (1.22)$$

$$x_f^{(3)} = \ddot{v}_1 + x_m^{(3)} + \dot{x}_m (-\omega_2^2 - \omega_3^2) - 2\ddot{y}_m \omega_3 + \dot{y}_m (\omega_1 \omega_2 - \epsilon_3) + 2\ddot{z}_m \omega_2; \quad (1.23)$$

the second rows yield

$$\dot{y}_f = v_2 + \dot{y}_m, \quad (1.24)$$

$$\ddot{y}_f = \dot{v}_2 + \ddot{x}_m \omega_3 + \ddot{y}_m, \quad (1.25)$$

$$y_f^{(3)} = \ddot{v}_2 + 2\ddot{x}_m \omega_3 + \dot{x}_m (\omega_1 \omega_2 + \epsilon_3) + y_m^{(3)} + \dot{y}_m (-\omega_1^2 - \omega_3^2) - 2\ddot{z}_m \omega_1; \quad (1.26)$$

the third rows yield

$$v_3 = 0, \quad (1.27)$$

$$\dot{v}_3 = \ddot{z}_f - \ddot{z}_m + \dot{x}_m \omega_2 - \dot{y}_m \omega_1, \quad (1.28)$$

$$v_3^{(3)} = z_f^{(3)} - z_m^{(3)} + 2\ddot{x}_m \omega_2 - \dot{x}_m (\omega_1 \omega_3 - \epsilon_2) - 2\ddot{y}_m \omega_1 - \dot{y}_m (\omega_2 \omega_3 + \epsilon_1). \quad (1.29)$$

Constraints on the moving point

Let the position vector for the moving point

$$P_{fm} = \begin{pmatrix} p_x \\ p_y \\ p_z \end{pmatrix}.$$

We substitute $n = 0, 1$ and 2 into (17). The first rows of the resulting matrix equations yield

$$\dot{p}_x = v_1, \quad (1.30)$$

$$\ddot{p}_x = \dot{v}_1 + \dot{y}_m \omega_3, \quad (1.31)$$

$$p_x^{(3)} = \ddot{v}_1 + 2\dot{x}_m(\omega_2^2 + \omega_3^2) + \ddot{y}_m \omega_3 - 2\dot{y}_m(\omega_1 \omega_2 - \epsilon_3) - \ddot{z}_m \omega_2; \quad (1.32)$$

the second rows yield

$$\dot{p}_y = v_2, \quad (1.33)$$

$$\ddot{p}_y = \dot{v}_2 - \dot{x}_m \omega_3, \quad (1.34)$$

$$p_y^{(3)} = \ddot{v}_2 - \ddot{x}_m \omega_3 - 2\dot{x}_m(\omega_1 \omega_2 + \epsilon_3) + 2\dot{y}_m(\omega_1^2 + \omega_3^2) + \ddot{z}_m \omega_1; \quad (1.35)$$

the third rows yield

$$\dot{p}_z = 0, \quad (1.36)$$

$$\ddot{p}_z = \ddot{z}_f - \ddot{z}_m + 2(\dot{x}_m \omega_2 - \dot{y}_m \omega_1), \quad (1.37)$$

$$p_z^{(3)} = z_f^{(3)} - z_m^{(3)} + 3\ddot{x}_m \omega_2 - 3\dot{x}_m(\omega_1 \omega_3 - \epsilon_2) - 3\ddot{y}_m \omega_1 - 3\dot{y}_m(\omega_2 \omega_3 + \epsilon_1). \quad (1.38)$$

3.2 Motion properties for point contact between surfaces

From the basic constraints in the last section, we derive the the contact trajectories up to second order, and the moving point's trajectory up to third order.

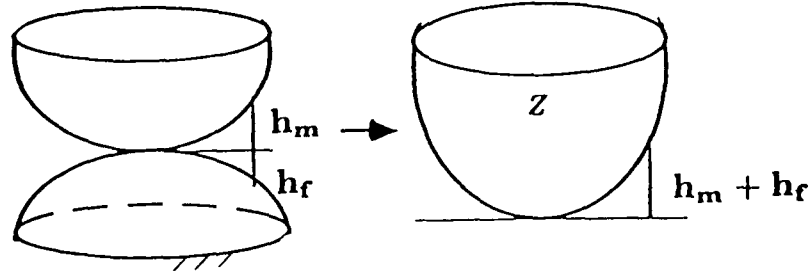


Figure 3.4 A relative surface

First order properties

A function Z describes in the reference position a "relative surface," $Z = H(x, y) = h_m(x, y) + h_f(x, y)$ (Fig. 3.4). Similar to $k_{i,x}$, $k_{i,y}$ and g_i for the m and f surfaces, we have for this relative surface at the reference position

$$K_x = k_{m,x} + k_{f,x}, \quad K_y = k_{m,y} + k_{f,y}, \quad G = g_m + g_f.$$

From these, the Gaussian curvature of the surface at the reference point is given by

$$K = K_x K_y - G^2.$$

K_x , K_y , G and K of the relative surface are important to the relative motion between two surfaces, and will be used throughout this chapter. We substitute (1.21) and (1.24) into (1.8) and (1.10), and solve the linear equations for tangential contact velocity:

$$\dot{x}_m = \frac{1}{K} [G(\omega_1 + g_f v_1 + k_{f,y} v_2) - K_y(-\omega_2 + k_{f,x} v_1 + g_f v_2)], \quad (2.1)$$

$$\dot{y}_m = \frac{1}{K} [-K_x(\omega_1 + g_f v_1 + k_{f,y} v_2) + G(-\omega_2 + k_{f,x} v_1 + g_f v_2)], \quad (2.2)$$

$$\dot{x}_f = \frac{1}{K} [-G(-\omega_1 + g_m v_1 + k_{m,y} v_2) + K_y(\omega_2 + k_{m,x} v_1 + g_m v_2)], \quad (2.3)$$

$$\dot{y}_f = \frac{1}{K} [K_x(-\omega_1 + g_m v_1 + k_{m,y} v_2) - G(\omega_2 + k_{m,x} v_1 + g_m v_2)]. \quad (2.4)$$

The contact velocities do not depend on ω_3 , the normal component of the angular velocity.

For pure rolling, by definition $v_x = v_y = 0$,

$$\dot{x}_m = \dot{x}_f = \frac{1}{K}(G\omega_1 + K_y\omega_2), \quad (2.5)$$

$$\dot{y}_m = \dot{y}_f = -\frac{1}{K}(K_x\omega_1 + G\omega_2). \quad (2.6)$$

Assume that there exists a tactile sensor at the contact point and that it allows us to calculate the tangential contact velocity. Given the geometry and the sensor reading we can calculate the tangential angular velocity (ω_1 and ω_2), or vice versa. It can be noted that \dot{x}_i and \dot{y}_i are related only to the geometry of the relative surface.

When ω_i in equations (1)-(4) vanish, we have the relationships for pure sliding. From the sensor reading for the tangential contact velocity we can calculate the tangential sliding velocity, and vice versa.

Second order properties

Substituting (1.22) and (1.25) into (1.9) and (1.11), we obtain the tangential contact acceleration for the general motion,

$$\begin{aligned} \ddot{x}_m = \frac{1}{K} \{ & K_y[A + k_{f,x}(\dot{y}_m\omega_3 - \dot{v}_1) - g_f(\dot{x}_m\omega_3 + \dot{v}_2)] \\ & - G[B + g_f(\omega_3\dot{y}_m - \dot{v}_1) - k_{f,y}(\dot{x}_m\omega_3 + \dot{v}_2)] \}, \end{aligned} \quad (2.7)$$

$$\begin{aligned} \ddot{y}_m = \frac{1}{K} \{ & K_x[B + g_f(\omega_3\dot{y}_m - \dot{v}_1) - k_{f,y}(\dot{x}_m\omega_3 + \dot{v}_2)] \\ & - G[A + k_{f,x}(\dot{y}_m\omega_3 - \dot{v}_1) - g_f(\dot{x}_m\omega_3 + \dot{v}_2)] \}, \end{aligned} \quad (2.8)$$

$$\begin{aligned} \ddot{x}_f = \frac{1}{K} \{ & K_y[A + k_{m,x}(-\dot{y}_m\omega_3 + \dot{v}_1) + g_m(\dot{x}_m\omega_3 + \dot{v}_2)] \\ & - G[B + g_m(-\omega_3\dot{y}_m + \dot{v}_1) + k_{m,y}(\dot{x}_m\omega_3 + \dot{v}_2)] \}, \end{aligned} \quad (2.9)$$

$$\begin{aligned} \ddot{y}_f = \frac{1}{K} \{ & K_x[B + g_m(-\omega_3\dot{y}_m + \dot{v}_1) + k_{m,y}(\dot{x}_m\omega_3 + \dot{v}_2)] \\ & - G[A + k_{m,x}(-\dot{y}_m\omega_3 + \dot{v}_1) + g_m(\dot{x}_m\omega_3 + \dot{v}_2)] \}, \end{aligned} \quad (2.10)$$

where

$$A = \epsilon_2 + \omega_1\omega_3 + 2\omega_3(g_m\dot{x}_m + k_{m,y}\dot{y}_m) - \sum_i (k_{i,xx}\dot{x}_i^2 + 2k_{i,xy}\dot{x}_i\dot{y}_i + k_{i,yx}\dot{y}_i^2), \quad (2.11)$$

$$B = -\epsilon_1 + \omega_2 \omega_3 - 2\omega_3(k_{m,x}\dot{x}_m + g_m \dot{y}_m) - \sum_i (k_{i,xy}\dot{x}_i^2 + 2k_{i,yx}\dot{x}_i \dot{y}_i + k_{i,yy}\dot{y}_i^2). \quad (2.12)$$

For pure rolling up to second order, by definition, the sliding terms (v_1 , v_2 , \dot{v}_1 and \dot{v}_2) vanish in equations (7)-(12). If in addition $\omega_3 = 0$, then

$$\ddot{x}_m = \ddot{x}_f, \quad \ddot{y}_m = \ddot{y}_f. \quad (2.13)$$

These accelerations are only related to the geometry of the relative surface. When $\epsilon_1 = \epsilon_2 = \omega_3 = 0$, then $\ddot{x}_m = \ddot{x}_f = \ddot{y}_m = \ddot{y}_f = 0$.

The tangential angular acceleration and tangential contact acceleration are in one-to-one correspondence with each other; from either one we can determine the other.

For pure sliding up to second order, by definition, Ω and \mathcal{E} vanish in equations (7)-(12), and we have relationships between the tangential contact acceleration and sliding acceleration which are in one-to-one correspondence with each other.

From (1.31) and (2), the x_f component of the acceleration of the moving point is

$$\ddot{p}_x = \dot{v}_1 + \frac{\omega_3}{K} [-K_x(\omega_1 + g_f v_1 + k_{f,y} v_2) + G(-\omega_2 + k_{f,x} v_1 + g_f v_2)]. \quad (2.14)$$

From (1.34) and (1), the y_f component of the acceleration of the moving point is

$$\ddot{p}_y = \dot{v}_2 - \frac{\omega_3}{K} [G(\omega_1 + g_f v_1 + k_{f,y} v_2) - K_y(-\omega_2 + k_{f,x} v_1 + g_f v_2)]. \quad (2.15)$$

Substituting (1.19) into (1.37), the z_f component of the acceleration of the moving point is

$$\ddot{p}_z = - \sum_i (k_{i,x}\dot{x}_i^2 + 2g_i \dot{x}_i \dot{y}_i + k_{i,y}\dot{y}_i^2) + 2(\omega_2 \dot{x}_m - \omega_1 \dot{y}_m), \quad (2.16)$$

where x_i and y_i are from (1)-(4). For the moving point, the normal acceleration is completely independent of ω_3 , and the tangential acceleration is equal to the tangential sliding acceleration when $\omega_3 = 0$.

For pure rolling up to second order,

$$\ddot{p}_x = -\frac{\omega_3}{K}(K_x\omega_1 + G\omega_2), \quad (2.17)$$

$$\ddot{p}_y = -\frac{\omega_3}{K}(K_y\omega_2 + G\omega_1), \quad (2.18)$$

$$\ddot{p}_z = \frac{1}{K}(K_y\omega_2^2 + K_x\omega_1^2 + 2G\omega_1\omega_2). \quad (2.19)$$

The acceleration of the moving point depends only on the geometry of the relative surface and the angular velocity.

If we define the coordinate frame such that $\dot{y}_f = 0$ (we are free to choose the orientation of the reference frame about the contact normal), then $\omega_1 = -G\omega_2/K_x$, and

$$\ddot{p}_x = 0, \quad (2.20)$$

$$\ddot{p}_y = -\frac{\omega_2\omega_3}{K_x}. \quad (2.21)$$

Unlike rolling with point contact between two planar curves, for spatial pure rolling if the tangential and normal angular velocities do not vanish, there exists tangential acceleration, and its direction is perpendicular to that of the contact velocity with respect to the fixed surface.

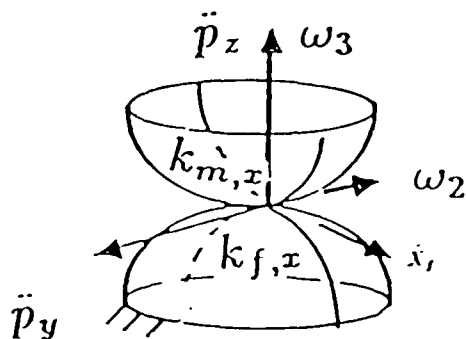


Figure 3.5 Moving point's acceleration under pure rolling

With this special reference frame, \ddot{p}_z takes the simplified form

$$\ddot{p}_z = \frac{\omega_2^2}{K_x} = \frac{\omega_2^2}{k_{m,x} + k_{f,x}}, \quad (2.22)$$

where $k_{m,x}$ and $k_{f,x}$ are the curvatures of the curves cut from the surfaces by a plane through the surface normal and the tangent to the contact velocity with respect to the fixed surface, and ω_2 is the tangential angular velocity component perpendicular to this plane (Fig. 3.5). This formula resembles the analogous one for two planar curves in pure rolling contact. No matter what contact trajectories are traced by Q_f on the fixed surface, when the angular velocity and the path tangent are the same, the normal acceleration of the moving point must be the same.

For the moving point, the ratio of the magnitude of the tangential acceleration to the normal acceleration is equal to ω_3/ω_2 . This is the ratio of the angular velocity's normal component and its tangential component which is perpendicular to the contact velocity with respect to the fixed surface.

From (14)-(16), for pure sliding the tangential components of the acceleration of the moving point are

$$\ddot{p}_x = \dot{v}_1, \quad (2.23)$$

$$\ddot{p}_y = \dot{v}_2. \quad (2.24)$$

The general expression for the normal acceleration of the moving point when the relative motion between surfaces is pure sliding can be obtained by substituting (1)-(4) into (11), and setting the angular velocity to zero. If both surfaces in contact are symmetric, $g_m = g_f = 0$, and if we define the reference frame such that $v_2 = 0$ (also $\dot{y}_f = 0$ from (4)), and $v_1 = v$ (v is the sliding speed) then

$$\ddot{p}_z = -\frac{v^2}{\rho_{m,x} + \rho_{f,x}}. \quad (2.25)$$

$\rho_{m,x} = 1/k_{m,x}$ and $\rho_{f,x} = 1/k_{f,x}$ are the radii of curvature of the curves cut from the surfaces by a plane through the motion tangent and the contact normal (Fig.3.6).

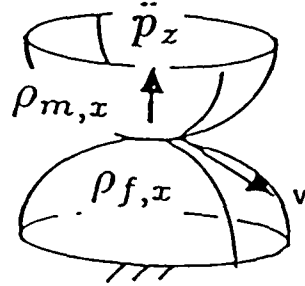


Figure 3.6 Moving point's acceleration under pure sliding

This formula resembles the one for point contact between two planar curves when the relative motion is a translation.

Third order properties

Substituting (1.19) into (1.32), we have the x , component of the jerk of the moving point

$$p_x^{(3)} = \ddot{v}_1 + 2\dot{x}_m(\omega_2^2 + \omega_3^2) + \ddot{y}_m\omega_3 - 2\dot{y}_m(\omega_1\omega_2 - \epsilon_3) - (k_{m,x}\dot{x}_m^2 + 2g_m\dot{x}_m\dot{y}_m + k_{m,y}\dot{y}_m^2)\omega_2 \quad (2.26)$$

Substituting (1.19) into (1.35), we have the y , component of the jerk of the moving point

$$p_y^{(3)} = \ddot{v}_2 + 2\dot{y}_m(\omega_1^2 + \omega_3^2) - \ddot{x}_m\omega_3 - 2\dot{x}_m(\omega_1\omega_2 + \epsilon_3) + (k_{m,x}\dot{x}_m^2 + 2g_m\dot{x}_m\dot{y}_m + k_{m,y}\dot{y}_m^2)\omega_1 \quad (2.27)$$

Substituting (1.20) into (1.38), we have the z , component of the jerk of the moving point

$$p_z^{(3)} = - \sum_i [k_{i,xx}\dot{x}_i^3 + 3(k_{i,xy}\dot{x}_i + k_{i,yx}\dot{y}_i)\dot{x}_i\dot{y}_i + k_{i,yy}\dot{y}_i^3 + 3(k_{i,x}\dot{x}_i\ddot{x}_i + k_{i,y}\dot{y}_i\ddot{y}_i + g_i(\dot{x}_i\ddot{y}_i + \dot{y}_i\ddot{x}_i))] + 3\ddot{x}_m\omega_2 - 3\dot{x}_m(\omega_1\omega_3 - \epsilon_2) - 3\ddot{y}_m\omega_1 - 3\dot{y}_m(\omega_2\omega_3 + \epsilon_1) \quad (2.28)$$

where \dot{x}_i , \dot{y}_i , \ddot{x}_i and \ddot{y}_i have already been calculated earlier in this section.

For pure rolling, up to third order, by definition $v_1^{(k)} = v_2^{(k)} = 0$ for $k = 0, 1$ to 3. We can substitute these into (26)-(28) and also the values from the previously derived \dot{x}_i , \dot{y}_i , \ddot{x}_i and \ddot{y}_i for pure rolling up to second order.

For pure sliding up to second order, by definition, $\Omega = 0$ and $\mathcal{E} = 0$. The expressions (26)-(28) take the simplified forms

$$p_x^{(s)} = \ddot{v}_1, \quad (2.29)$$

$$p_y^{(s)} = \ddot{v}_2, \quad (2.30)$$

$$p_z^{(s)} = - \sum_i [k_{i,xx} \dot{x}_i^3 + 3(k_{i,xy} \dot{x}_i + k_{i,yx} \dot{y}_i) \dot{x}_i \dot{y}_i + k_{i,yy} \dot{y}_i^3 + 3(k_{i,x} \dot{x}_i \ddot{x}_i + k_{i,y} \dot{y}_i \ddot{y}_i + g_i(\dot{x}_i \ddot{y}_i + \dot{y}_i \ddot{x}_i))], \quad (2.31)$$

where the previously derived values of \dot{x}_i , \dot{y}_i , \ddot{x}_i and \ddot{y}_i , for a pure sliding motion will be substituted.

For pure rolling up to n^{th} order, assuming all derivatives of the angular velocity up to $(n-2)^{\text{th}}$ order are known, there is a one-to-one correspondence between the tangential $(n-1)^{\text{th}}$ derivatives of contact velocity and angular velocity. Similarly, for pure sliding up to n^{th} order, when given the derivatives of the sliding velocity up to $(n-2)^{\text{th}}$ order, there is a one-to-one correspondence between the tangential $(n-1)^{\text{th}}$ order derivatives of the contact velocity and the sliding velocity.

3.3 Spatial motion with point contact between two spheres

As an example to illustrate the general relationships developed in the last section, we consider spatial motion with point contact between two spheres of radii ρ_m and ρ_f .

The h_m and h_f defined in (1.1) and (1.2) can be explicitly written as

$$h_m = \rho_m - \sqrt{\rho_m^2 - x_m^2 - y_m^2}, \quad h_f = \rho_f - \sqrt{\rho_f^2 - x_f^2 - y_f^2}. \quad (3.1)$$

Substituting (1) into Appendix D (D1) and (D3), we have

$$k_{m,x} = k_{m,y} = \frac{1}{\rho_m}, \quad k_{f,x} = k_{f,y} = \frac{1}{\rho_f}, \quad g_m = g_f = 0. \quad (3.2)$$

Substituting (1) into Appendix D (D2), we have

$$k_{i,xx} = k_{i,xy} = k_{i,yx} = k_{i,yy} = 0. \quad (3.3)$$

To simplify the following expressions, we define

$$\bar{\rho} = \frac{\rho_m \rho_f}{\rho_m + \rho_f}, \quad \rho_s = \rho_m + \rho_f.$$

Substituting (2) and (3) into (2.1)-(2.4), we have the expressions for the tangential contact velocities,

$$\dot{x}_m = \bar{\rho}(\omega_2 - \frac{v_1}{\rho_f}), \quad \dot{y}_m = \bar{\rho}(-\omega_1 - \frac{v_2}{\rho_f}), \quad (3.4)$$

$$\dot{x}_f = \bar{\rho}(\omega_2 + \frac{v_1}{\rho_m}), \quad \dot{y}_f = \bar{\rho}(-\omega_1 + \frac{v_2}{\rho_m}). \quad (3.5)$$

For pure rolling, the contact velocity (\dot{x}_i and \dot{y}_i) is sensitive to the radii of the spheres. When one sphere is small, $\bar{\rho}$ will be small, and the contact velocity (sensed by a tactile sensor) will be less sensitive to the sliding velocity (v_i). If one sphere's radius increases to infinity it becomes a plane, in which case the contact speed is proportional to the radius of the remaining sphere.

For pure sliding,

$$\dot{x}_m = -\frac{1}{1 + \rho_f/\rho_m} v_1, \quad \dot{y}_m = -\frac{1}{1 + \rho_f/\rho_m} v_2, \quad (3.6)$$

$$\dot{x}_f = \frac{1}{1 + \rho_m/\rho_f} v_1, \quad \dot{y}_f = \frac{1}{1 + \rho_m/\rho_f} v_2. \quad (3.7)$$

When one sphere is very small in radius compared to the other sphere, a tactile sensor on it will have poor sensitivity for measuring the sliding velocity.

Substituting (2)-(5) into (2.7)-(2.12), we have expressions for the tangential contact acceleration:

$$\ddot{x}_m = \bar{\rho}[\epsilon_2 + \omega_1 \omega_3 - \frac{2\rho_f + \rho_m}{\rho_s} \omega_3(\omega_1 + \frac{v_2}{\rho_f}) - \frac{\dot{v}_1}{\rho_f}], \quad (3.8)$$

$$\ddot{y}_m = \bar{\rho}[-\epsilon_1 + \omega_2 \omega_3 - \frac{2\rho_f + \rho_m}{\rho_s} \omega_3(\omega_2 - \frac{v_1}{\rho_f}) - \frac{\dot{v}_2}{\rho_f}], \quad (3.9)$$

$$\ddot{x}_f = \bar{\rho}[\epsilon_2 + \omega_1 \omega_3 - \frac{\rho_f}{\rho_s} \omega_3(\omega_1 + \frac{v_2}{\rho_f}) + \frac{\dot{v}_1}{\rho_m}], \quad (3.10)$$

$$\ddot{y}_f = \bar{\rho}[-\epsilon_1 + \omega_2\omega_3 - \frac{\rho_f}{\rho_s}\omega_3(\omega_2 - \frac{v_1}{\rho_f}) + \frac{\dot{v}_2}{\rho_m}]. \quad (3.11)$$

When v_i and \dot{v}_i in (8)-(11) vanish, we have the tangential contact acceleration for pure rolling up to second order. Its sensitivity to the angular acceleration depends on the radii of the spheres in a similar way to that discussed earlier in this section for the angular velocity.

When ω_i and ϵ_i vanish in (8)-(11), we have relationships between the tangential contact acceleration and sliding acceleration, which are exactly the same as those between tangential contact velocity and sliding velocity.

Substituting (2)-(5) into (2.14)-(2.16), we have the acceleration of the moving point,

$$\ddot{p}_x = \bar{\rho}(-\omega_1 - \frac{v_2}{\rho_f})\omega_3 + \dot{v}_1, \quad (3.12)$$

$$\ddot{p}_y = \bar{\rho}(-\omega_2 + \frac{v_1}{\rho_f})\omega_3 + \dot{v}_2, \quad (3.13)$$

$$\ddot{p}_z = \bar{\rho}(\omega_1^2 + \omega_2^2) - \frac{v_1^2 + v_2^2}{\rho_s} + \frac{2\rho_m}{\rho_s}(\omega_1 v_2 - \omega_2 v_1). \quad (3.14)$$

For pure rolling,

$$\ddot{p}_x = -\bar{\rho}\omega_1\omega_3, \quad \ddot{p}_y = -\bar{\rho}\omega_2\omega_3, \quad \ddot{p}_z = \bar{\rho}(\omega_1^2 + \omega_2^2). \quad (3.15)$$

The normal acceleration is proportional to the square of the magnitude of the tangential angular velocity, and the ratio of the magnitude of the tangential acceleration to normal acceleration is

$$\frac{\sqrt{\ddot{p}_x^2 + \ddot{p}_y^2}}{\ddot{p}_z} = \frac{|\omega_3|}{\sqrt{\omega_1^2 + \omega_2^2}}.$$

We can easily calculate the acceleration of the center point of the moving sphere under pure rolling. When $\epsilon_1 = \epsilon_2 = 0$, the acceleration at the center point has the magnitude ratio ρ_m/ρ_f , and is along the opposite direction to the acceleration of the moving contact point.

For pure sliding, up to second order,

$$\ddot{p}_x = \dot{v}_1, \quad \ddot{p}_y = \dot{v}_2, \quad \ddot{p}_z = -\frac{v_1^2 + v_2^2}{\rho_s}. \quad (3.16)$$

The normal acceleration is inversely proportional to the sum of the radii of the spheres, and proportional to the square of the sliding velocity.

Substituting (2)-(5) and (8)-(11) into (2.26)-(2.28), we have expressions for the components of the jerk of the moving point:

$$\begin{aligned} p_x^{(3)} = & \ddot{v}_1 + 2\bar{\rho}(\omega_2 - \frac{v_1}{\rho_f})(\omega_2^2 + \omega_3^2) + \bar{\rho}\omega_3[-\epsilon_1 + \omega_2\omega_3 - \frac{2\rho_f + \rho_m}{\rho_s}\omega_3(\omega_2 - \frac{v_1}{\rho_f}) \\ & - \frac{\dot{v}_2}{\rho_f}] + 2\bar{\rho}(\omega_1\omega_2 - \epsilon_3)(\omega_1 + \frac{v_2}{\rho_f}) - \frac{\bar{\rho}^2}{\rho_m}\omega_2[\omega_1^2 + \omega_2^2 + \frac{1}{\rho_f^2}(v_1^2 + v_2^2) \\ & + \frac{2}{\rho_f}(\omega_1v_2 - \omega_2v_1)], \end{aligned} \quad (3.17)$$

$$\begin{aligned} p_y^{(3)} = & \ddot{v}_2 - 2\bar{\rho}(\omega_1 + \frac{v_2}{\rho_f})(\omega_1^2 + \omega_3^2) - \bar{\rho}\omega_3[\epsilon_2 + \omega_1\omega_3 - \frac{2\rho_f + \rho_m}{\rho_s}\omega_3(\omega_1 + \frac{v_2}{\rho_f}) \\ & - \frac{\dot{v}_1}{\rho_f}] - 2\bar{\rho}(\omega_1\omega_2 + \epsilon_3)(\omega_2 - \frac{v_1}{\rho_f}) + \frac{\bar{\rho}^2}{\rho_m}\omega_1[\omega_1^2 + \omega_2^2 + \frac{1}{\rho_f^2}(v_1^2 + v_2^2) \\ & + \frac{2}{\rho_f}(\omega_1v_2 - \omega_2v_1)], \end{aligned} \quad (3.18)$$

$$\begin{aligned} p_z^{(3)} = & \frac{\dot{v}_1v_2 + \dot{v}_2v_1}{\rho_s} + \bar{\rho}[\omega_1\epsilon_1 + \omega_2\epsilon_2] - \frac{\bar{\rho}}{\rho_s}\omega_3(v_1\omega_1 + v_2\omega_2) \\ & + 3\bar{\rho}\{-(\omega_1\omega_3 - \epsilon_2)(\omega_2 - \frac{v_1}{\rho_f}) + (\omega_2\omega_3 + \epsilon_1)(\omega_1 + \frac{v_2}{\rho_f}) \\ & + \omega_2[\epsilon_2 + \omega_1\omega_3 - \frac{2\rho_f + \rho_m}{\rho_s}\omega_3(\omega_1 + \frac{v_2}{\rho_f}) - \frac{\dot{v}_1}{\rho_f}] \\ & - \omega_1[-\epsilon_1 + \omega_2\omega_3 - \frac{2\rho_f + \rho_m}{\rho_s}\omega_3(\omega_2 - \frac{v_1}{\rho_f}) - \frac{\dot{v}_2}{\rho_f}]\}. \end{aligned} \quad (3.19)$$

For pure rolling up to third order,

$$\begin{aligned} p_x^{(3)} = & \bar{\rho}\{2\omega_2(\omega_2^2 + \omega_3^2) + \omega_3[-\epsilon_1 - \frac{\rho_f}{\rho_s}\omega_2\omega_3] + 2\omega_1(\omega_1\omega_2 - \epsilon_3) \\ & - \frac{\bar{\rho}}{\rho_m}\omega_2(\omega_1^2 + \omega_2^2)\}, \end{aligned} \quad (3.20)$$

$$p_y^{(3)} = -\bar{\rho}\{2\omega_1(\omega_1^2 + \omega_3^2) + \omega_3[\epsilon_2 - \frac{\rho_f}{\rho_s}\omega_1\omega_3] + 2\omega_2(\omega_1\omega_2 + \epsilon_3) - \frac{\bar{\rho}}{\rho_m}\omega_1(\omega_1^2 + \omega_2^2)\}, \quad (3.21)$$

$$p_z^{(3)} = 3\bar{\rho}(\omega_1\epsilon_1 + \omega_2\epsilon_2). \quad (3.22)$$

When $\omega_3 = \epsilon_3 = 0$, $p_y^{(3)}/p_x^{(3)} = -\omega_1/\omega_2$. In words, when the normal angular velocity and the normal angular acceleration vanish, the ratio of the two perpendicular components of the tangential jerk (of the moving point) is equal to the inverse of the ratio of angular velocity components along the same axes.

When $\epsilon_1 = \epsilon_2 = 0$, $p_z^{(3)} = 0$, i.e., the normal jerk of the moving point vanishes when there is no tangential angular acceleration.

For pure sliding,

$$p_x^{(3)} = \ddot{v}_1, \quad p_y^{(3)} = \ddot{v}_2, \quad p_z^{(3)} = -\frac{3}{\rho_s}(\dot{v}_1 v_1 + \dot{v}_2 v_2) \quad (3.23)$$

The normal jerk of the moving point is inversely proportional to the sum of the radii of the spheres and linearly proportional to the sliding velocity and sliding acceleration. When either the tangential sliding velocity or sliding acceleration vanishes, the normal jerk of the moving point vanishes.

3.4 Special geometry of contacting surfaces

We can extend our general relationships to the special cases where one contact surface is a sharp vertex (a point), or a sharp edge (a line) or a plane (Fig. 3.7). We model a point and a plane as the limit of a sphere, and a line as the limit of a circular cylinder.

Moving surface is a point

When the moving surface is modeled as the decreasing limit of a sphere, $k_{m,x}$ and $k_{m,y}$ approach ∞ ; g_m , $k_{m,xx}$, $k_{m,xy}$, $k_{m,yx}$ and $k_{m,yy}$ vanish. By taking the limit in (2.1)-(2.4) and (2.7)-(2.10) (after substituting in (2.11) and (2.12)),

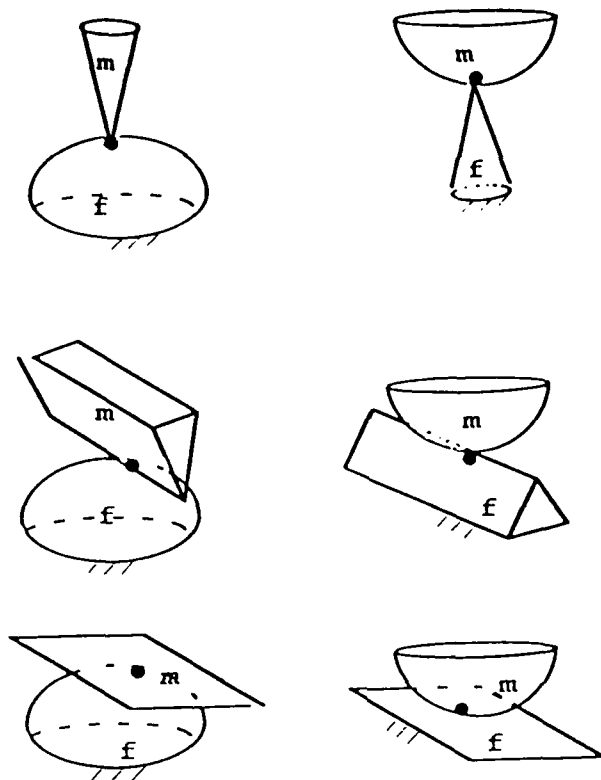


Figure 3.7 *Special geometries for point contact between surfaces*

the tangential contact velocity and the contact acceleration with respect to the moving frame are, respectively,

$$\dot{x}_m = \dot{y}_m = 0, \ddot{x}_m = \ddot{y}_m = 0. \quad (4.1)$$

Obviously the contact trajectory with respect to the moving frame reduces to a point.

The tangential contact velocity and acceleration with respect to the fixed surface are, respectively,

$$\dot{x}_f = v_1, \dot{y}_f = v_2, \quad (4.2)$$

$$\ddot{x}_f = \dot{v}_1, \ddot{y}_f = \dot{v}_2. \quad (4.3)$$

The tangential contact velocity and acceleration with respect to the fixed surface are equal to the tangential sliding velocity and acceleration. Substituting (1)

into (1.17), we see that they are also equal to the tangential acceleration of the moving point. By taking the limit in (2.16), one obtains the normal acceleration of the moving point,

$$\ddot{p}_z = -(k_{f,x}v_1^2 + 2g_f v_1 v_2 + k_{f,y}v_2^2). \quad (4.4)$$

Fixed surface is a point

When the fixed surface is modeled as the decreasing limit of a sphere, $k_{f,x}$ and $k_{f,y}$ approach ∞ , g_f , $k_{f,xx}$, $k_{f,xy}$, $k_{f,yx}$ and $k_{f,yy}$ vanish. By taking the limit in (2.1)-(2.4) and (2.7)-(2.10), the tangential contact velocity and acceleration with respect to the moving frame are, respectively,

$$\dot{x}_m = -v_1, \quad \dot{y}_m = -v_2, \quad (4.5)$$

$$\ddot{x}_m = -\dot{v}_1 - \omega_3 v_2, \quad \ddot{y}_m = -\dot{v}_2 + \omega_3 v_1. \quad (4.6)$$

The tangential contact velocity and acceleration with respect to the fixed frame are, respectively,

$$\dot{x}_f = \dot{y}_f = 0, \quad (4.7)$$

$$\ddot{x}_f = \ddot{y}_f = 0. \quad (4.8)$$

Taking the limit in (2.14)-(2.16), the components for the acceleration of the moving point are, respectively,

$$\ddot{p}_x = \dot{v}_1 - \omega_3 v_2, \quad (4.9)$$

$$\ddot{p}_y = \dot{v}_2 - \omega_3 v_1, \quad (4.10)$$

$$\ddot{p}_z = -(k_{m,x}v_1^2 + 2g_m v_1 v_2 + k_{m,y}v_2^2) + 2(-\omega_2 v_1 + \omega_1 v_2). \quad (4.11)$$

Comparing (11) to (3.9), when either surface in contact is reduced to a point, the sliding velocity becomes the dominant term in the expression for the normal acceleration of the moving point, which is not the case for convex surfaces (for

our purposes, we have convex surfaces when P_m and P_f are elliptic points of their surfaces, and locally the surfaces are bent away from the tangent plane in different directions).

Moving surface is a line

When the moving line is modeled as the decreasing limit of a circular cylinder with its direction coincident with the x axis (by virtue of the choice of the orientation of the reference frames about the contact normal), $k_{m,y}$ approaches ∞ , and $k_{m,x}$, g_m , $k_{m,xx}$, $k_{m,xy}$, $k_{m,yx}$ and $k_{m,yy}$ vanish.

Taking the limit in (2.1) and (2.2),

$$\dot{x}_m = -\frac{1}{k_{f,x}}(-\omega_2 + k_{f,x}v_1 + g_f v_2), \quad \dot{y}_m = 0. \quad (4.12)$$

Taking the limit in (2.7) and (2.8),

$$\ddot{x}_m = \frac{1}{k_{f,x}} \left\{ \epsilon_2 + \omega_1 \omega_3 + 2 \frac{\omega_3}{k_{f,x}} [-k_{f,x}(\omega_1 + k_{f,y}v_2) + g_f(-\omega_2 + g_f v_2)] \right. \\ \left. - (k_{f,xx}\dot{x}_f^2 + 2k_{f,xy}\dot{x}_f\dot{y}_f + k_{f,yx}\dot{y}_f^2) - k_{f,x}\dot{v}_1 - g_f(\dot{x}_m\omega_3 + \dot{v}_2) \right\}, \quad (4.13)$$

$$\ddot{y}_m = 0. \quad (4.14)$$

Obviously, the contact trajectory with respect to the moving frame is a point along the y_m direction, and it is a general function of the motion along the x_m direction.

Taking the limit in (2.3) and (2.4),

$$\dot{x}_f = \frac{1}{k_{f,x}}(\omega_2 - g_f v_2), \quad \dot{y}_f = v_2. \quad (4.15)$$

Taking the limit in (2.9) and (2.10),

$$\ddot{x}_f = \frac{1}{k_{f,x}} \left\{ \epsilon_2 + \omega_1 \omega_3 + \frac{2\omega_3}{k_{f,x}} [-k_{f,x}(\omega_1 + k_{f,y}v_2) + g_f(-\omega_2 + g_f v_2)] \right. \\ \left. - (k_{f,xx}\dot{x}_f^2 + 2k_{f,xy}\dot{x}_f\dot{y}_f + k_{f,yx}\dot{y}_f^2) - g_f(\dot{x}_m\omega_3 + \dot{v}_2) \right\}, \quad (4.16)$$

$$\ddot{y}_f = \dot{v}_2 + \dot{x}_m\omega_3. \quad (4.17)$$

From the tangential contact velocity with respect to the fixed frame, we can uniquely determine the components of the angular velocity and sliding velocity along the y , direction, and from the tangential contact acceleration with respect to the fixed frame, we can determine the components of the angular acceleration and sliding acceleration along the y , direction.

Taking the limit in (2.14)-(2.16), we have

$$\ddot{p}_x = \dot{v}_1, \quad (4.18)$$

$$\ddot{p}_y = \dot{v}_2 + \frac{\omega_3}{k_{f,x}}(-\omega_2 + k_{f,x}v_1 + g_f v_2), \quad (4.19)$$

$$\ddot{p}_z = \frac{\omega_2^2}{k_{f,x}} + \left(\frac{g_f^2}{k_{f,x}} - k_{f,y}\right)v_2^2 - 2\omega_2\left(v_1 + \frac{g_f v_2}{k_{f,x}}\right). \quad (4.20)$$

In the x , direction, this result resembles the case of pure sliding.

Fixed surface is a line

When the fixed surface is modeled as the decreasing limit of a circular cylinder with its axis parallel to the x axis, $k_{f,y}$ approaches ∞ , and $k_{f,x}$, g_f , $k_{f,xx}$, $k_{f,xy}$, $k_{f,yx}$ and $k_{f,yy}$ vanish. By taking the limit in (2.1) and (2.2),

$$\dot{x}_m = \frac{1}{k_{m,x}}(\omega_2 + g_m v_2), \quad \dot{y}_m = -v_2. \quad (4.21)$$

By taking the limit in (2.7) and (2.8),

$$\begin{aligned} \ddot{x}_m = \frac{1}{k_{m,x}}[& \epsilon_2 + \omega_1 \omega_3 + 2\omega_3(g_m \dot{x}_m + k_{m,y} \dot{y}_m) \\ & - (k_{m,xx} \dot{x}_m^2 + 2k_{m,xy} \dot{x}_m \dot{y}_m + k_{m,yx} \dot{y}_m^2) + g_m(\dot{x}_m \omega_3 + \dot{v}_2), \end{aligned} \quad (4.22)$$

$$\ddot{y}_m = -(\dot{x}_m \omega_3 + \dot{v}_2). \quad (4.23)$$

As in the previous case, the tangential contact velocity with respect to the moving frame is completely determined by the y , components of the angular velocity and sliding velocity. When all the velocity terms are given, the tangential contact acceleration with respect to the moving frame is completely determined by the y , component of the angular acceleration and the sliding acceleration.

Taking the limit in (2.3) and (2.4),

$$\dot{x}_f = \frac{1}{k_{m,x}}(\omega_2 + k_{m,x}v_1 + g_mv_2), \quad \dot{y}_f = 0. \quad (4.24)$$

and taking the limit in (2.9) and (2.10),

$$\begin{aligned} \ddot{x}_f = \frac{1}{k_{m,x}} [& \epsilon_2 + \omega_1\omega_3 + 2\omega_3(g_m\dot{x}_m + k_{m,y}\dot{y}_m) - (k_{m,xx}\dot{x}_m^2 + 2k_{m,xy}\dot{x}_m\dot{y}_m \\ & + k_{m,yx}\dot{y}_m^2) + k_{m,x}(-\dot{y}_m\omega_3 + \dot{v}_1) + g_m(\dot{x}_m\omega_3 + \dot{v}_2)]. \end{aligned} \quad (4.25)$$

$$\ddot{y}_f = 0. \quad (4.26)$$

Obviously, the contact trajectory with respect to the fixed frame is a point along the y_f direction.

By taking the limit in (2.14)-(2.16),

$$\ddot{p}_x = \dot{v}_1 - \omega_3v_2, \quad (4.27)$$

$$\ddot{p}_y = \dot{v}_2 - \frac{\omega_3}{k_{m,x}}[g_mv_2 - (-\omega_2 + k_{f,x}v_1 + g_fv_2)], \quad (4.28)$$

$$\ddot{p}_z = -\left[\frac{1}{k_{m,x}}(\omega_2 + g_mv_2)^2 - 2\frac{g_m}{k_{m,x}}(\omega_2 + g_mv_2)v_2 + k_{m,y}v_2^2\right] + \frac{2\omega_2}{k_{m,x}}(\omega_2 + g_mv_2) + 2\omega_1v_2 \quad (4.29)$$

Moving surface is a plane

When the moving surface is modeled as the increasing limit of a sphere, $k_{m,x}$, $k_{m,y}$, g_m , $k_{m,xx}$, $k_{m,xy}$, $k_{m,yx}$ and $k_{m,yy}$ vanish. We denote the Gaussian curvature of the fixed surface at the reference point as K_f ,

$$K_f = k_{f,x}k_{f,y} - g_f^2.$$

Taking the limit in (2.1), (2.2), (2.7) and (2.8), the contact velocity and acceleration with respect to the moving frame are, respectively,

$$\dot{x}_m = \frac{1}{K_f}[g_f\omega_1 + k_{f,y}\omega_2] - v_1, \quad \dot{y}_m = \frac{-1}{K_f}[k_{f,x}\omega_1 + g_f\omega_2] - v_2, \quad (4.30)$$

$$\ddot{x}_m = \frac{1}{K_f} \{k_{f,y}[\epsilon_2 + \omega_1\omega_3 - (k_{f,xx}\dot{x}_f^2 + 2k_{f,xy}\dot{x}_f\dot{y}_f + k_{f,yx}\dot{y}_f^2)] + g_f[\epsilon_1 - \omega_2\omega_3 + (k_{f,xy}\dot{x}_f^2 + 2k_{f,yx}\dot{x}_f\dot{y}_f + k_{f,yy}\dot{y}_f^2)]\} - \dot{v}_1 + \dot{y}_m\omega_3, \quad (4.31)$$

$$\ddot{y}_m = \frac{-1}{K_f} \{k_{f,x}[\epsilon_1 - \omega_2\omega_3 + (k_{f,xy}\dot{x}_f^2 + 2k_{f,yx}\dot{x}_f\dot{y}_f + k_{f,yy}\dot{y}_f^2)] + g_f[\epsilon_2 + \omega_1\omega_3 - (k_{f,xx}\dot{x}_f^2 + 2k_{f,xy}\dot{x}_f\dot{y}_f + k_{f,yx}\dot{y}_f^2)]\} - \dot{v}_2 - \dot{x}_m\omega_3. \quad (4.32)$$

All these quantities are functions of both the rotational and sliding motion.

Taking the limit in (2.3), (2.4), (2.9) and (2.10), the contact velocity and acceleration with respect to the fixed frame are, respectively,

$$\dot{x}_f = \frac{1}{K_f} [g_f\omega_1 + k_{f,y}\omega_2], \quad \dot{y}_f = \frac{-1}{K_f} [k_{f,x}\omega_1 + g_f\omega_2], \quad (4.33)$$

$$\ddot{x}_f = \frac{1}{K_f} \{k_{f,y}[\epsilon_2 + \omega_1\omega_3 - (k_{f,xx}\dot{x}_f^2 + 2k_{f,xy}\dot{x}_f\dot{y}_f + k_{f,yx}\dot{y}_f^2)] + g_f[\epsilon_1 - \omega_2\omega_3 + (k_{f,xy}\dot{x}_f^2 + 2k_{f,yx}\dot{x}_f\dot{y}_f + k_{f,yy}\dot{y}_f^2)]\}, \quad (4.34)$$

$$\ddot{y}_f = \frac{-1}{K_f} \{k_{f,x}[\epsilon_1 - \omega_2\omega_3 + (k_{f,xy}\dot{x}_f^2 + 2k_{f,yx}\dot{x}_f\dot{y}_f + k_{f,yy}\dot{y}_f^2)] + g_f[\epsilon_2 + \omega_1\omega_3 - (k_{f,xx}\dot{x}_f^2 + 2k_{f,xy}\dot{x}_f\dot{y}_f + k_{f,yx}\dot{y}_f^2)]\}. \quad (4.35)$$

These are functions only of the rotational motion. In other words, when there is a tactile sensor on the fixed surface, from the tangential contact velocity reading, we can calculate the tangential angular velocity. Having knowledge of the first order motion, from the tangential contact acceleration, we can calculate the tangential angular acceleration.

Taking the limit in (2.14)-(2.16), the acceleration components of the moving point with respect to the reference frame are, respectively,

$$\ddot{p}_x = \dot{v}_1 - \frac{\omega_3}{K_f} (k_{f,x}\omega_1 + g_f\omega_2) - v_2\omega_3, \quad (4.36)$$

$$\ddot{p}_y = \dot{v}_2 + \frac{\omega_3}{K_f} (k_{f,y}\omega_2 - g_f\omega_1) + v_1\omega_3, \quad (4.37)$$

$$\ddot{p}_z = \frac{1}{K_f} (k_{f,x}\omega_1^2 + 2g_f\omega_1\omega_2 + k_{f,y}\omega_2^2) + 2(\omega_1v_2 - \omega_2v_1). \quad (4.38)$$

Fixed surface is a plane

When the fixed surface is modeled as the increasing limit of a sphere, $k_{f,x}$, $k_{f,y}$, g_f , $k_{f,xx}$, $k_{f,xy}$, $k_{f,yx}$ and $k_{f,yy}$ vanish. We denote the Gaussian curvature of the moving surface as K_m ;

$$K_m = k_{m,x}k_{m,y} - g_m^2.$$

Taking the limit in (2.1), (2.2), (2.7) and (2.8), the contact velocity and acceleration with respect to the moving frame are, respectively,

$$\dot{x}_m = \frac{1}{K_m}[g_m\omega_1 + k_{m,y}\omega_2], \quad \dot{y}_m = \frac{-1}{K_m}[k_{m,x}\omega_1 + g_m\omega_2], \quad (4.39)$$

$$\ddot{x}_m = \frac{1}{K_m}\{k_{m,y}[\epsilon_2 - \omega_1\omega_3 - (k_{m,xx}\dot{x}_f^2 + 2k_{m,xy}\dot{x}_f\dot{y}_f + k_{m,yx}\dot{y}_f^2)] \\ + g_m[\epsilon_1 + \omega_2\omega_3 + (k_{m,xy}\dot{x}_f^2 + 2k_{m,yx}\dot{x}_f\dot{y}_f + k_{m,yy}\dot{y}_f^2)]\}, \quad (4.40)$$

$$\ddot{y}_m = \frac{-1}{K_m}\{k_{m,x}[\epsilon_1 + \omega_2\omega_3 + (k_{m,xy}\dot{x}_f^2 + 2k_{m,yx}\dot{x}_f\dot{y}_f + k_{m,yy}\dot{y}_f^2)] \\ + g_m[\epsilon_2 - \omega_1\omega_3 - (k_{m,xx}\dot{x}_f^2 + 2k_{m,xy}\dot{x}_f\dot{y}_f + k_{m,yx}\dot{y}_f^2)]\}. \quad (4.41)$$

All these quantities are functions of the rotational aspects of the motion only.

Taking the limit in (2.3), (2.4), (2.9) and (2.10), the contact velocity and acceleration with respect to the fixed frame are, respectively,

$$\dot{x}_f = \frac{1}{K_m}[g_m\omega_1 + k_{m,y}\omega_2] + v_1, \quad \dot{y}_f = \frac{-1}{K_m}[k_{m,x}\omega_1 + g_m\omega_2] + v_2, \quad (4.42)$$

$$\ddot{x}_f = \frac{1}{K_m}\{+k_{m,y}[\epsilon_2 - \omega_1\omega_3 - (k_{m,xx}\dot{x}_f^2 + 2k_{m,xy}\dot{x}_f\dot{y}_f + k_{m,yx}\dot{y}_f^2)] \\ + g_m[\epsilon_1 + \omega_2\omega_3 + (k_{m,xy}\dot{x}_f^2 + 2k_{m,yx}\dot{x}_f\dot{y}_f + k_{m,yy}\dot{y}_f^2)]\} - \dot{y}_m\omega_3 + \dot{v}_1, \quad (4.43)$$

$$\ddot{y}_f = \frac{-1}{K_m}\{k_{m,x}[\epsilon_1 + \omega_2\omega_3 + (k_{m,xy}\dot{x}_f^2 + 2k_{m,yx}\dot{x}_f\dot{y}_f + k_{m,yy}\dot{y}_f^2)] \\ + g_m[\epsilon_2 - \omega_1\omega_3 - (k_{m,xx}\dot{x}_f^2 + 2k_{m,xy}\dot{x}_f\dot{y}_f + k_{m,yx}\dot{y}_f^2)]\} + \dot{v}_2 + \dot{x}_m\omega_3. \quad (4.44)$$

By taking the limit in (2.14)-(2.16), the components of the acceleration of the moving point are, respectively,

$$\ddot{p}_x = \dot{v}_1 - \frac{\omega_3}{K_m}(k_{m,x}\omega_1 + g_m\omega_2), \quad (4.45)$$

$$\ddot{p}_y = \dot{v}_2 - \frac{\omega_3}{K_m}(g_m\omega_1 + k_{m,y}\omega_2), \quad (4.46)$$

$$\ddot{p}_z = \frac{1}{K_m}(k_{m,x}\omega_1^2 + 2g_m\omega_1\omega_2 + k_{m,y}\omega_2^2). \quad (4.47)$$

Comparing (45)-(47) with (36)-(38), we see that whenever one contact surface is a plane, the angular velocity becomes a more dominant part of the contact acceleration (as compared to the case of contacting between two convex surfaces).

3.5 Planning spatial motion with point contact

The independent motion variables which appear in the general relationships, and their special cases developed in the previous sections can be determined from a preplanned path for the contact. In the following paragraphs we discuss the calculations needed to determine the motion variables.

Contact speed planning

Assuming we know the desired contact trajectory $\mathbf{r}(s_f)$ on the fixed surface, where s_f is the arc-length variable, then the derivatives of $\mathbf{r}(s_f)$ with respect to s_f can be expressed in terms of the unit tangent \mathbf{t} , principal normal \mathbf{n} , and bi-normal \mathbf{b} , as well as the curvature κ , its derivative with respect to s_f , κ' , and the torsion τ . It is well known that

$$\mathbf{r}' = \mathbf{t}, \quad \mathbf{r}'' = \kappa\mathbf{n}, \quad \mathbf{r}''' = \kappa'\mathbf{n} + \kappa(\tau\mathbf{b} - \kappa\mathbf{t}). \quad (5.1)$$

If we pick the x-axis so that it is aligned with \mathbf{t} , then the components t_2 , t_3 , n_1 and b_1 vanish. Now if we know the desired speed along the contact trajectory, we know \dot{s}_f , hence we have the time-based derivatives of $\mathbf{r}(s_f)$ from the relationship $\dot{\mathbf{r}} = \mathbf{r}'\dot{s}_f$. The tangential contact velocity, acceleration and jerk are, respectively,

$$\dot{x}_f = \dot{s}_f, \quad \dot{y}_f = 0, \quad (5.2)$$

$$\ddot{x}_f = \ddot{s}_f, \quad \ddot{y}_f = \kappa\dot{s}_f^2 n_2, \quad (5.3)$$

$$x_f^{(3)} = -\kappa^2\dot{s}_f^3 + \dot{s}_f^{(3)}, \quad y_f^{(3)} = \dot{s}_f^3(\kappa'n_2 + \kappa\tau b_2) + 3\kappa n_2\dot{s}_f\ddot{s}_f. \quad (5.4)$$

One interesting case is that of constant contact speed where we have the requirement $\dot{s}_f(t) = \dot{s}_f(0)$, or

$$\ddot{s}_f = \dot{s}_f^{(3)} = \dots = \dot{s}_f^{(n)} = 0. \quad (5.5)$$

Substituting (5) into (3) and (4), the tangential acceleration and jerk under constant contact speed are, respectively,

$$\ddot{x}_f = 0, \quad \ddot{y}_f = \kappa \dot{s}_f^2 n_2. \quad (5.6)$$

$$x_f^{(3)} = -\kappa^2 \dot{s}_f^{(3)}, \quad y_f^{(3)} = \dot{s}_f^3 (\kappa' n_2 + \kappa \tau b_2). \quad (5.7)$$

The z_f component of \mathbf{r}'' is equal to $-k_{f,x}$. From (1) we can derive

$$\kappa = -\frac{k_x}{n_3} = -\frac{k_x}{\cos \phi}, \quad (5.8)$$

where ϕ is the angle between the principal normal of the curve and the surface normal.

When the contact trajectory is a geodesic curve, the curve's principal normal is coincident with the surface normal, hence $n_2 = 0$, and

$$\ddot{y}_f = 0, \quad y_f^{(3)} = \pm \dot{s}_f^3 k \tau. \quad (5.9)$$

The positive sign is used here for contact between convex surfaces.

If we instead use preplanning of the contact speed with respect to the moving surface, the relationships will be similar to the above except that we replace f by m .

Sliding speed planning with respect to the fixed surface

In practice it is hard to specify the sliding velocity trajectory, however, sometimes we do have constraints on the sliding speed, such as constant sliding speed, which can be combined with other constraints to determine the path.

The magnitude of the sliding speed with respect to the fixed surface is $v(t) = (v_1^2 + v_2^2 + v_3^2)^{\frac{1}{2}}$. Taking its derivatives we have constraints which relate the two

tangential components of the sliding velocity, and similarly for the acceleration and higher derivatives.

In addition to preplanning the contact path, there is also the possibility of preplanning the relative rotations. The rotation "path" planned with respect to the fixed frame requires us to specify the angular velocity and angular acceleration directly. We consider one interesting case in the following.

Orientation fixed with respect to the contact frame

The contact frame here is defined to have its x and z axes respectively coincident with the unit contact velocity tangent \mathbf{t} and the surface normal \mathbf{n} . We consider the rate of change of the unit tangent. From the contact trajectory $\dot{\mathbf{t}} = \mathbf{t}'\dot{s}_f = \dot{s}_f\kappa\mathbf{n}$, and from the motion of the body $\dot{\mathbf{t}} = [0, \omega_3, -\omega_2]^T$, by equivalence

$$\omega_2 = -\dot{s}_f\kappa n_3, \quad (5.10)$$

$$\omega_3 = \dot{s}_f\kappa n_2. \quad (5.11)$$

We consider the motion of the unit surface normal. Substituting \dot{x}_m and \dot{y}_m to be zero in (1.8) and (1.10),

$$\omega_1 = -g_f\dot{s}_f, \quad (5.12)$$

$$\omega_2 = k_{f,x}\dot{s}_f. \quad (5.13)$$

We equate (10) and (13), $k_{f,x} = -\kappa n_3$, which is the same as (8). For a geodesic curve, we have (on a convex surface)

$$k_{f,x} = \kappa, \quad \omega_2 = \dot{s}_f\kappa, \quad \omega_3 = 0. \quad (5.14)$$

The required angular acceleration can be determined in a similar way. We first consider the acceleration of the unit tangent. From the contact trajectory,

$$\frac{d^2\mathbf{t}}{dt^2} = \ddot{s}_f\kappa\mathbf{n} + \kappa'\dot{s}_f^2\mathbf{n} + \dot{s}_f^2\kappa\mathbf{n}', \quad \text{where } \mathbf{n}' = -\kappa\mathbf{t} + \tau\mathbf{b},$$

and from the motion of the body ,

$$\frac{d^2 t}{dt^2} = [-(\omega_2^2 + \omega_3^2), \epsilon_3 + \omega_1 \omega_2, -\epsilon_2 + \omega_1 \omega_3]^T.$$

By equivalence,

$$-\omega_2^2 - \omega_3^2 = -\kappa^2 \dot{s}_f^2, \quad (5.15)$$

$$-\epsilon_2 + \omega_1 \omega_3 = (\kappa' \dot{s}_f^2 + \ddot{s}_f \kappa) n_3 + \dot{s}_f^2 \kappa \tau b_3, \quad (5.16)$$

$$\epsilon_3 + \omega_1 \omega_2 = (\kappa' \dot{s}_f^2 + \ddot{s}_f \kappa) n_2 + \kappa \dot{s}_f^2 \tau b_2. \quad (5.17)$$

We then consider the acceleration of the unit surface normal. Substituting the null contact velocity and acceleration with respect to the moving frame into (1.9) and (1.11), we have

$$\epsilon_1 = -(k_{f,xy} \dot{s}_f^2 + g_f \ddot{x}_f + k_{f,y} \ddot{y}_f) + \omega_2 \omega_3, \quad (5.18)$$

$$\epsilon_2 = k_{f,xx} \dot{s}_f^2 + k_{f,x} \ddot{x}_f + g_f \ddot{y}_f + \omega_1 \omega_3. \quad (5.19)$$

From (11) and (13), (15) is automatically satisfied, and from (16) and (19), we have the constraint

$$k_{f,xx} \dot{s}_f^2 + k_{f,x} \ddot{x}_f + g_f \ddot{y}_f - \omega_2 \omega_3 = \omega_1 \omega_3 - (\kappa' \dot{s}_f^2 + \ddot{s}_f \kappa) n_3 - \kappa \tau \dot{s}_f^2 b_3.$$

When the moving body has fixed orientation with respect to the contact frame, the angular velocity and acceleration are functions of the contact speed and its rate of change with respect to the fixed frame.

Motion planning of a finger's spatial motion

In Section 2.5 we have given an example of the planning of the planar motion of a two-degrees-of-freedom finger of a robot hand. By using Appendix E, and the types of relative motion planning explained earlier in this section, we can easily extend the procedure of Section 2.5 to plan the spatial motion under point contact of a finger with three or more controllable degrees of freedom.

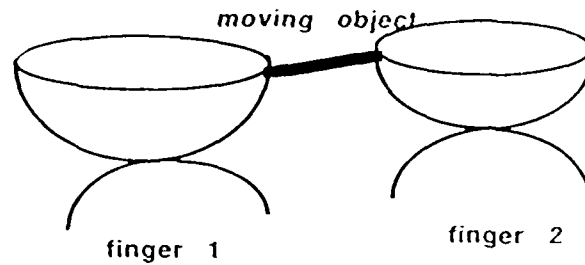


Figure 3.8 Two point contact between surfaces

3.6 Two or three point contacts between surfaces

Except for the special motions (pure rolling or pure sliding), the information from one tactile sensor can not completely determine the motion of the moving body. In this section we shall show that with two points of contact, each with a tactile sensor, we can in general (except for some special geometries) completely determine the angular velocity and sliding velocity, and their derivatives.

We now assume that the moving body is composed of two or more rigidly connected surfaces, each of which continuous and differentiable in the neighborhood of the point of contact (Fig. 3.8).

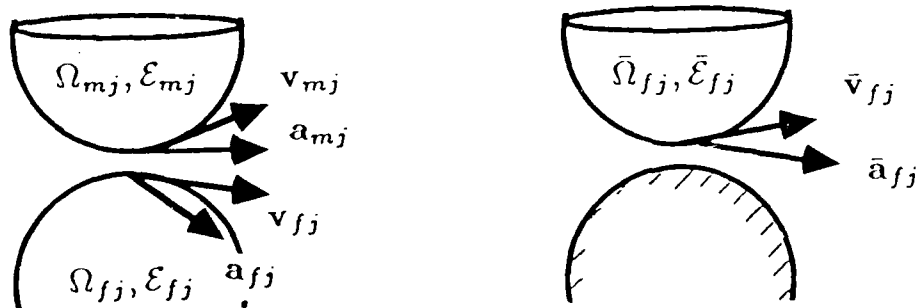


Figure 3.9 Motion variables for multiple contacts

We replace the fixed surfaces by two fingers of a robot hand, each one in motion. We label the two contacts as point 1 and point 2. Associated with them, V_{n_j} ,

Ω_{mj} , a_{mj} and \mathcal{E}_{mj} are respectively the velocity of the j^{th} moving point, the angular velocity of the moving body relative to ground (expressed in the j^{th} reference frame), and their rates of change (Fig. 3.9(a)); V_{fj} , Ω_{fj} , \mathbf{a}_{fj} and \mathcal{E}_{fj} are the same variables for the motion of the point of contact on the surface of the j^{th} finger and the motion of the j^{th} finger (Fig. 3.9(a)); \bar{V}_j , $\bar{\Omega}_j$, $\bar{\mathbf{a}}_j$ and $\bar{\mathcal{E}}_j$ characterize the relative motion for the moving point and the moving body relative to the j^{th} finger (Fig. 3.9(b)); \dot{x}_{fj} , \dot{y}_{fj} , \ddot{x}_{fj} and \ddot{y}_{fj} are the tangential contact velocity and acceleration at the j^{th} point of contact. For a geometric variable, we add the subscript j to indicate that it is associated with the j^{th} point of contact.

Calculating the angular velocity from two contacts

For two points in the moving rigid body we have

$$V_{m2} = R[V_{m1} + \Omega_{m1} \times \mathbf{r}], \quad (6.1)$$

or

$$V_{m2} = RV_{m1} + RL\Omega_{m1}. \quad (6.2)$$

Here, \mathbf{r} is a position vector to the second point of contact measured in the first reference frame, R is a rotation matrix which transforms the coordinates in the first reference frame to those in the second reference frame, and

$$L = \begin{pmatrix} 0 & r_3 & -r_2 \\ -r_3 & 0 & r_1 \\ r_2 & -r_1 & 0 \end{pmatrix}.$$

In order to solve for the angular velocity, we need to know V_{m2} , V_{m1} . From (2.3), (2.4), Appendix E (E1) and (E3) we have,

$$\begin{aligned} K_j \dot{x}_{fj} = & G_j(\omega_{mj,1} - \omega_{fj,1}) + K_{j,y}(\omega_{mj,2} - \omega_{fj,2}) + (v_{mj,1} - v_{fj,1}) \\ & \times (K_{j,y}k_{mj,x} - G_j g_{mj}) + (v_{mj,2} - v_{fj,2})(K_{j,y}g_{mj} - G_j k_{mj,y}), \end{aligned} \quad (6.3)$$

$$\begin{aligned} K_j \dot{y}_{fj} = & -K_{j,x}(\omega_{mj,1} - \omega_{fj,1}) - G_j(\omega_{mj,2} - \omega_{fj,2}) + (v_{mj,1} - v_{fj,1}) \\ & \times (K_{j,x}g_{mj} - G_j k_{mj,x}) + (v_{mj,2} - v_{fj,2})(K_{j,x}k_{mj,y} - G_j g_{mj}). \end{aligned} \quad (6.4)$$

Solving these equations for $v_{mj,1}$ and $v_{mj,2}$, and obtaining $v_{mj,3}$ from (E3), we have the matrix expression

$$V_{mj} = A(j)\Omega + B(j), \quad (6.5)$$

$$A(j) = \frac{1}{K_{mj}} \begin{pmatrix} -g_{mj} & -k_{mj,y} & 0 \\ k_{mj,x} & g_{mj} & 0 \\ 0 & 0 & 0 \end{pmatrix}, \quad (6.6)$$

$$B(j) = \begin{pmatrix} v_{fj,1} + \frac{1}{K_{mj}} [(K_{j,x}k_{mj,y} - G_jg_{mj})\dot{x}_{fj} + (G_jk_{mj,y} - K_{j,y}g_{mj})\dot{y}_{fj}] \\ v_{fj,2} + \frac{1}{K_{mj}} [(K_{j,y}k_{mj,x} - G_jg_{mj})\dot{y}_{fj} - (K_{j,x}g_{mj} - G_jk_{mj,x})\dot{x}_{fj}] \\ v_{fj,3} \\ +g_{mj}\omega_{fj,1} + k_{mj,y}\omega_{fj,2} \\ -g_{mj}\omega_{fj,2} - k_{mj,x}\omega_{fj,1} \\ 0 \end{pmatrix}, \quad (6.7)$$

where K_{mj} is the Gaussian curvature of the moving surface at contact j .

Substituting (5) (with $i = 1, 2$) into (2),

$$A(2)\Omega_{m2} + B(2) = R[A(1)\Omega_{m1} + B(1)] + RL\Omega_{m1},$$

and from $\Omega_{m2} = R\Omega_{m1}$ we have

$$\Omega_{m1} = [A(2)R - RA(1) - RL]^{-1}[RB(1) - B(2)]. \quad (6.8)$$

Equation (8) can be used to calculate the angular velocity of the moving body from the readings of two contact sensors.

Calculating the angular acceleration from two contacts

For the two contact points in the same rigid moving body we have

$$\mathbf{a}_{m2} = R[\mathbf{a}_{m1} + \boldsymbol{\varepsilon} \times \mathbf{r} + \Omega \times (\Omega \times \mathbf{r})], \quad (6.9)$$

or

$$\mathbf{a}_{m2} = R(\mathbf{a}_{m1} + L\boldsymbol{\varepsilon}_{m1} + C), \quad (6.10)$$

where

$$C = \begin{pmatrix} \omega_1(\omega_2 r_2 + \omega_3 r_3) - r_1(\omega_2^2 + \omega_3^2) \\ \omega_2(\omega_3 r_3 + \omega_1 r_1) - r_2(\omega_3^2 + \omega_1^2) \\ \omega_3(\omega_1 r_1 + \omega_2 r_2) - r_3(\omega_1^2 + \omega_2^2) \end{pmatrix}$$

In order to solve for the angular acceleration, we need to know \mathbf{a}_{m2} and \mathbf{a}_{m1} . Similar to the previous case solving for $\mathbf{a}_{mj,1}$ and $\mathbf{a}_{mj,2}$ from (2.9), (2.10), (E2) and (E4), and obtaining $\mathbf{a}_{mj,3}$ from (E4), we have

$$\mathbf{a}_{mj} = A(j)\mathcal{E} + D(j), \quad (6.11)$$

$$D(j) = \frac{1}{K_{mj}} \begin{pmatrix} [(K_{j,x}k_{mj,y} - G_j g_{mj})\ddot{x}_{fj} + (G_j k_{mj,y} - K_{j,y}g_{mj})\ddot{y}_{fj} + g_{mj}T_{j2} - k_{mj,y}T_{j1}] \\ [(K_{j,y}k_{mj,x} - G_j g_{mj})\ddot{y}_{fj} - (K_{j,x}g_{mj} - G_j g_{mj})\ddot{x}_{fj} + g_{mj}T_{j1} - k_{mj,x}T_{j2}] \end{pmatrix} +$$

$$\begin{aligned} a_{fj,1} - 2\ddot{v}_{j,2}\omega_{fj,3} + \dot{y}_{mj}\ddot{\omega}_{j,3} + \frac{1}{K_{mj}}[g_{mj}(\epsilon_{fj,1} + \omega_{fj,2}\ddot{\omega}_{j,3} - \omega_{fj,3}\ddot{\omega}_{j,2}) + k_{mj,y}(\epsilon_{fj,2} + \omega_{fj,3}\ddot{\omega}_{j,1} - \omega_{fj,1}\ddot{\omega}_{j,3})] \\ a_{fj,2} + 2\ddot{v}_{j,1}\omega_{fj,3} - \dot{x}_{mj}\ddot{\omega}_{j,3} - \frac{1}{K_{mj}}[k_{mj,x}(\epsilon_{fj,1} + \omega_{fj,2}\ddot{\omega}_{j,3} - \omega_{fj,3}\ddot{\omega}_{j,2}) + g_{mj}(\epsilon_{fj,2} + \omega_{fj,3}\ddot{\omega}_{j,1} - \omega_{fj,1}\ddot{\omega}_{j,3})] \\ a_{fj,3} + \ddot{v}_{j,2}\omega_{fj,1} - \ddot{v}_{j,1}\omega_{fj,2} \end{aligned} \quad (6.12)$$

where

$$\begin{aligned} T_{j1} &= \ddot{\omega}_{j,1}\ddot{\omega}_{j,3} + 2\ddot{\omega}_{j,3}(g_{mj}\dot{x}_{mj} + k_{mj,y}\dot{y}_{mj}) - \sum_i (k_{ij,xx}\dot{x}_i^2 + 2k_{ij,xy}\dot{x}_i\dot{y}_i + k_{ij,yx}\dot{y}_i^2) \\ &\quad - k_{mj,x}\dot{y}_{mj}\ddot{\omega}_{j,3} + g_{mj}\dot{x}_{mj}\ddot{\omega}_{j,3}, \\ T_{j2} &= \ddot{\omega}_{j,2}\ddot{\omega}_{j,3} - 2\ddot{\omega}_{j,3}(k_{mj,x}\dot{x}_{mj} + g_{mj}\dot{y}_{mj}) - \sum_i (\dot{k}_{ij,xy}\dot{x}_i^2 + 2k_{ij,yx}\dot{x}_i\dot{y}_i + k_{ij,yy}\dot{y}_i^2) \\ &\quad - g_{mj}\ddot{\omega}_{j,3}\dot{y}_{mj} + k_{mj,y}\dot{x}_{mj}\ddot{\omega}_{j,3}. \end{aligned}$$

Here the summation is over m and f .

Substituting (11) (with $j = 1, 2$) into (10), we have

$$A(2)\mathcal{E}_{m2} + D(2) = R[A(1)\mathcal{E}_{m1} + D(1)] + RL\mathcal{E}_{m1} + RC.$$

From $\mathcal{E}_{m2} = R\mathcal{E}_{m1}$, we have

$$\mathcal{E}_{m1} = [A(2)R - RA(1) - RL]^{-1}[RD(1) + RC - D(2)]. \quad (6.13)$$

Equation (13) can be used to calculate the angular acceleration of the moving body from the contact accelerations at the two point contacts.

Moving body is two or three spheres

When the moving surface is a sphere, $A(j)$ is an anti-symmetric matrix. In the general formulas (8) and (13), we can rewrite the matrix as

$$[A(2)R - RA(1) - RL] = R[R^{-1}A(2)R - A(1) - L].$$

Since L is also an anti-symmetric matrix, $[R^{-1}A(2)R - A(1) - L]$ is anti-symmetric, hence a singular matrix. The general formulas (8) and (13) can not be applied.

In order to determine the moving body's angular velocity from tactile sensor readings it becomes necessary to add a third finger. If the finger is such that the third surface is also a sphere, applying (2) and (5) for the second and third contacts, and adding the resulting equations, we have

$$\Omega_{m1} = \left[\sum_{j=2}^3 (A(j)R_{1j} - R_{1j}L_{1j} - R_{1j}A(1)) \right]^{-1} [(R_{12} + R_{13})B(1) - B(2) - B(3)]. \quad (6.14)$$

Similarly applying (10) and (11) repeatedly for the second and third contacts, and adding the resulting equations, we have

$$\varepsilon_{m1} = \left[\sum_{j=2}^3 (A(j)R_{1j} - R_{1j}L_{1j} - R_{1j}A(1)) \right]^{-1} \sum_{j=2}^3 [R_{1j}D(1) + R_{1j}C_{1j} - D(j)]. \quad (6.15)$$

A point and a plane are two extreme cases of a sphere. When the moving body's contact surfaces reduce to two planes, or two points, or one plane and one point, we need three contacts to determine the motion.

However, when the moving body's contact surface reduces to one sphere, there may be an unobservable slipping mode. This is because the sphere can always rotate about its center without being affected by its supports. As an extreme case, when the moving body reduces to one plane the same observation pertains.

Approximate integration for position

If we can assume that in a small time interval, the geometry is invariant, we can

approximate the position by the differential form of (8)

$$\Phi = [A(2)R - RA(1) - RL]^{-1}[RB^*(1) - B^*(2)]. \quad (6.16)$$

where Φ is a vector whose components are the three infinitesimal incremental angles the moving body has successively rotated about the x, y and z axes, $\Phi = (\delta\theta_1, \delta\theta_2, \delta\theta_3)$. From these angles one can make a rotation matrix $R(\delta\theta_1, \delta\theta_2, \delta\theta_3)$. The $B^*(j)$, $j = 1, 2$, are similar to B in (7), except the velocity terms are replaced by the infinitesimal rotation angles.

This completes our discussion of point contact between surfaces. In the next chapter we study surfaces moving under line contact.

Chapter 4

SPATIAL MOTION WITH LINE CONTACT

It is a classical result that any instantaneous spatial motion of a rigid body can be represented as a moving axode in line contact with a fixed axode along the instantaneous screw axis of the motion [Bottema and Roth, '79]. However, for rigid body motions with line contact *between two ruled surfaces*, the surfaces are not necessarily the axodes, and the contact line is not necessarily the screw axis. A simple example is the line contact between a finger of a robot hand, with a (circular) cylindrical shape, and a (circular) cone while the two are in relative motion.

Here, we derive the equations which govern the kinematics of the contact between ruled surfaces. We are interested in knowing the velocity, acceleration and jerk of a reference point on the moving body, the angular velocity and angular acceleration components, which are perpendicular to the contact line of the moving body, and the contact speeds and their rates of change on the reference curves for maintaining line contact. In particular, we are interested in obtaining the relationships between these quantities and the parameters which define the moving body's motion at the contact line.

Following a similar route to the one taken for point contact, in this chapter we first analyze the basic constraints associated with line contact, then obtain the motion properties and their variations under special geometries. These properties are further extended for two-line contact.

Besides the general line contact motions, which are called roll-slide motions, we discuss three types of special motions: 1) there is no rotation about the line of contact; 2) there is no sliding perpendicular to the line of contact at one point, which can be assumed to be the reference point; 3) there is no sliding along the contact line. If both ruled surfaces in contact are cylindrical surfaces and the last condition is satisfied, the first two special motions become, respectively, 1) pure translation and 2) pure rotation about the instantaneous line of contact.

4.1 Constraints on line contact

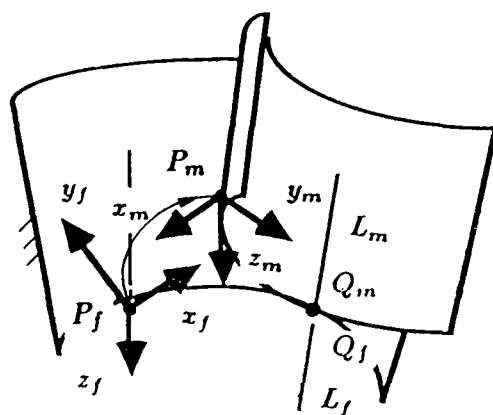


Figure 4.1 Arbitrary position of a moving surface in line contact

In this section, we specify a contact model, then consider the basic constraints on the contact normal, contact line, contact trajectories, moving point, and special motions.

The contact model is illustrated in Fig. 4.1. To be practical and for simplicity, we exclude skew ruled surfaces, and consider only developable ruled surfaces, i.e., ruled surfaces whose consecutive generators intersect each other. The moving ruled surface is labeled as m , and the fixed ruled surface as f . The contact is between a fixed line and a moving line. A point P_m on the initial moving line is designated as the moving point, and its trajectory the moving point trajectory.

Symmetrically, a fixed point P_f , which is coincident with P_m in the initial instant, is designated as the fixed point and used for reference purposes.

We imagine a pair of unit vectors L_m and L_f , with their tails at a fixed origin, which do not belong to either body and are always parallel to the current position of the instantaneous contact line of the moving and fixed ruled surfaces, respectively. As the contact changes, the vectors L_m and L_f trace cones of unit length. Associated with each contact line, we specify a pair of points, Q_m and Q_f , which as we move from contact line to contact line trace spatial curves on the ruled surfaces. The points are coincident with P_m in the initial position. When viewed from the moving and fixed surface, the trajectories of Q_m and Q_f (the curves) and those of L_m and L_f (unit length cones) characterize the contacting ruled surfaces (Fig. 4.1).

We define the moving frame and the fixed frame so that they are coincident with each other in the initial instant: the points P_m and P_f are used as the frame origins; the z axes (z_m and z_f) are along the coinciding lines of contact; the y axes (y_m and y_f) are along the common surface normal (directed in toward the moving surface); and the x axes (x_m and x_f) are in the common tangential plane and perpendicular to the line of contact. Below, when we specify the motion components with respect to these axes we use the subscripts L, N, T , which represent the direction of the line of contact, surface normal and orthogonal tangent, respectively.

We denote the trajectories of Q_m and Q_f by the variables \mathbf{r}_m and \mathbf{r}_f (the position vectors), respectively. A moving ruled surface can be represented by

$$R_m = \mathbf{r}_m + d_m L_m, \quad (1.1)$$

and a fixed ruled surface can be represented by

$$R_f = \mathbf{r}_f + d_f L_f. \quad (1.2)$$

R_m and R_f are the position vectors for generic points on the ruled surfaces, and d_m and d_f are the distances measured from \mathbf{r}_m and \mathbf{r}_f to the specified

points along the corresponding rulings. To simplify our derivation, we assume the tangents to the curves, denoted by all values of \mathbf{r}_m and \mathbf{r}_f , are perpendicular to the corresponding rulings at each instant. (In Appendix D we show that such curves and their corresponding \mathbf{r}_m and \mathbf{r}_f , are easily obtainable from an arbitrary representation of a ruled surface).

We will use the subscript i whenever either m or f can be used. This convention implies that the same quantity must be used throughout the entire equation.

Constraints on contact normal

A unit vector, which is parallel to the inwardly directed normal of the moving surface or the outwardly directed normal of the fixed surface, can be expressed as:

$$N_i = \frac{\partial R_i}{\partial d_i} \times \frac{\partial R_i}{\partial s_i} = L_i \times (\mathbf{r}_i' + d_i L_i') / |L_i \times (\mathbf{r}_i' + d_i L_i')|.$$

The unit surface normals along the same generator of a developable ruled surface are all parallel, i.e., they are independent of d_i . Hence, L_i' must be a linear combination of L_i and \mathbf{r}_i' , and the expression for N_i can be simplified to

$$N_m = L_m \times \mathbf{r}' / |L_m \times \mathbf{r}'|, \quad (1.3)$$

$$N_f = L_f \times \mathbf{r}' / |L_f \times \mathbf{r}'|. \quad (1.4)$$

In order to maintain line contact, the inwardly directed surface normal associated with L_m and the outwardly directed surface normal associated with L_f must be coincident. Thus we require that

$$N_f = R N_m, \quad (1.5)$$

where $R(t)$ is a 3×3 rotation matrix which transforms the coordinates of the moving system to their values in the fixed system; the derivatives of $R(t)$ have been analyzed in [Bottema and Roth, '79] (on p. 22).

On the other hand, from differential geometry, the derivatives of a spatial curve with respect to its arc length satisfy the relationships:

$$\mathbf{r}' = \mathbf{t}, \quad \mathbf{r}'' = \kappa \mathbf{n}, \quad \mathbf{r}''' = \kappa \tau \mathbf{b} - \kappa^2 \mathbf{t} + \kappa' \mathbf{n},$$

where κ is the curvature and τ the torsion of the curve, and $\mathbf{t}, \mathbf{n}, \mathbf{b}$ are the unit vectors along the tangent, normal and bi-normal directions, respectively. For simplicity, we define $n_{iN} = \mathbf{n}_i \cdot \mathbf{N}$, $n_{iL} = \mathbf{n}_i \cdot \mathbf{L}$, $b_{iN} = \mathbf{b}_i \cdot \mathbf{N}$, $b_{iL} = \mathbf{b}_i \cdot \mathbf{L}$, the angular velocity of the moving body $\Omega = [\omega_T \ \omega_N \ \omega_L]^T$, and the body's angular acceleration vector $\mathcal{E} = [\epsilon_T \ \epsilon_N \ \epsilon_L]^T$.

Now we can obtain the first order and the second order constraints on the contact normals. Substituting (3) and (4) into (5), and using the above curve kinematics, the first order constraints on the contact normal are:

$$\omega_T = 0, \quad \omega_L = \kappa_f n_{fN} \dot{s}_f - \kappa_m n_{mN} \dot{s}_m, \quad (1.6)$$

where \dot{s}_m, \dot{s}_f are the contact speeds along \mathbf{r}_m and \mathbf{r}_f , respectively. Similarly, the second order constraints on the contact normal are:

$$\epsilon_T = -\omega_L \omega_N - 2\omega_N \kappa_m n_{mN} \dot{s}_m + 2\dot{L}_{fT} \kappa_f n_{fN} \dot{s}_f - \ddot{L}_{fN} - 2\dot{L}_{mT} \kappa_m n_{mN} \dot{s}_m + \ddot{L}_{mN}, \quad (1.7)$$

$$\epsilon_L = -\kappa_m n_{mN} \ddot{s}_m - (\kappa_m \tau_m b_{mN} + \kappa'_m n_{mN}) \dot{s}_m^2 + \kappa_f n_{fN} \ddot{s}_f + (\kappa_f \tau_f b_{fN} + \kappa'_f n_{fN}) \dot{s}_f^2. \quad (1.8)$$

The dots denote the time derivatives, and we have used the conventions that $\dot{L}_{iT} = \dot{L}_i \cdot \mathbf{T}$, $\ddot{L}_{iT} = \ddot{L}_i \cdot \mathbf{T}$, $\ddot{L}_{iN} = \ddot{L}_i \cdot \mathbf{N}$ and $\ddot{L}_{iL} = \ddot{L}_i \cdot \mathbf{L}$. The normal component of the derivative equation from (5) does not provide new information, since we have the constraints $N_i^T N_i = 1$.

Constraints on contact line

To maintain line contact, the unit vectors parallel to the contacting moving ruling and contacting fixed ruling at each instant must be parallel to each other, therefore

$$L_f = R(t)L_m. \quad (1.9)$$

Taking the first two derivatives, we obtain the conditions for the normal angular velocity and angular acceleration to maintain line contact:

$$\omega_N = \dot{L}_{fT} - \dot{L}_{mT}; \quad (1.10)$$

$$\epsilon_N = \ddot{L}_{fT} - \ddot{L}_{mT}. \quad (1.11)$$

The rest of the components of the constraint equations from the derivatives of (9) are consistent with those contact normal constraints.

From spherical differential geometry, it is known that the derivatives of L , with respect to the arc length of the spherical curve, are related to the geodesic curvature, γ_s , of the spherical curve:

$$L' = \bar{T}, \quad \bar{T}' = \gamma_s G - L, \quad G' = -\gamma_s \bar{T}, \quad (1.12)$$

where L, \bar{T} and G are three perpendicular unit vectors. From our previous analysis, we know that $\partial L_i / \partial s_i$ is a linear combination of L_i and \mathbf{r}'_i (or T), and from the relation $L^T L = 1$, we conclude that \dot{L} is parallel to T . Hence, in (12) \bar{T} is parallel to T , and G is parallel to the surface normal N . Thus,

$$L' = T, \quad L'' = \gamma_s N - L.$$

For the time-based derivatives, there exists the relation $dL/dt = (dL/d\alpha_s) \cdot (d\alpha_s/dt)$, or

$$\dot{L} = L' \dot{\alpha}_s, \quad \ddot{L} = L'' \dot{\alpha}_s^2 + L' \ddot{\alpha}_s, \quad (1.13)$$

where α_s designates the spherical arc length.

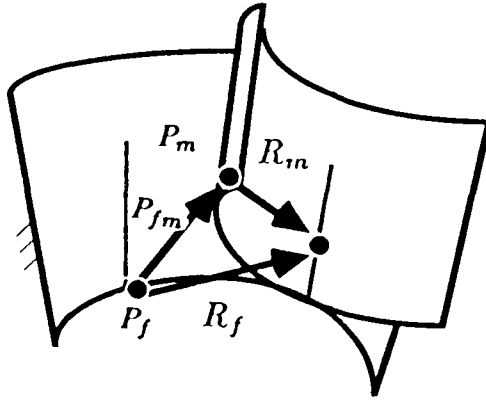


Figure 4.2 Contact trajectories on ruled surfaces

Constraints on contact trajectories

The need for contact constrains the points on the contact trajectories; this provides the relationship between R_m in (1) and R_f in (2), and the relationship leads to the introduction of a quantity we call the sliding velocity.

We let R_m in (1) represent the trajectory of Q_m by taking $d_m = 0$, and let R_f in (2) traces the locus of Q_m in the fixed space, then from Fig. 4.2:

$$R_f = P_{fm} + R(t)R_m, \quad (1.14)$$

where P_{fm} is the position vector for the moving point P_m . The first order time derivative of (14) is

$$\dot{R}_f = [\dot{P}_{fm} + \dot{R}(t)R_m] + R(t)\dot{R}_m. \quad (1.15)$$

As in the previous two chapters, the content of the first square bracket is a general expression for the sliding velocity at Q_m , and the introduction of sliding velocity is meaningful to the application. By Taylor series expansion, the sliding velocity can be expressed as

$$V(t) = V(0) + \dot{V}(0)t + \dots$$

Using this notation, we can write the n^{th} order time derivative of (15) as

$$\dot{R}_f^{(n)} = V^{(n)} + [R(t)\dot{R}_m]^n. \quad (1.16)$$

Taking $n = 0$ in equation (16), we have

$$v_T = \dot{s}_f - \dot{s}_m, \quad v_L = \dot{d}_f, \quad v_N = 0. \quad (1.17)$$

When $n = 1$ we have

$$\dot{v}_T = \ddot{s}_f - \ddot{s}_m + 2\dot{d}_f\dot{L}_f, \quad (1.18)$$

$$\dot{v}_L = \kappa_f n_{fL} \dot{s}_f^2 - \kappa_m n_{mL} \dot{s}_m^2 + \ddot{d}_f + \omega_N \dot{s}_m, \quad (1.19)$$

$$\dot{v}_N = \kappa_f n_{fN} \dot{s}_f^2 - \kappa_m n_{mN} \dot{s}_m^2 - \omega_L \dot{s}_m. \quad (1.20)$$

For the n^{th} order moving point's kinematics, we have from (15),

$$P_{fm}^{(n+1)} = V^{(n)} - [\dot{R}(t)R_m]^{(n)}. \quad (1.21)$$

Constraints on special motions

We now look at the special motions up to second order.

When there is no rotation about the line of contact, we have

$$\Omega \cdot L = 0 \quad (1.22)$$

Taking the first two derivatives, and solving for the angular velocity and angular acceleration about the line of contact, we have

$$\omega_L = 0, \quad \epsilon_L = 0. \quad (1.23)$$

When there is no sliding velocity perpendicular to the line of contact at the reference point, we have

$$V - (V \cdot L)L = 0. \quad (1.24)$$

Taking the first two derivatives and solving for the sliding velocity and acceleration which is along T , we have

$$v_T = 0, \quad \dot{v}_T = v_L \dot{L}_T. \quad (1.25)$$

When there is no sliding along the line of contact, we have

$$\mathbf{v} \cdot L = 0. \quad (1.26)$$

This and its derivative yield

$$v_L = 0, \quad \dot{v}_L = -v_T \dot{L}_T. \quad (1.27)$$

AD-A190 709

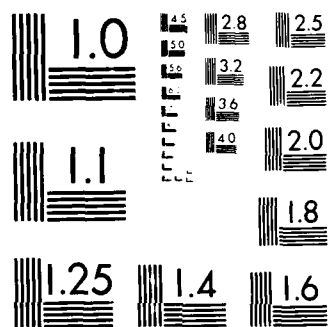
INSTANTANEOUS ROBOT MOTION WITH CONTACT BETWEEN
SURFACES(U) STANFORD UNIV CA DEPT OF COMPUTER SCIENCE
C CRI JAN 88 STAN-CS-88-1191 NDA903-86-K-0002

2/2

UNCLASSIFIED

F/G 12/9

44



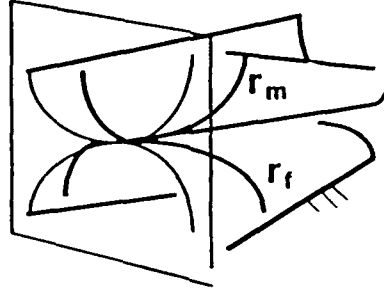


Figure 4.3 Projectional curves

4.2 Motion properties for line contact

From the constraint relationships, in this section we derive the first and second order contact speeds along the reference curves, and the first, second and third order motion derivatives of the moving reference point; these results are expressed as functions of sliding at the reference point and the rotation about the line of contact. We also illustrate how to plan for line contact motions which maintain a desired contact trajectory.

We define

$$K = \kappa_m n_{mN} - \kappa_f n_{fN}.$$

$\kappa_m n_{mN}$ and $-\kappa_f n_{fN}$ are the curvatures of the curves obtained when \mathbf{r}_m and \mathbf{r}_f are projected onto a plane perpendicular to the line of contact (Fig. 4.3). Up to second order, \mathbf{r}_m and \mathbf{r}_f can be replaced by circles with curvature κ_m and κ_f , and principal normals \mathbf{n}_m and \mathbf{n}_f , respectively. The projection of these two circles onto a plane which is perpendicular to the line of contact, is two ellipses in contact, and their curvatures at contact are $\kappa_m n_{mN}$ and $-\kappa_f n_{fN}$, respectively. When two convex projected curves (curves bent in opposite directions) are in contact, K is always positive since by our coordinate convention only n_{fN} is negative.

The speeds of Q_m and Q_f , \dot{s}_m and \dot{s}_f , are obtainable from (1.6) and (1.10):

$$\dot{s}_m = -\frac{1}{K}[\omega_L - \kappa_f n_{fN} v_T], \quad (2.1)$$

$$\dot{s}_f = -\frac{1}{K}[\omega_L - \kappa_m n_{mN} v_T]. \quad (2.2)$$

Independent of v_L , \dot{s}_m and \dot{s}_f are proportional to the angular velocity about the contact line and the sliding velocity perpendicular to the contact line at the reference point. This result is exactly the same as if the motion were constrained by point contact of the two projected curves. These relations are useful for path planning and sensing purposes.

When there is no sliding perpendicular to the contact line at the moving point,

$$\dot{s}_m = \dot{s}_f = -\frac{1}{K}\omega_L. \quad (2.3)$$

In words, \dot{s}_m and \dot{s}_f are equal to the negative of the ratio of ω_L and the sum of the curvatures of the projected curves. If we can calculate \dot{s}_m or \dot{s}_f from a tactile sensor reading, we can determine ω_L from (3), assuming we know the surface geometry and position of contact.

When there is no rotation about the contact line,

$$\dot{s}_m = \frac{1}{K}\kappa_f n_{fN} v_T, \quad \dot{s}_f = -\frac{1}{K}\kappa_m n_{mN} v_T. \quad (2.4)$$

When the ratio of the curvature of the projected moving curve to that of the projected fixed curve is very small, \dot{s}_m is approximately equal to v_T , \dot{s}_f is approximately proportional to this ratio, and vice versa.

The moving point's velocity is equal to the sliding velocity if we take $n = 0$ in (1.21):

$$\dot{p}_T = v_T, \quad \dot{p}_L = v_L, \quad \dot{p}_N = 0. \quad (2.5)$$

No matter whether v_T vanishes or not, there is usually sliding perpendicular to the line of contact for a generic point on the line of contact, and the sliding velocity has a linear distribution along the line. When both spherical image curves (see foot note on p. 6), of L_m and L_f , advance at the same speed, from (1.12) and (1.13) the normal angular velocity vanishes, and the sliding velocity is the same (it can be zero) for every point on the contact line. On the other

hand, the normal velocity v_N vanishes at every point on the contact line since $\omega_T = 0$. This property can be useful in searching for the contact line (provided the geometry and motion of the moving rigid body are given). The velocity component along the contact line v_L is the same for every point on the line. If a point of the contact line is in the sensing range of a tactile sensor, we can determine v_L .

The rates of change of the contact speeds on the curves \mathbf{r}_m and \mathbf{r}_f are obtainable from (1.8) and (1.19):

$$\ddot{s}_m = -\frac{1}{K}[\epsilon_L - \kappa_f n_{fN} \dot{v}_T + 2\kappa_f n_{fN} \dot{L}_{fT} v_L + (\kappa_m \tau_m b_{mN} + \kappa'_m n_{mN}) \dot{s}_m^2 - (\kappa_f \tau_f b_{fN} + \kappa'_f n_{fN}) \dot{s}_f^2]; \quad (2.6)$$

$$\ddot{s}_f = -\frac{1}{K}[\epsilon_L - \kappa_m n_{mN} \dot{v}_T + 2\kappa_m n_{mN} \dot{L}_{fT} v_L + (\kappa_m \tau_m b_{mN} + \kappa'_m n_{mN}) \dot{s}_m^2 - (\kappa_f \tau_f b_{fN} + \kappa'_f n_{fN}) \dot{s}_f^2]. \quad (2.7)$$

When the first order motion properties are determined, equations (6) and (7) give the relationships between the rates of change of contact speeds on curves \mathbf{r}_m and \mathbf{r}_f , the sliding acceleration component which is perpendicular to both the contact line and contact normal, and the angular acceleration about the line of contact.

When there is no sliding perpendicular to the contact line at the reference point, substituting (1.25) into (6) and (7) yields

$$\ddot{s}_m = -\frac{1}{K}[\epsilon_L + 2\kappa_f n_{fN} \dot{L}_{fT} v_L] + \frac{\omega_L^2}{K^3}[(\kappa_m \tau_m b_{mN} + \kappa'_m n_{mN}) - (\kappa_f \tau_f b_{fN} + \kappa'_f n_{fN})], \quad (2.8)$$

$$\ddot{s}_f = -\frac{1}{K}[\epsilon_L + 2\kappa_m n_{mN} \dot{L}_{fT} v_L] + \frac{\omega_L^2}{K^3}[(\kappa_m \tau_m b_{mN} + \kappa'_m n_{mN}) - (\kappa_f \tau_f b_{fN} + \kappa'_f n_{fN})]. \quad (2.9)$$

The accelerations \ddot{s}_m and \ddot{s}_f are linearly related to ϵ_L . When $v_L = 0$, $\ddot{s}_m = \ddot{s}_f$.

When there is no rotation about the contact line, substituting (1.25) into (6) and (7) yields

$$\ddot{s}_m = -\frac{1}{K}[-\kappa_f n_{fN} \dot{v}_T + 2\kappa_f n_{fN} \dot{L}_{fT} v_L] + [(\kappa_m \tau_m b_{mN} + \kappa'_m n_{mN}) \kappa_f^2 n_{fN}^2 - (\kappa_f \tau_f b_{fN} + \kappa'_f n_{fN}) \kappa_m^2 n_{mN}^2] \frac{v_T^2}{K^3}, \quad (2.10)$$

$$\begin{aligned}\ddot{s}_f = & -\frac{1}{K}[-\kappa_m n_{mN} \dot{v}_T + 2\kappa_m n_{mN} \dot{L}_{fT} v_L] + [(\kappa_m \tau_m b_{mN} + \kappa'_m n_{mN}) \kappa_f^2 n_{fN}^2 \\ & - (\kappa_f \tau_f b_{fN} + \kappa'_f n_{fN}) \kappa_m^2 n_{mN}^2] \frac{v_T^2}{K^3}.\end{aligned}\quad (2.11)$$

The accelerations \ddot{s}_m and \ddot{s}_f are linearly related to \dot{v}_T .

The second order properties of the moving point are obtainable by taking $n = 2$ in (1.21) and substituting the results into (2.1) and (2.2):

$$\ddot{p}_T = \dot{v}_T, \quad (2.12)$$

$$\ddot{p}_L = \dot{v}_L + \frac{1}{K} \omega_N (\omega_L - \kappa_f n_{fN} v_T), \quad (2.13)$$

$$\ddot{p}_N = \frac{1}{K} \omega_N^2 + \frac{1}{K} \kappa_m \kappa_f n_{mN} n_{fN} v_T^2 - \frac{2}{K} \kappa_f n_{fN} \omega_L v_T. \quad (2.14)$$

The normal acceleration is independent of v_L , and is determined from the first order relative motion of the projected moving and fixed curves.

When there is no sliding perpendicular to the contact line at the moving point,

$$\ddot{p}_T = \dot{L}_{fT} v_L, \quad (2.15)$$

$$\ddot{p}_L = \dot{v}_L - \frac{1}{K} \omega_L \omega_N, \quad (2.16)$$

$$\ddot{p}_N = \frac{1}{K} \omega_L^2. \quad (2.17)$$

When either v_L vanishes or $\dot{\alpha}$, vanishes (the spherical image is stationary), \ddot{p}_T vanishes. The normal acceleration is proportional to the square of the angular velocity about the line of contact, and inversely proportional to the sum of the curvatures of the projected curves. This resembles planar pure rolling about the point of contact.

When $v_L = \dot{v}_L = 0$, then

$$\frac{\ddot{p}_N}{\ddot{p}_L} = -\frac{\omega_L}{\omega_N}.$$

This resembles spatial pure rolling about the point of contact.

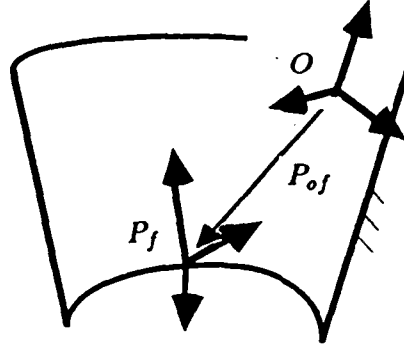


Figure 4.4 Two reference frames on a fixed surface

When there is no rotation about the line of contact,

$$\ddot{p}_T = \dot{v}_T, \quad (2.18)$$

$$\ddot{p}_L = \dot{v}_L + \frac{1}{K} \kappa_f n_{fN} \omega_N v_T, \quad (2.19)$$

$$\ddot{p}_N = \frac{1}{K} \kappa_m \kappa_f n_{mN} n_{fN} v_T^2. \quad (2.20)$$

The normal acceleration is proportional to the square of the sliding velocity component perpendicular to the line of contact, and is inversely proportional to the sum of the radii of curvatures of the projected curves. This formula resembles the one for planar pure translation between two curves with point contact.

For the third order properties of the moving point, we take $n = 3$ in (1.21) and obtain

$$p_T^{(3)} = \ddot{v}_T + 2(\omega_N^2 + \omega_L^2) \dot{s}_m + \kappa_m n_{mN} \omega_L \dot{s}_m^2 - \kappa_m n_{mL} \omega_N \dot{s}_m^2, \quad (2.21)$$

$$p_L^{(3)} = \ddot{v}_L + 2\epsilon_N \dot{s}_m + \omega_N \ddot{s}_m, \quad (2.22)$$

$$p_N^{(3)} = (\kappa_f \tau_f b_{fN} + \kappa'_f n_{fN}) \dot{s}_f^3 - (\kappa_m \tau_m b_{mN} + \kappa'_m n_{mN}) \dot{s}_m^3 + 3\kappa_f n_{fN} \dot{s}_f \ddot{s}_f - 3\kappa_m n_{mN} \dot{s}_m \ddot{s}_m + 3v_L \ddot{L}_{fN} - 3\epsilon_L \dot{s}_m - 3\omega_L \ddot{s}_m, \quad (2.23)$$

where \dot{s}_m and \dot{s}_f are given by (6) and (7). The expressions for special motions are obtainable by substituting the corresponding special cases for \dot{s}_i, \ddot{s}_i .

The constraints on the angular velocity and angular acceleration for the components, other than about the contact line, have already been obtained in (1.6), (1.7), (1.10) and (1.11).

The foregoing first and second order motion properties are useful for path planning, even if we originally have two different representations for the contacting surfaces. Assuming that with respect to arbitrary moving and fixed frames (we call them the original moving and fixed frames), both contacting developable ruled surfaces are represented by

$$\bar{R}_i = \bar{r}_i + \bar{d}_i \bar{L}_i.$$

We can preplan, with respect to the original frames, the trajectories of \bar{r}_m , \bar{d}_f and \bar{r}_f , then transform the variables with respect to the contact reference frames. For example, on the fixed surface (Fig. 4.4) we assume P_{of} is the position vector for the reference point with respect to the original frame, and T is the rotation matrix transforming the coordinates of the contact reference frame to the original frame, then from the relation

$$\bar{R}_f = P_{of} + TR_f, \quad \dot{\bar{R}}_f = T\dot{R}_f, \quad \ddot{\bar{R}}_f = T\ddot{R}_f,$$

we can determine the values of \dot{s}_f , v_L , v_T and those of their derivatives which we would need in order to evaluate the motion expressions we have studied so far.

4.3 Line contact between two circular cones

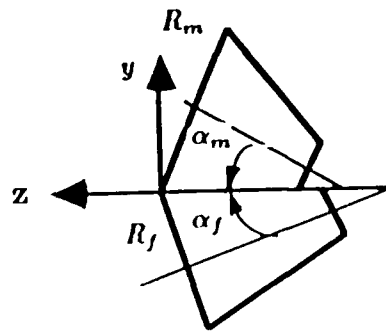


Figure 4.5 Two circular cones under line contact

To illustrate the general properties, we now apply them to the case where two circular cones are in relative motion with line contact.

We pick \mathbf{r}_m and \mathbf{r}_f as position vectors for the points on the two circles cut by planes perpendicular to the cone axes and going through the reference point (Fig. 4.5). Hence,

$$\kappa_m = \frac{1}{\rho_m}, \quad \kappa_f = \frac{1}{\rho_f}, \quad \kappa'_m = \kappa'_f = \tau_m = \tau_f = 0.$$

The principal normals for the circles \mathbf{r}_m and \mathbf{r}_f at the reference point are, respectively,

$$\mathbf{n}_m = \begin{pmatrix} 0 \\ \cos \alpha_m \\ -\sin \alpha_m \end{pmatrix}, \quad \mathbf{n}_f = \begin{pmatrix} 0 \\ -\cos \alpha_f \\ -\sin \alpha_f \end{pmatrix}.$$

Here, the coordinate axes are as described in Fig. 4.5.

To evaluate L_i , we define a second set of moving and fixed frames with their z axes parallel to the cone axes, and their x axes parallel to those of the original reference frames, respectively. We can express L_m in the second moving frame,

$$L_{m2} = \begin{pmatrix} \sin \alpha_m \sin \theta_m \\ -\sin \alpha_m \cos \theta_m \\ \cos \alpha_m \end{pmatrix}.$$

Taking the first two derivatives, and evaluating them at $\theta_m = 0$ yields

$$\dot{L}_{m2} = \begin{pmatrix} \sin \alpha_m \\ 0 \\ 0 \end{pmatrix} \dot{\theta}_m, \quad \ddot{L}_{m2} = \begin{pmatrix} 0 \\ \sin \alpha_m \\ 0 \end{pmatrix} \dot{\theta}_m^2 + \begin{pmatrix} \sin \alpha_m \\ 0 \\ 0 \end{pmatrix} \ddot{\theta}_m.$$

By a simple coordinate rotation, we obtain the desired derivatives of L with respect to the original moving frame,

$$L_m = T_m L_{m2}, \quad T_m = \begin{pmatrix} 1 & 0 & 0 \\ 0 & \cos \alpha_m & \sin \alpha_m \\ 0 & -\sin \alpha_m & \cos \alpha_m \end{pmatrix}.$$

Similarly, L_f expressed with respect to the second fixed frame is

$$L_{f2} = \begin{pmatrix} \sin \alpha_f \sin \theta_f \\ \sin \alpha_f \cos \theta_f \\ \cos \alpha_f \end{pmatrix}.$$

Taking the first two derivatives, and setting $\theta_f = 0$ yields

$$\dot{L}_{f2} = \begin{pmatrix} \sin \alpha_f \\ 0 \\ 0 \end{pmatrix} \dot{\theta}_f, \quad \ddot{L}_{f2} = \begin{pmatrix} 0 \\ -\sin \alpha_f \\ 0 \end{pmatrix} \dot{\theta}_f^2 + \begin{pmatrix} \sin \alpha_f \\ 0 \\ 0 \end{pmatrix} \ddot{\theta}_f.$$

By a simple coordinate rotation, we obtain the desired derivatives of L_f with respect to the original fixed frame.

$$L_f = T_f L_{f2}, \quad T_f = \begin{pmatrix} 1 & 0 & 0 \\ 0 & \cos \alpha_f & -\sin \alpha_f \\ 0 & \sin \alpha_f & \cos \alpha_f \end{pmatrix}.$$

The speeds of Q_m and Q_f , \dot{s}_m and \dot{s}_f , are obtained by substituting the above expressions into equations (2.1) and (2.2)

$$\dot{s}_m = -\bar{\rho}[\omega_L + \frac{1}{\rho_f} \cos \alpha_f v_T], \quad (3.1)$$

$$\dot{s}_f = -\bar{\rho}[\omega_L - \frac{1}{\rho_m} \cos \alpha_m v_T], \quad (3.2)$$

where

$$\bar{\rho} = \frac{\rho_m \rho_f}{\rho_m \cos \alpha_f + \rho_f \cos \alpha_m}.$$

As far as \dot{s}_m and \dot{s}_f are concerned, a line contact between two developable ruled surface is equivalent to a line contact between two circular cones.

For the corresponding special motions, when there is no sliding velocity perpendicular to the line of contact at the moving point, \dot{s}_m and \dot{s}_f will be small (the sensitivity of tangential contact speed to rotational motion is reduced) when either ρ_m or ρ_f is small. When there is no rotation about the line of contact,

$$\dot{s}_m = -\frac{v_T}{1 + \cos \alpha_m \rho_f / (\cos \alpha_f \rho_m)}, \quad \dot{s}_f = \frac{v_T}{1 + \cos \alpha_f \rho_m / (\cos \alpha_m \rho_f)}. \quad (3.3)$$

If the ratio $\cos \alpha_f \rho_m / (\cos \alpha_m \rho_f)$ decreases, \dot{s}_m decreases while \dot{s}_f increases, and vice versa.

The rates of change of the contact speeds, \ddot{s}_m and \ddot{s}_f , are obtained by substituting the above expressions into (2.6) and (2.7):

$$\ddot{s}_m = -\bar{\rho}[\epsilon_L + \frac{1}{\rho_f} \cos \alpha_f \dot{v}_T - \frac{1}{\rho_f^2} \sin(2\alpha_f) v_L \dot{s}_f], \quad (3.4)$$

$$\ddot{s}_f = -\bar{\rho}[\epsilon_L - \frac{1}{\rho_m} \cos \alpha_m \dot{v}_T + \frac{1}{\rho_m \rho_f} \sin(2\alpha_f) v_L \dot{s}_f]. \quad (3.5)$$

When $v_L = 0$, one obtains similar relationships for \ddot{s}_m , \ddot{s}_f , ϵ_L and \dot{v}_T to those we found for \dot{s}_m , \dot{s}_f , ω_L and v_T .

The moving point's acceleration are obtained from (2.12)-(2.14):

$$\ddot{p}_T = \dot{v}_T, \quad (3.6)$$

$$\ddot{p}_L = \dot{v}_L - \bar{\rho} \omega_N [\omega_L + \frac{1}{\rho_f} \cos \alpha_f v_T], \quad (3.7)$$

$$\ddot{p}_N = \bar{\rho} \omega_L^2 - \frac{\bar{\rho}}{\rho_m \rho_f} \cos \alpha_m \cos \alpha_f v_T^2 + \frac{2\bar{\rho}}{\rho_f} \cos \alpha_f \omega_L v_T. \quad (3.8)$$

The normal acceleration is exactly the same as when two ellipses with semi radii ρ_i and $\rho_i \cos \alpha_i$ are in contact with each other at the symmetric point associated with the normal radii. As far as the normal acceleration is concerned, any line contact between two developable ruled surface is equivalent to line contact between two circular cones.

The jerk components of the moving point are obtained from (2.21)-(2.23):

$$p_T^{(3)} = \ddot{v}_T + 2(\omega_N^2 + \omega_L^2) \dot{s}_m + \frac{\cos \alpha_m}{\rho_m} \omega_L \dot{s}_m^2 + \frac{\sin \alpha_m}{\rho_m} \omega_N \dot{s}_m^2, \quad (3.9)$$

$$p_L^{(3)} = \ddot{v}_L + 2\epsilon_N \dot{s}_m + \omega_N \ddot{s}_m, \quad (3.10)$$

$$p_N^{(3)} = -3\left(\frac{\cos \alpha_f}{\rho_f} \dot{s}_f \ddot{s}_f + \frac{\cos \alpha_m}{\rho_m} \dot{s}_m \ddot{s}_m\right) - \frac{3 \sin \alpha_f}{\rho_f^2} \cos \alpha_f v_L \dot{s}_f^2 - 3\epsilon_L \dot{s}_m - 3\omega_L \ddot{s}_m. \quad (3.11)$$

It is also easy to see the orientation constraints for maintaining line contact. The angular velocity constraints are obtained from (1.6) and (1.10):

$$\omega_T = 0, \quad \omega_N = \frac{1}{\rho_f} \sin \alpha_f \dot{s}_f - \frac{1}{\rho_m} \sin \alpha_m \dot{s}_m. \quad (3.12)$$

For two identical circular cones, when there is no sliding perpendicular to the line of contact at the moving point, the normal component of the angular velocity vanishes. The angular acceleration constraints are obtained from (1.7) and (1.11):

$$\epsilon_T = -\omega_N \omega_L - \frac{2 \cos \alpha_m}{\rho_m} \omega_N \dot{s}_m - \frac{3 \sin(2\alpha_f)}{2\rho_f^2} \dot{s}_f^2 - \frac{3 \sin(2\alpha_m)}{2\rho_m^2} \dot{s}_m^2, \quad (3.13)$$

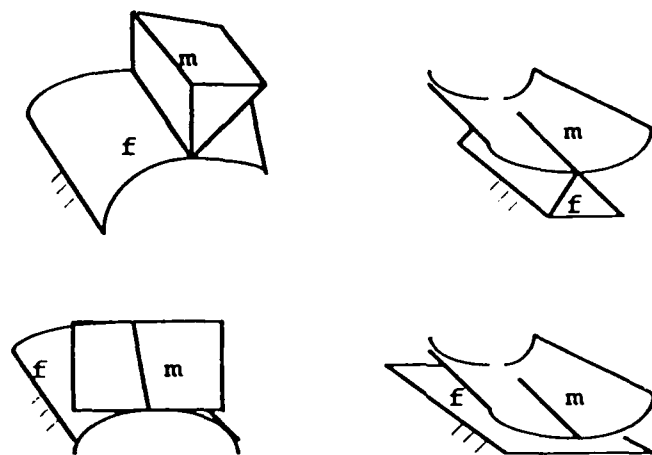


Figure 4.6 Special geometries for line contact

$$\epsilon_N = \frac{\sin \alpha_f}{\rho_f} \ddot{s}_f - \frac{\sin \alpha_m}{\rho_m} \ddot{s}_m. \quad (3.14)$$

4.4 Special geometries of ruled surfaces

The motion constraints will take simpler forms for special geometries. We consider the following four special cases of developable ruled surfaces: the moving surface is a line, the fixed surface is a line, the moving surface is a plane and the fixed surface is a plane (Fig. 4.6). When the angle α , for the circular cone in the previous example vanishes, we have an expression for a circular cylinder, which becomes a line if $\rho_i \rightarrow 0$, and becomes a plane if $\rho_i \rightarrow \infty$.

Moving surface is a line

The speeds of Q_m and Q_f , and their rates of change are obtainable by taking the limit as $\mathbf{r}_m \rightarrow 0$ in (2.1) and (2.6),

$$\dot{s}_m = \ddot{s}_m = 0. \quad (4.1)$$

This is obvious since the moving surface is a line. Taking the limit as $\mathbf{r}_m \rightarrow 0$ in (2.2) and (2.7),

$$\dot{s}_f = v_T, \quad \ddot{s}_f = \dot{v}_T. \quad (4.2)$$

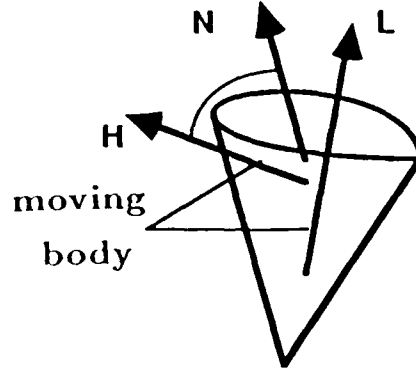


Figure 4.7 Reference lines of a moving body

Hence, the contact speed along \mathbf{r}_f and its rate of change are equal to the component of sliding velocity and sliding acceleration along the curve tangent, respectively.

Similarly, we have the acceleration and the jerk of the moving point. The moving point's acceleration is obtained by substituting (1) and (2) into (2.12)-(2.14):

$$\ddot{p}_T = \dot{v}_T, \quad \ddot{p}_L = \dot{v}_L, \quad \ddot{p}_N = \kappa_f n_{fN} v_T^2. \quad (4.3)$$

And, the moving point's jerk is obtained by substituting (1) and (2) into (2.21)-(2.23):

$$p_T^{(3)} = \ddot{v}_T, \quad p_L^{(3)} = \ddot{v}_L, \quad p_N^{(3)} = \kappa_f \tau_f b_{fN} \dot{s}_f^3 + 3\kappa_f n_{fN} \dot{s}_f \ddot{s}_f + 3v_L \ddot{L}_{fN}. \quad (4.4)$$

Substituting (1) into (1.21), we see that the acceleration and jerk of the moving point are equal to the sliding velocity and its rate of change.

We can also have the special orientation constraints. The angular velocity satisfies the following conditions from (1.6) and (1.10):

$$\omega_T = 0, \quad \omega_N = \dot{L}_{fT}. \quad (4.5)$$

This means that the normal angular velocity is equal to the speed on the fixed spherical curve. The angular acceleration satisfies the following conditions from (1.7)-(1.11):

$$\epsilon_T = -\omega_N \omega_L + 2\omega_L (\omega_L - \kappa_f n_{fN} v_T) - \ddot{L}_{fN} + 2\kappa_f n_{fN} L_{fT} \dot{s}_f, \quad \epsilon_N = \ddot{L}_{fT}. \quad (4.6)$$

The case where a moving surface reduces to a line is useful for path planning with regard to orientation. A robot's orientation "path" can be partially represented by a cone, with each ruling parallel to a different position of the same reference line of the moving body (the axis of a circular peg is an example of a useful reference line). The orientation of the moving body, relative to the cone, can be represented by an angle ϕ between the surface normal N of the cone and a second line H , which is fixed in the moving body and perpendicular to the original reference line L (Fig. 4.7). The motion of L is equivalent to that of a line moving on a cone with line contact. Since L does not slide along itself, \mathbf{r}_f is a spherical curve. Rotation about the line of contact gives the relative angular velocity and the angular acceleration (from (6)).

Fixed surface is a line

This occurs when the fixed surface becomes an edge. Symmetric to the previous case, the speeds of Q_m , Q_f and their rates of change are:

$$\dot{s}_m = -v_T, \quad \ddot{s}_m = -\dot{v}_T, \quad (4.7)$$

$$\dot{s}_f = \ddot{s}_f = 0. \quad (4.8)$$

The components of the moving point's acceleration are obtained from (2.12)-(2.14):

$$\ddot{p}_T = \dot{v}_T, \quad (4.9)$$

$$\ddot{p}_L = \dot{v}_L - \omega_N v_T, \quad (4.10)$$

$$\ddot{p}_N = -\kappa_m n_{mN} v_T^2 + 2\omega_L v_T. \quad (4.11)$$

The moving point's jerk is obtained by substituting (7) and (8) into (2.21)-(2.23):

$$p_T^{(3)} = \ddot{v}_T + 2(\omega_L^2 + \omega_N^2)\dot{s}_m + \kappa_m n_{mN}\omega_L \dot{s}_m^2 - \kappa_m n_{mL}\omega_N \dot{s}_m^2, \quad (4.12),$$

$$p_L^{(3)} = \ddot{v}_L + 2\epsilon_N + \omega_N \ddot{s}_m, \quad (4.13)$$

$$p_N^{(3)} = -(\kappa_m \tau_m b_{mN} + \kappa'_m n_{mN})\dot{s}_m^3 - 3\kappa_m n_{mN}\dot{s}_m \ddot{s}_m - 3\epsilon_L \dot{s}_m - 3\omega_L \ddot{s}_m. \quad (4.14)$$

The sliding terms, in the direction perpendicular to the line of contact, are dominant for the normal acceleration and jerk.

The angular velocity satisfies the following conditions from (1.6) and (1.10),

$$\omega_T = 0, \quad \omega_N = -\dot{L}_{mT}, \quad (4.15)$$

and the angular acceleration satisfies the following conditions from (1.7)-(1.11),

$$\epsilon_T = -\omega_N \omega_L - 2\kappa_m n_{mN} \omega_N \dot{s}_m + \ddot{L}_{mN} - 2\kappa_m n_{mN} \dot{s}_m \dot{L}_{mN}, \quad \epsilon_N = -\ddot{L}_{mT}. \quad (4.16)$$

The above constraints are useful in path planning for assembly, if we are required to rotate a part (with a developable ruled surface) about a sharp edge on another part.

Moving surface is a plane

To find the speeds of Q_m , Q_f and their rates of change, we first take the limit as $r_m \rightarrow \infty$ in (2.1) and (2.6),

$$\dot{s}_m = \frac{1}{\kappa_f n_{fN}} [\omega_L - \kappa_f n_{fN} v_T], \quad (4.17)$$

$$\ddot{s}_m = \frac{1}{\kappa_f n_{fN}} [\epsilon_L - \kappa_f n_{fN} \dot{v}_T + 2\kappa_f n_{fN} v_L \dot{L}_{fL} - (\kappa_f \tau_f b_{fN} + \kappa'_f n_{fN}) \dot{s}_f^2]. \quad (4.18)$$

Then, we take the limit as $r_m \rightarrow \infty$ in (2.2) and (2.7):

$$\dot{s}_f = \frac{\omega_L}{\kappa_f n_{fN}}, \quad (4.19)$$

$$\ddot{s}_f = \frac{1}{\kappa_f n_{fN}} [\epsilon_L - (\kappa_f \tau_f b_{fN} + \kappa'_f n_{fN}) \dot{s}_f^2]. \quad (4.20)$$

As long as the fixed surface is not planar, the instantaneous rotation about the contact line, ω_L and ϵ_L , can be determined from \dot{s}_f and \ddot{s}_f .

We have the moving point's acceleration by substituting (17) and (18) into (2.12)-(2.14),

$$\ddot{p}_T = \dot{v}_T, \quad (4.21)$$

$$\ddot{p}_L = \dot{v}_L + \frac{\omega_N}{\kappa_f n_{fN}} (\omega_L - \kappa_f n_{fN} v_T), \quad (4.22)$$

$$\ddot{p}_N = \frac{1}{\kappa_f n_{fN}} [-\omega_L^2 + 2\kappa_f n_{fN} v_T \omega_L]. \quad (4.23)$$

We also have the moving point's jerk by substituting (17) and (18) into (2.21)-(2.23),

$$p_T^{(3)} = \ddot{v}_T + 2(\omega_N^2 + \omega_L^2) \dot{s}_m, \quad (4.24)$$

$$p_L^{(3)} = \ddot{v}_L + 2\epsilon_N \dot{s}_m + \omega_N \ddot{s}_m, \quad (4.25)$$

$$p_N^{(3)} = (\kappa_f \tau_f b_{fN} + \kappa'_f n_{fN}) \dot{s}_f^3 + 3\kappa_f n_{fN} \dot{s}_f \ddot{s}_f + 3v_L \ddot{L}_{fN} - 3\dot{s}_m \epsilon_L - 3\omega_L \ddot{s}_m. \quad (4.26)$$

The dominant term in the normal acceleration and jerk of the moving point is ω_L .

The tangential angular velocity and angular acceleration perpendicular to the line of contact are from (1.6) and (1.7):

$$\omega_T = 0, \quad \epsilon_T = -\omega_N \omega_L - \ddot{L}_{fN} + 2\kappa_f n_{fN} \dot{L}_f \dot{s}_f. \quad (4.27)$$

When the moving surface reduces to a plane, any line in the plane can be a ruling; the contact line constraint (1.9) is not valid. Hence, ω_N and ϵ_N become free variables.

Fixed surface is a plane

Symmetric to the previous cases, the speed of Q_m and its rate of change are, respectively,

$$\dot{s}_m = -\frac{\omega_L}{\kappa_m n_{mN}}, \quad (4.28)$$

$$\ddot{s}_m = -\frac{1}{\kappa_m n_{mN}} [\epsilon_L + (\kappa_m \tau_m b_{mN} + \kappa'_m n_{mN}) \dot{s}_m^2]. \quad (4.29)$$

And, for Q_f ,

$$\dot{s}_f = -\frac{1}{\kappa_m n_{mN}} [\omega_L - \kappa_m n_{mN} v_T], \quad (4.30)$$

$$\ddot{s}_f = -\frac{1}{\kappa_m n_{mN}} [\epsilon_L - \kappa_m n_{mN} \dot{v}_T + (\kappa_m \tau_m b_{mN} + \kappa'_m n_{mN}) \dot{s}_m^2]. \quad (4.31)$$

As long as the moving surface is not planar, we can calculate ω_L from \dot{s}_m , and ϵ_L from \dot{s}_f .

We have the moving point's acceleration by substituting (21) and (29) into (2.12)-(2.14):

$$\ddot{p}_T = \dot{v}_T, \quad (4.32)$$

$$\ddot{p}_L = \dot{v}_L - \frac{\omega_L \omega_N}{\kappa_m n_{mN}}, \quad (4.33)$$

$$\ddot{p}_N = \frac{\omega_L^2}{\kappa_m n_{mN}}. \quad (4.34)$$

The moving point's jerk is obtained by substituting (21) and (29) into (2.21)-(2.23):

$$p_T^{(3)} = \ddot{v}_T + 2(\omega_N^2 + \omega_L^2) \dot{s}_m + \kappa_m n_{mN} \omega_L \dot{s}_m^2 - \kappa_m n_{mL} \omega_N \dot{s}_m^2, \quad (4.35)$$

$$p_L^{(3)} = \ddot{v}_L + 2\epsilon_N + \omega_N \ddot{s}_m, \quad (4.36)$$

$$p_N^{(3)} = -(\kappa_m \tau_m b_{mN} + \kappa'_m n_{mN}) \dot{s}_m^3 - 3\kappa_m n_{mN} \dot{s}_m \ddot{s}_m - 3\epsilon_L \dot{s}_m - 3\omega_L \ddot{s}_m. \quad (4.37)$$

The rotation about the line of contact is the dominant term in the normal acceleration and jerk of the moving point.

The tangential angular velocity and angular acceleration perpendicular to the line of contact are obtained from (1.6) and (1.7):

$$\omega_T = 0, \quad \epsilon_T = -\omega_N \omega_L - 2\kappa_m n_{mN} \omega_N \dot{s}_m + \ddot{L}_{mN} - 2\kappa_m n_{mN} \dot{L}_m \dot{s}_m. \quad (4.38)$$

By similar reasoning as in the previous case, ω_N and ϵ_N are free variables.

It is often desired for a robot to rotate an object while the object avoids hitting some obstacle which can be modeled as a planar surface. The equations developed above are the limit conditions which prevent a moving body from breaking into a fixed plane.

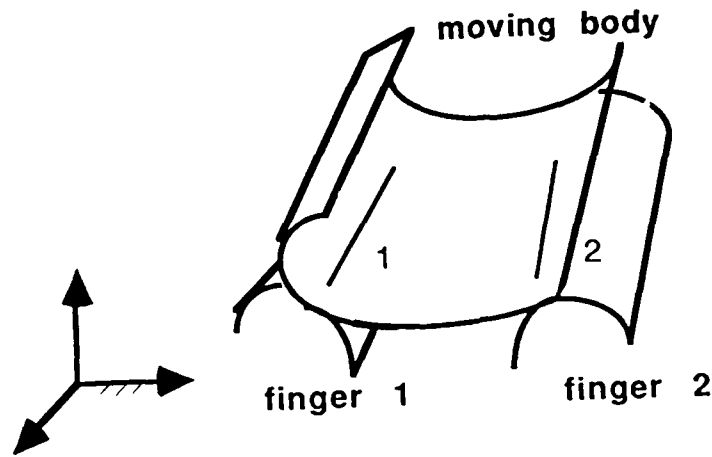


Figure 4.8 Two line contacts

4.5 Two line contacts between surfaces

This section extends the motion constraints for single line contact to those for two line contacts (Figure 4.8).

We notice from the previous sections that with one line contact, the motion of a rigid body is not completely determined. It will be useful for path planning and motion sensing to study the motion of a rigid body with two line contacts. An example of this occurs when a body is in contact with two fingers of a robot hand (if the fingers of the hand have a fixed relative position they act as one rigid body).

Here we assume a moving object is composed of two rigidly connected developable ruled surfaces. We order the contact lines and call them line 1 and line 2 (Fig. 4.8), and use subscript j to indicate that: 1) the variable is expressed in the reference frame j associated with the j^{th} contact line, and 2) either the first line or the second line can be substituted into the equation (Fig. 4.8). We consider that the “moving body” and the fingers are in relative motion to each other, and in absolute motion relative to a fixed body. Ω_{mj} , \mathcal{E}_{mj} , V_{mj} and \mathbf{a}_{mj} are variables associated with the object’s motion with respect to the fixed space: Ω_{mj} and \mathcal{E}_{mj} are the angular velocity and the angular acceleration of the moving object, and V_{mj} and \mathbf{a}_{mj} are the velocity and acceleration of the j^{th} reference point

relative to the fixed body. $\bar{\Omega}_j, \bar{\mathcal{E}}_j, \bar{V}_j$ and $\bar{\mathbf{a}}_j$ are the variables for the object's motion relative to the j^{th} finger, $\Omega_{fj}, \mathcal{E}_{fj}, V_{fj}$ and \mathbf{a}_{fj} are these variables for the j^{th} finger's motion with respect to the fixed body, κ_{mj} and \mathbf{n}_{mj} are the geometric variables associated with the j^{th} contact line of the moving object, and κ_{fj} and \mathbf{n}_{fj} are the geometric variables associated with the j^{th} finger.

From the velocity relation between two points on the same rigid body $V_{m2} = RV_{m1} + R(\Omega \times \mathbf{r})$ (where \mathbf{r} is a position vector pointing from the first to the second moving point), we have

$$\begin{pmatrix} v_{f2,T} + \bar{v}_{2,T} \\ v_{f2,N} \\ v_{f2,L} + \bar{v}_{2,L} \end{pmatrix} = R \begin{pmatrix} v_{f1,T} + \bar{v}_{1,T} \\ v_{f1,N} \\ v_{f1,L} + \bar{v}_{1,L} \end{pmatrix} + RL \begin{pmatrix} \omega_{m1,T} \\ \omega_{m1,N} \\ \omega_{m1,L} \end{pmatrix}, \quad (5.1)$$

where $\bar{v}_{j,T}$ is from (2.2)

$$\bar{v}_{j,T} = \frac{1}{\kappa_{mj}n_{mj,N}} [(\omega_{mj,T} - \omega_{fj,T}) + (\kappa_{mj}n_{mj,N} - \kappa_{fj}n_{fj,N})\dot{s}_{fj}]. \quad (5.2)$$

We have the relation $\Omega_{m2} = R\Omega_{m1}$. If $R = [\beta_{ij}]_{3 \times 3}$, then from (1.6) $\omega_{m2,T} = \beta_{12}\omega_{m1,N} + \beta_{13}\omega_{m1,L} = 0$. When the x axis of the second frame is not parallel to that of the first frame, $\omega_{m1,N}$ and $\omega_{m1,L}$ are not independent, and we have $\omega_{m2,L} = \beta_{32}\omega_{m1,N} + \beta_{33}\omega_{m1,L}$. From the first two rows of equation (1), we can solve for the unknown motion variables associated with the first contact line.

Substituting the acceleration relation between two moving points on the same rigid body, $\mathbf{a}_{m2} = R\mathbf{a}_{m1} + R(\mathcal{E} \times \mathbf{r}) + R[\Omega_{m1} \times (\Omega_{m1} \times \mathbf{r})]$, we have

$$\begin{pmatrix} a_{f2,T} + \bar{a}_{2,T} - 2\bar{v}_{2,N}\omega_{f2,L} \\ a_{f2,N} + \bar{a}_{2,N} + 2\bar{v}_{2,T}\omega_{f2,L} \\ a_{f2,L} + \bar{a}_{2,L} + 2(\bar{v}_{2,N}\omega_{f2,T} - \bar{v}_{2,T}\omega_{f2,N}) \end{pmatrix} = R \begin{pmatrix} a_{f1,T} + \bar{a}_{1,T} - 2\bar{v}_{1,N}\omega_{f1,L} \\ a_{f1,N} + \bar{a}_{1,N} + 2\bar{v}_{1,T}\omega_{f1,L} \\ a_{f1,L} + \bar{a}_{1,L} + 2(\bar{v}_{1,N}\omega_{f1,T} - \bar{v}_{1,T}\omega_{f1,N}) \end{pmatrix} + RB\Omega_{m1} + RC. \quad (5.3)$$

The expressions $\bar{a}_{j,T}$, $\bar{a}_{j,L}$ and $\bar{a}_{j,N}$ are from (2.12)-(2.14):

$$\bar{a}_{j,T} = \dot{v}_{j,T}, \quad (5.4)$$

$$\bar{a}_{j,L} = \dot{v}_{j,L} + \frac{1}{K_j} \bar{\omega}_{j,N} (\bar{\omega}_{j,L} - \kappa_{fj} n_{fj,N} \bar{v}_{j,T}), \quad (5.5)$$

$$\bar{a}_{j,N} = \frac{1}{K_j} \bar{\omega}_{j,N}^2 + \frac{1}{K_j} \kappa_{mj} \kappa_{fj} n_{mj,N} n_{fj,N} v_{j,T}^2 - \frac{2}{K_j} \kappa_{fj} n_{fj,N} \bar{\omega}_{j,L} v_{j,T}, \quad (5.6)$$

and $\bar{v}_{j,T}$ in (4.4) can be obtained from (2.7) as

$$\begin{aligned} \dot{v}_{j,T} = & \frac{1}{\kappa_{mj} n_{mj,N}} [K_j \ddot{s}_{fj} + \epsilon_{j,L} + 2\kappa_{mj} n_{mj,N} \dot{L}_{fj,x} \bar{v}_L \\ & + (\kappa_{mj} \tau_{mj} b_{mj,N} + \kappa'_{mj} n_{mj,N}) \dot{s}_{mj}^2 - (\kappa_{fj} \tau_{fj} b_{fj,N} + \kappa'_{fj} n_{fj,N}) \dot{s}_{fj}^2]. \end{aligned} \quad (5.7)$$

B and C in (3) are two matrix expressions in (3.6.6) and (3.6.10).

Similarly, we have the relation $\mathcal{E}_{m2} = R\mathcal{E}_{m1}$, and the relation, from (1.7), $\epsilon_{m2,T} = \beta_{12}\epsilon_{m1,N} + \beta_{13}\epsilon_{m1,L} = 0$. When the x axis of the second frame is not parallel to that of the first frame, $\epsilon_{m1,N}$ and $\epsilon_{m1,L}$ are not independent, and we have $\epsilon_{m2,L} = \beta_{32}\epsilon_{m1,N} + \beta_{33}\epsilon_{m1,L}$. From the first two rows of equation (2), we can solve for the unknown motion variables associated with the first contact line. Hence, all the quantities for a complete second order motion description are determined.

When the moving body is reduced to two lines, at each reference frame we know $\omega_{j,T} = 0$ (4.5), and from a tactile sensor reading we also know $\omega_{j,N} = \dot{L}_{fT,j}$. Hence, we can determine the complete angular velocity from $\Omega_{m2} = R\Omega_{m1}$. We already know $\bar{v}_{j,N} = 0$, from (4.2) we also know $\bar{v}_{j,T} = \dot{s}_{fj}$, by using the velocity transformation between the two moving points we can completely determine the first order motion variables. By a similar argument, we can determine the second order motion variables.

When the moving body is reduced to two planes, in addition to $\omega_{j,T} = 0$, we know $\omega_{j,L} = \dot{s}_{fj}$ from (3.19). By virtue of the angular velocity transformation between two reference frames, we can determine the complete angular velocity. If $v_{j,L}$ is not obtainable from tactile sensors, we have to have a third contact, and then we can obtain the velocity of the first moving point from the condition that the relative normal velocities all vanish. The second order motion variables are similarly obtainable.

When the moving body is reduced to a line and a plane, or a line and a general developable ruled surface, or a plane and a general ruled surface, we can generally determine all the motion variables using only two line contacts.

This completes our study of the kinematics of spatial motion with line contact. In the next chapter we study control schemes which can be used to control a robot's motion variables so that they satisfy the kinematic relationships developed in this and earlier chapters.

Chapter 5

A CONTROL FORMULATION FOR CONTACT

The previous three chapters are focused on contact kinematics. The relationships we obtained are useful for path planning, especially when the hardware includes tactile sensors. The relationships we obtained for the moving point's trajectory are useful in implementing robot position and force control. Robot control formulations can be written in terms of many different variables. In our study, in this chapter, we use and extend the so-called "operational space control."

Under operational space control, if the control gain matrices are diagonal, the motion-error equations in that space will be decoupled [Khatib, '80; Khatib and Burdick, '86]. However, in this formulation the control frame (the frame which spans the operational space) remains unchanged along the entire trajectory. The operational space frame should not be confused with the so-called task frames [Mason, '81; Raibert and Craig, '81]; it is important to note that task frames are used to obtain motion specifications and are not control frames. In conventional operational space control, the normal acceleration at the contact is ignored. Hence, in operational space control under environmental contact, the control error is not necessarily directly meaningful to the task (since the operational frames are not necessarily parallel to the task frames), and the applied control force may not be accurate (since inertial forces due to normal acceleration are neglected). Therefore, we propose the use of task space control with the

inclusion of normal acceleration. Although this is at the cost of additional computation, it is worthwhile for manipulators under force control when the contact points vary with respect to the moving body.

In this chapter, we discuss operational space coordinates and task space variables, control law formulation in task variables, a motion compatibility filter, the calculation of the manipulator's dynamic model for a task space from the model in other reference systems, an efficient scheme for obtaining the Jacobian matrix inverse for calculating the dynamics model, and an extension to multiple finger contacts. With regard to sensing and applying static forces, we discuss the number of force unknowns at one contact and the use of force for manipulation.

Contact stability is not considered in this dissertation.

5.1 Operational coordinates and task variables

The operational space coordinates can be any set of independent variables of interest in an operation. For the end-effector of a spatial manipulator, we usually are interested in a reference point and the orientation, so the operational space coordinates can be taken as the coordinates of the point, a unit vector directed from the point, and a rotation angle about this vector. Sometimes we wish to consider the position of the elbow and only some of the parameters of the end-effector, etc.. The coordinates can be Cartesian, spherical, or cylindrical coordinates, or even be associated with a frame with three skew axes.

Although the operational space coordinates can be quite general, for a typical contact task where a contact point varies with respect to the moving surface, the trajectory's reference point and the task point are not the same. This is also true when there are multiple contacts with varying contact normals on the end-effector or component links. As in Fig. 5.1, let us assume the original reference frame is O , and the current task frame is P . Usually, the desired stiffness matrix will be diagonal when specified with respect to the current task frame. If we map this into a stiffness matrix with respect to the original reference frame, the new matrix is not diagonal. Hence, there will no longer be a decoupling of motion

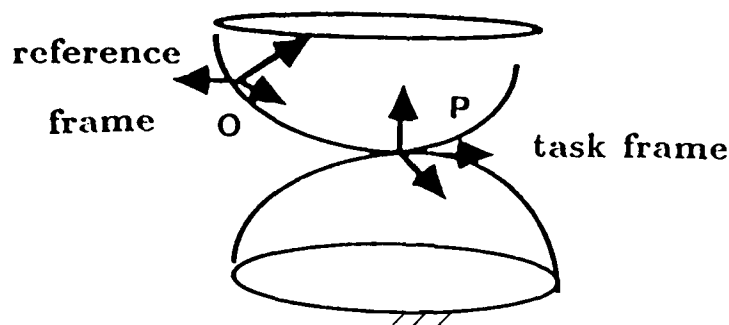


Figure 5.1 Original reference frame and task frame

errors. It follows that we desire to control in terms of a varying “operational space” in order to maintain the error decoupling feature. That is, for each (tiny) segment of a trajectory we let the current “operational space” to be the task space.

The task variables associated with contact can be specified depending on the types of contact: point contact, line contact or planar contact. Many contact-ing situations (such as a peg insertion) can be reduced to these types or their combinations.

For point contact, the task variable is naturally associated with the distance along the contact normal. Let us denote, for the i^{th} contact point, the surface normal \mathbf{n}_i , and a position vector \mathbf{p}_i , which is directed from the instantaneous contact point on the fixed body to the contact point in the moving body. The requirements for maintaining the point contact are that the normal components of \mathbf{p}_i and $\dot{\mathbf{p}}_i$ vanish, and that the normal component of $\ddot{\mathbf{p}}_i$ has a specific value $\ddot{p}_{z,i}$. $\ddot{p}_{z,i}$ is determined by the angular and sliding velocities of the moving body and the surface curvatures at the contact, using formulae which have been obtained in previous chapters. Thus

$$\mathbf{x}_i = \mathbf{n}_i \cdot \mathbf{p}_i = 0, \quad \dot{\mathbf{x}}_i = \mathbf{n}_i \cdot \dot{\mathbf{p}}_i = 0, \quad \ddot{\mathbf{x}}_i = \mathbf{n}_i \cdot \ddot{\mathbf{p}}_i = \ddot{p}_{z,i}. \quad (1.1)$$

While the expression for $\ddot{p}_{z,i}$ depends on the geometries of both surfaces at the contact, it is actually calculable from the moving surface geometry and tactile

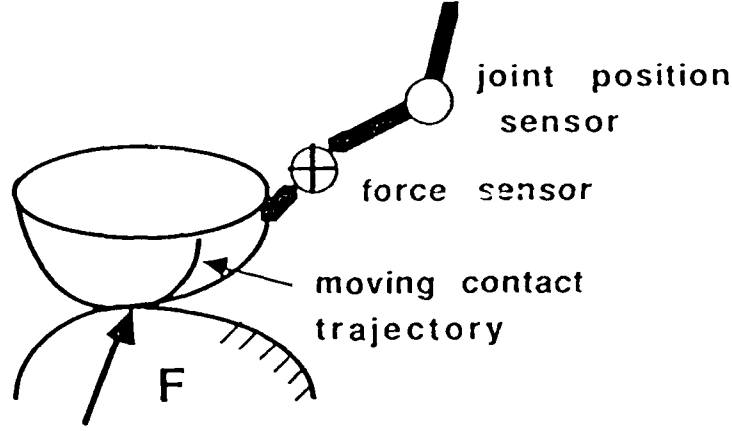


Figure 5.2 Moving body connected to a manipulator with force and position sensors

sensor readings. By tactile sensing – from either a tactile sensor or one force sensor we can determine the moving contact velocity \dot{x}_m and \dot{y}_m (assuming the inertia force between the contact point and sensing point is negligible; otherwise we need two force sensors*). From the position sensors (such as optical encoders at joints of a manipulator), we can determine the sliding velocity and angular velocity of the moving body (Fig. 5.2). Thus, from (3.1.21) and (3.1.24), we can determine the contact velocity on the fixed surface: $\dot{x}_f = v_1 - \dot{x}_m$, $\dot{y}_f = v_2 - \dot{y}_m$. Substituting (3.1.18), (3.1.10) and (3.1.19) into (3.1.37), we obtain the normal acceleration of the moving point

$$\begin{aligned} \ddot{p}_z = & -(k_{m,x}\dot{x}_m + g_m\dot{y}_m)(\dot{x}_m + \dot{x}_f) - (g_m\dot{x}_m + k_{m,y}\dot{y}_m)(\dot{y}_m + \dot{y}_f) \\ & - \omega_1\dot{y}_f + \omega_2\dot{x}_f + 2(\dot{x}_m\omega_2 - \dot{y}_m\omega_1). \end{aligned} \quad (1.2)$$

For the case where the moving surface becomes a point, from (3.4.4)

$$\ddot{p}_z = -k_{f,x}\dot{v}_1 - 2g_f v_1 v_2 - k_{f,y}\dot{v}_2^2 = -\omega_{fx}v_1 - \omega_{fy}v_2.$$

Here, ω_{fx} and ω_{fy} are the x and y components of the angular velocity of the contact normal on the fixed surface. If by use of a force sensor we can accurately

* We assume here that a dynamics model is valid for the members between the contact point and the force sensors.

determine the contact normal of the fixed surface, we are able to determine ω_{fx} and ω_{fy} .

For planar motion with point contact between two curves, from (2.2.9) and (2.2.28) we obtain

$$N \cdot \ddot{\mathbf{p}}_i = \omega \dot{x}_f - 2\dot{x}_m \omega - k_m(\dot{x}_m + \dot{x}_f)\dot{x}_m,$$

and when the moving curve becomes a point

$$N_i \cdot \ddot{\mathbf{p}}_i = -\omega_f v,$$

where ω_f is the angular velocity of the contact normal on the fixed curve.

For a line contact between two developable ruled surfaces, as pointed out in Chapter 4, there are three pairs of independent scalar constraints on the first order and second order properties of the motion. One pair of constraints is on the normal components of the velocity and the acceleration of a reference point on the contact line of the moving surface. One pair of constraints is on the angular velocity and angular acceleration along a direction perpendicular to both the contact line and the surface normal, and, the third pair is on the normal components of the angular velocity and the angular acceleration (this constraint diminishes when the fixed surface is planar).

Similarly, for a planar contact there are three sets of constraints. One set is on the normal distance of a reference point in the plane, and the other two can be on the rotations about tangential axes.

Except for the normal angular velocity under line contact, all first-order constraints for contact can be replaced by static force constraints. The null normal velocity for a point contact will be guaranteed by the presence of an appropriate normal contact force. The sufficient condition for maintaining a line contact is that the resultant normal force acts on the contact line in a sense to maintain contact, or that there are normal forces of sufficient magnitude and sense at two different reference points on the line. The sufficient condition for a planar contact

is that the resultant normal force acts on the contact plane in the appropriate sense, or that there are sufficiently large normal forces at three different reference points in the plane.

When used for obstacle avoidance, the constraints on contact velocity and contact acceleration become inequalities. When the motion produced by the other control variables does not satisfy the inequality constraints, we need to add these constraints to our controller, otherwise these inequalities serve simply as conditions which need to be checked for satisfaction.

5.2 Control in task variable space

In each small time interval, a model based manipulator control law [Khatib and Burdick, '86] can be directly applied to the task variables X :

$$\tau = J^T F = J^T [M_t(\ddot{X}^* + K_v \delta \dot{X} + K_p \delta X) + N_t + F_{control}]. \quad (2.1)$$

In this equation, τ is a command vector for joint torques; J and M_t are the Jacobian matrix and inertia matrix corresponding to the task space; \ddot{X}^* is the acceleration vector; K_v and K_p are diagonal gain matrices for controlling task space velocity and position; N_t is the vector of nonlinear velocity dependent inertia forces; the vector $F_{control}$ is the force applied to the environment.

For each task variable, we either control force or position. In force-controlled directions, if we can physically measure the accelerations, we use the actual acceleration components for \ddot{X}^* , whereas in position-controlled directions and for unmeasured acceleration directions we use the desired acceleration. The Jacobian matrix can be formulated as follows. The velocities along the force-controlled directions, \dot{X}_c , can be expressed as $\dot{X}_c = J_c \dot{\Theta}$. Position-controlled variables (other than the contact task variables), \dot{X}_m , can be expressed as $\dot{X}_m = J_m \dot{\Theta}$. Combining both, we have a complete set of task velocity variables $\dot{X} = [\dot{X}_c^T, \dot{X}_m^T]^T$ and the Jacobian matrix $J = [J_c^T, J_m^T]^T$.

Under the assumption that all desired force contacts are taking place, and there is zero velocity associated with these directions, we can determine from J_c if

there is any mobility for the manipulator under the current constraints. If $|J_c|$ is a square matrix of full rank, then a vector of zero joint rates is the only solution. Alternatively, if a unit screw associated with a contact normal is reciprocal to all the unit screws associated with the joint axes, that contact direction is uncontrollable and does not impose any restriction on the joint rates. In such a case, if the contact constraint is redundant instantaneously, the rank of J_c will be reduced by one.

M_t is a square inertia matrix corresponding to the set of task variables. It is known that $M_t = [JM_\theta^{-1}J^T]^{-1}$ [Khatib, '80], where M_θ is the inertia matrix in joint space. If $\ddot{\Theta}$ is the joint rate vector corresponding to the minimum kinetic energy of the manipulator under the constraint $\dot{X} = J\dot{\Theta}$, M_t satisfies the relation $\dot{X}^T M_t \dot{X} = \ddot{\Theta}^T M_\theta \ddot{\Theta}$. If we define $\ddot{\Theta} = \bar{J}\ddot{X}$, where $\bar{J} = M_\theta^{-1}J^T M_t$ [Khatib, '80], then $M_t = \bar{J}^T M_\theta \bar{J}$.

The control law in (2.1) can be partitioned into $F = F_{feed-forward} + F_{feedback}$, a desired feed-forward command force and an error-control force based on feedback. The $F_{feed-forward} = M_t \ddot{X}^* + N_t + F_a$, contains the inertial forces and the desired contact force, F_a , while $F_{feedback}$ involves the motion and force error correction commands. For the feed-forward inertia forces, since $\tau = J^T F$ and $F = \bar{J}^T \tau$ we have

$$\tau_{feed-forward} = J^T [M_t \ddot{X}^* + N_t] = J^T \bar{J}^T (M_\theta \ddot{\Theta} + N_\theta), \quad (2.2)$$

hence $J^T \bar{J}^T$ is a projector which maps joint inertia forces into the permissible torque space. For a non-redundant manipulator $\bar{J} = J^{-1}$, and the feed-forward inertia vectors are the same as those in joint space. So in this case, only the error-correction vector differs between controls formulated in task space and joint space.

The decoupling, which is associated with the diagonal control gain matrices, will remain unchanged in the presence of contact forces acting in arbitrary directions (This is of course provided that we can neglect the friction at the contacts and that there are biased contact forces applied for maintaining the contacts. If the effect of friction is not negligible, compensating for the frictional forces in the

control law will also help). This is because contact wrench and motion screws are mutually reciprocal, and no mechanical work is done at the contact. Hence, the contact force will not affect the motion of the object, although the motion dynamics will affect the contact forces. Lipkin and Duffy [Lipkin and Duffy, '86] have stressed the difference between reciprocity and orthogonality for contact forces and motion. In support of their results that force controlling directions may not be orthogonal to the motion directions, assume several contact forces are at different points and exerted in different directions, with resultant force \mathbf{f} and angular velocity ω at the reference frame origin, the velocity is \mathbf{v} and the resultant moment is \mathbf{m} , the screw reciprocity indicates that at the origin of the reference frame

$$\mathbf{f} \cdot \mathbf{v} + \mathbf{m} \cdot \omega = 0. \quad (2.3)$$

In general $\mathbf{f} \cdot \mathbf{v} \neq 0$ and $\mathbf{m} \cdot \omega \neq 0$, so orthogonality is not guaranteed.

Although there are no computations needed for control gains (which are usually specified in task frames) model based control in task space requires more computation than in operational space. First, there is the need for trajectory mapping. For example, assume that there exists a task point X_2 , an original reference point X_1 , and a relationship $P_o + RX_2 = X_1$. Here, P_o is a position vector for the origin of the task frame with respect to the reference frame, and R is a rotation matrix from the task frame coordinates to the reference frame. Once X_1 is specified, the trajectory with respect to the task frame becomes $X_2 = R^T(X_1 - P_o)$, $\dot{X}_2 = R^T \dot{X}_1$, and $\ddot{X}_2 = R^T \ddot{X}_1$. Second, there is a need for relatively faster updating of dynamics parameters than for controlling in an operational space system. The dynamics parameters are usually updated at a slower rate than that of the trajectory. However, if these are updated too slowly, then we will again encounter again the problems mentioned for operational space control.

5.3 Motion compatibility filter

When the accelerations in the force control directions are known, they should be included in the controller since this will facilitate smooth force control. If the

control is performed directly on the task variables or if the task point and the original reference point are coincident, applying the so-called motion compatibility filter to the error-correction vector is equivalent to having null components of K_p and K_v matrices in the force-control directions. We can also have a compatibility filter for the error-correction vector (on velocity and force) in other control spaces when the contact directions are given.

Khatib and Burdick [Khatib and Burdick, '86] introduced a motion compatibility filter ΩF_m^* , and we now consider it under the assumption that the task point is coincident with the original reference point. Ω is a matrix involving two sub-matrices, which can be regarded in our context as $R_1^T \sum_f R_1$ and $R_2^T \sum_r R_2$. R_1 and R_2 are two rotation matrices relating the positional and rotational operational frames to the analogous task frames. \sum_f and \sum_r are unit matrices but with null elements in the force-control directions. If we assume F_m^* is of the form $\ddot{X}_d + K_v \delta \dot{X} + K_p \delta X$, $\Omega \ddot{X}_d$ actually filters out the acceleration along the force-control directions, and these accelerations do not necessarily vanish.

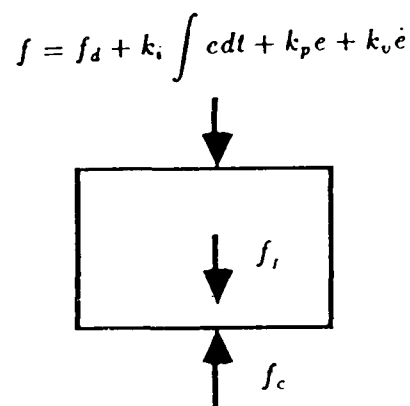


Figure 5.3 Free body diagram for single mass contact

We can look at the effect of normal acceleration on force control through the study of a single mass contact. As in Fig. 5.3, we define f_c , f_d and f_I to be the actual contact force, desired contact force and the inertia force, k_p , k_i , and

k_v to be the control gains for a PID control law, and the contact-force error to be $e(t) = f_d - f_c$. If we neglect the inertia force in the control command $f = f_d + k_I \int e dt + k_p e + k_v \dot{e}$, then the Laplace transformations for the actual contact force and the contact-force error are:

$$f_c(s) = f_d - \frac{s f_I}{s^2 k_v + s(1 + k_p) + k_i}, \quad c(s) = \frac{s f_I}{s^2 k_v + s(1 + k_p) + k_i}. \quad (3.1)$$

For a general *PID* or *PI* controller, there will be a static error in contact force with magnitude proportional to f_I whenever it is a ramp signal, and for a *PD* controller there will be a static force error for a constant f_I signal. If we consider the dynamic error characteristics of contact force, the f_I term will be more significant for a smooth contact.

For error control vectors, we use an upper bar on \sum to indicate its sub-matrix for the point's position, and use subscripts o or t for a variable to indicate that it is associated either with the operational reference frame or the task frame. Then

$$(R_1^T \sum_f R_1) \bar{K}_{po} \delta \bar{X}_o = (R_1^T \sum_f R_1) R_1^T \bar{K}_{pt} R_1 \delta \bar{X}_o = R_1^T \sum_f \bar{K}_{pt} \delta \bar{X}_t. \quad (3.2)$$

The product $\sum_f \bar{K}_{pt}$ demands that the components of \bar{K}_{pt} along force-control directions vanish. An analogous result is true for the rotation part. Hence, the explicit calculation of such a filter at run-time is not necessary, since we can simply let the corresponding components of K_p and K_v vanish.

We now consider a general compatibility filters for velocity and force, such filters become necessary when control is performed in other than task space. We assume the contacting surface normals are known, since these can be obtained from force sensor information.

When there are multiple contacts on different links, we can almost directly use the joint-space filters proposed by West and Asada [West and Asada, '85]. The differences are that we can assume the control directions are already in the "essential work space," and that instead of a rigidly fixed point each contact can have relative motion. The filter is derived by substituting J_c , in which each

row represents a constraint associated with a contact, into the filter expressions developed by West and Asada.

When all contacts are on one rigid body in spatial motion, we apply a similar procedure to the one used by West and Asada. Assume that the control variables \dot{X}_o are related to the contact variables \dot{X}_c by a transformation matrix T_c , $\dot{X}_c = T_c \dot{X}_o = 0$. To satisfy this equation

$$\dot{X}_o = (I - T_c^+ T_c) a, \quad (3.3)$$

where a is an arbitrary scalar, and T_c^+ is a 1, 2-inverse [Ben-Israel, et. al, '74] of T_c . $(I - T_c^+ T_c)$ is a projector, hence a compatibility filter for velocity. From $F_o^T \dot{X}_o = F_1^T (I - T_c^+ T_c) y = 0$, we obtain

$$F_o = (T_c^+ T_c) b, \quad (3.4)$$

where b is an arbitrary scalar. $T_c^+ T_c$ is an orthogonal projector or a compatibility filter for force. We notice that the velocity component along a line in a rigid body is the the same for every point on the line. Hence, each row of T_c depends only on the corresponding axis associated with a contacting normal.

5.4 Transformation of dynamics parameters

We now consider the case that a preplanned trajectory of a moving body is associated with one reference point and the task variables are associated with another point (for example, the varying contact point on the moving body). Given the parameters of dynamics model associated with a reference frame, those for the task frame can be simple to calculate. If there exists only an orientation difference between the reference frame and the task frame, then controlling in the reference frame and in the task frame are equivalent provided their control gains are interchangeable.

We use subscripts o and t to denote variables which are associated with the reference frame and the task frame, respectively. Assume that T is a transformation matrix which relates the velocities of the two reference frames: $\dot{X}_t = T \dot{X}_o$.

($\dot{X}_t = [v_t, \omega_t]^T$ and $\dot{X}_o = [v_o, \omega_o]^T$). Then

$$M_t = T^{-T} M_o T^{-1}, \quad (4.1)$$

$$N_t = T^{-T} [N_o - M_o T^{-1} C], \quad (4.2)$$

$$F_t = T^{-1} F_o, \quad (4.3)$$

where C is a vector of the centrifugal acceleration between the two points.

If we assume that the point velocity and the angular velocity are expressed with respect to two different sets of frames, and the distance between the reference point and the task point vanishes, $T = \text{diagonal}(R_1, R_2)$, $M_t = T M_o T^T$, $N_t = T N_o$, and $F_t = T F_o$. Based on these, the motion expression in (2.1) satisfies

$$J_o^T [M_o \ddot{X}_{od} + K_{ov} \delta \dot{X}_o + K_{op} \delta X_o] = J_t^T [M_t \ddot{X}_{td} + K_{tv} \delta \dot{X}_t + K_{tp} \delta X_t], \quad (4.4)$$

as long as we take $K_{op} = T^T K_{tp} T$ and $K_{ov} = T^T K_{tv} T$. The control in the fixed reference frame will now lead to decoupled error equation in task variable space.

For a general coordinate transformation between two sets of variables of equal number, (1) and (3) are still valid, except in (2) $N_t = T^{-T} (N_o - M_o T^{-1} \dot{T} \dot{X}_o)$, where \dot{T} is to be determined from $\ddot{X}_t = \dot{T} \dot{X}_o + T \ddot{X}_o$.

5.5 An efficient inverse of the Jacobian matrix

As shown before, for a non-redundant general manipulator with environmental contact, the inertia matrix in a reference frame can be treated as directly related to the inverse Jacobian-matrix. Generally the reference point is not at the wrist point, and the last three joints have motion as well, so the Jacobian matrix has no three-by-three zero sub-matrix. However, for a manipulator, such as the PUMA, in which the last three joint axes intersect at the wrist point, the job can be broken down to two simple three-by-three matrix inverses plus several matrix transformations and multiplication.

As in Fig. 5.4, from the wrist frame to the reference frame,

$$V_o = R_1 V_w + R_1 [\Omega_w \times r], \quad \Omega_o = R_2 \Omega_w$$

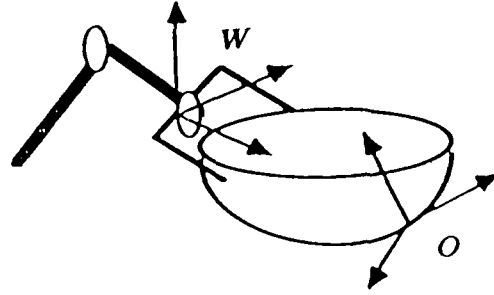


Figure 5.4 Wrist frame and a reference frame

where the subscript o (or w) denotes that a variable is with respect to the reference frame (or the wrist frame), and \mathbf{r} is a position vector from the wrist point to the reference point. In matrix form the above expressions become

$$\begin{pmatrix} V_o \\ \Omega_o \end{pmatrix} = \begin{pmatrix} R_1 & P \\ O & R_2 \end{pmatrix} \begin{pmatrix} V_w \\ \Omega_w \end{pmatrix}.$$

Here, R_1 is a coordinate rotation transformation matrix from the positional wrist frame to the positional reference frame and R_2 is the analogous matrix for the rotational wrist frame to the rotational reference frame, and O a three-by-three null matrix. The velocity and angular velocity at the wrist frame can be expressed in a standard way,

$$\begin{pmatrix} V_w \\ \Omega_w \end{pmatrix} = \begin{pmatrix} J_1 & O \\ J_2 & J_3 \end{pmatrix} \dot{\Theta},$$

where J_i is a three-by-three matrix. If we define J to be the Jacobian matrix relating the reference velocity to joint rates,

$$\begin{pmatrix} V_o \\ \Omega_o \end{pmatrix} = \begin{pmatrix} R_1 & P \\ O & R_2 \end{pmatrix} \begin{pmatrix} J_1 & O \\ J_2 & J_3 \end{pmatrix} \dot{\Theta} = J \dot{\Theta}. \quad (5.1)$$

Now J is expressed as a product of two 6 by 6 matrixes, and each one includes a null off-diagonal sub-matrix. By standard calculation the inverse of J becomes

$$\begin{aligned} J^{-1} &= \begin{pmatrix} J_1^{-1} & 0 \\ A & J_3^{-1} \end{pmatrix} \begin{pmatrix} R_1^T & B \\ 0 & R_2^T \end{pmatrix} \\ &= \begin{pmatrix} J_1^{-1} R_1^T & J_1^{-1} B \\ A R_1^T & AB + J_3^{-1} R_2^T \end{pmatrix}, \end{aligned} \quad (5.2)$$

where $A = -J_3^{-1} J_2 J_1^{-1}$, $B = -R_1^T P R_2^T$. This gives an efficient way to calculate the inverse.

For a general non-redundant manipulator with environmental contacts, the Jacobian matrix still can be divided into sub-matrices, with J_1 and J_4 square matrices

$$J = \begin{pmatrix} J_1 & J_2 \\ J_3 & J_4 \end{pmatrix}. \quad (5.3)$$

If J_1^{-1} exists, we have from [Kailath, '80],

$$J^{-1} = \begin{pmatrix} J_1^{-1} + E \Delta^{-1} F & -E \Delta^{-1} \\ -\Delta^{-1} F & \Delta^{-1} \end{pmatrix}, \quad (5.4)$$

where $\Delta = J_4 - J_3 J_1^{-1} J_2$, $E = J_1^{-1} J_2$ and $F = J_3 J_1^{-1}$. If J_4^{-1} exists, the (1,1) block element of the inverse can be written as $[J_1 - J_2 J_4^{-1} J_3]^{-1}$. If J_2^{-1} exists, similarly we can obtain

$$J^{-1} = \begin{pmatrix} -\Delta^{-1} J_4 J_2^{-1} & \Delta^{-1} \\ J_2^{-1} (I + J_1 \Delta^{-1} J_4 J_2^{-1}) & -J_2^{-1} J_1 \Delta^{-1} \end{pmatrix}, \quad (5.5)$$

where $\Delta = J_3 - J_4 J_2^{-1} J_1$.

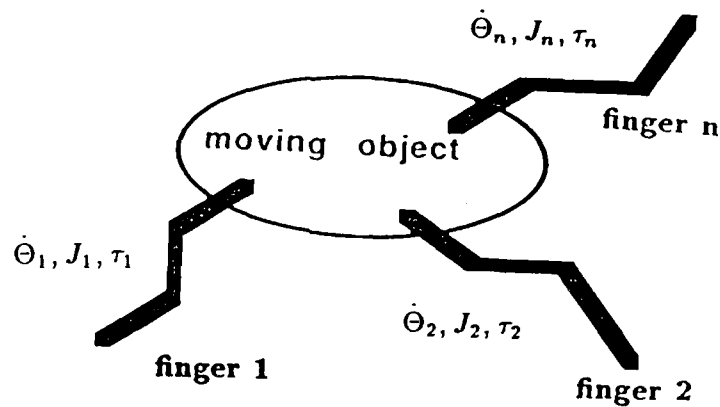


Figure 5.5 Multiple fingers in grasping

5.6 On extension to grasping

Model based control can be extended to grasping (Fig. 5.5), since force-controlled variables can be associated with internal grasping forces, and the grasped object and fingers can be considered as a complete system.

The internal forces when simultaneously applied, produce zero work if we neglect sliding. Under this assumption, the control of internal force will not affect the decoupling of error-correction terms in the motion controller.

Since the motions of the fingers and that of the grasped object interact with each other, the decoupling of the error-correction terms will be affected if we isolate the dynamics of the moving body. Assume an object is supported, through point contacts without slipping, by a group moving fingers and is capable of spatial motion $\dot{X} = [V_t, \Omega_t]^T$ (the velocity at a reference point and the angular velocity of the object). If we consider only the moving object, the driving force becomes

$$M_b(\ddot{X} + K_v\delta\dot{X} + K_p\delta X) + N_b + F_{control}. \quad (6.1)$$

Here, M_b is the inertia matrix for the grasped object, and N_b is its non-linear inertia force (it vanishes if X is associated with the object's mass center). Assume each finger's inertia force has been balanced, we encounter the problem of how to treat the finger-tip forces from $M_b(K_v\delta\dot{X} + K_p\delta X)$: without the premultiplication of a finger's equivalent inertia matrix, the response will be slow since the finger's tip has different acceleration responses to its different joint torques. However, if we premultiply the command force at the finger tip by the equivalent inertia matrix of the finger, the decoupling of the error-correcting terms for the moving body will be affected.

Hence, we need to consider the moving body and its supporting fingers together as a system, for which we change the subscripts b to s in (1), and M_s and N_s can be obtained as follows. We denote v_i as the velocity vector at the i^{th} contact point, $v_i = W_i\dot{X}$, and $W_i = [R_i L(r_i), R_i]$. Here, R_i is a rotation coordinate transformation matrix from the reference frame to the i^{th} contact frame, and $L(r_i)$ is a matrix resulting from $\Omega_i \times r_i = L(r_i)\Omega_i$, where r_i is a position vector

from the reference point to the i^{th} contact point. On the other hand, from the link Jacobian matrix we have $\mathbf{v}_i = \mathbf{J}_i \dot{\Theta}_i$. Redundant fingers could be treated on the basis that the minimum kinetic energy of the system corresponds to the minimum kinetic energy for each finger, we assume each finger is non-redundant: $\dot{\Theta}_i = \mathbf{J}_i^{-1} \mathbf{W}_i \dot{\mathbf{X}}$. The resultant force on the moving body can be expressed as the sum $\sum_{i=1}^n \mathbf{F}_i$, where $\mathbf{F}_i = \mathbf{W}_i^{-T} \mathbf{J}_i^{-T} \boldsymbol{\tau}_i$. Based on these the system's inertia matrix, \mathbf{M}_s , becomes

$$\mathbf{M}_s = \mathbf{W}_1^T \mathbf{J}_1^{-T} \mathbf{M}_1 \mathbf{J}_1^{-1} \mathbf{W}_1 + \mathbf{W}_2^T \mathbf{J}_2^{-T} \mathbf{M}_2 \mathbf{J}_2^{-1} \mathbf{W}_2 + \cdots + \mathbf{W}_n^T \mathbf{J}_n^{-T} \mathbf{M}_n \mathbf{J}_n^{-1} \mathbf{W}_n + \mathbf{M}_b. \quad (6.2)$$

If we consider the acceleration at the contact point on the moving body: $\ddot{\mathbf{J}}_i \dot{\Theta}_i + \mathbf{J}_i \ddot{\Theta}_i + \mathbf{a}_{r,i} + \mathbf{a}_{c,i} = \mathbf{W}_i \ddot{\mathbf{X}} + \mathbf{C}_i$; $\ddot{\Theta}_i = \mathbf{J}_i^{-1} [\mathbf{W}_i \ddot{\mathbf{X}} + \mathbf{C}_i - \ddot{\mathbf{J}}_i \dot{\Theta}_i - \mathbf{a}_{r,i} - \mathbf{a}_{c,i}]$. In this expression, $\mathbf{a}_{r,i}$ and $\mathbf{a}_{c,i}$ are the relative acceleration and the Coriolis acceleration of the contact point on the moving object with respect to that of the i^{th} finger, and $\mathbf{C}_i = \mathbf{R}_i [\boldsymbol{\Omega}_i \times (\mathbf{W}_i \dot{\mathbf{X}})]$. Mapping the inertia torques $\mathbf{M}_i \ddot{\Theta}_i + \mathbf{N}_{\Theta_i}$ in joint coordinates into the inertia force on moving object's reference system, we obtain

$$\mathbf{N}_s = \mathbf{N}_b + \sum_{i=1}^n \mathbf{N}_i; \quad (6.3)$$

where $\mathbf{N}_i = \mathbf{W}_i^T \mathbf{J}_i^{-T} [\mathbf{N}_{\Theta_i} + \mathbf{M}_i \mathbf{J}_i^{-1} (\mathbf{C}_i - \ddot{\mathbf{J}}_i \dot{\Theta}_i - \mathbf{a}_{r,i} - \mathbf{a}_{c,i})]$.

While $\mathbf{M}_b [\ddot{\mathbf{X}}_d + \mathbf{K}_p \delta \mathbf{X} + \mathbf{K}_v \delta \dot{\mathbf{X}}] + \mathbf{N}_b$ can be distributed among finger tips with redundancy, the $[\mathbf{W}_i^T \mathbf{J}_i^{-T} \mathbf{M}_i \mathbf{J}_i^{-1} \mathbf{W}_i] \ddot{\mathbf{X}} + \mathbf{N}_i$ naturally should be assigned back to the corresponding finger, since no additional force transmission through the contact point is necessary. This part can be assigned as $\mathbf{M}_i \mathbf{J}_i^{-1} (\mathbf{W}_i \ddot{\mathbf{X}} + \mathbf{C}_i - \ddot{\mathbf{J}}_i \dot{\Theta}_i - \mathbf{a}_{r,i} - \mathbf{a}_{c,i}) + \mathbf{N}_{\Theta_i}$ in the i^{th} finger's joint space. For the error-correcting term, similarly, we can assign $\mathbf{M}_i \mathbf{J}_i^{-1} \mathbf{W}_i [\mathbf{K}_p \delta \mathbf{X} + \mathbf{K}_v \delta \dot{\mathbf{X}}] = \boldsymbol{\tau}_i$ back to the corresponding finger. This makes the error-correcting force on the moving body proportional to each finger's inertia, and it is this term which makes a difference between defining a system by considering the moving body only and considering both the moving body and the supporting fingers.

When an object is operated by n fingers (manipulators) through rigid grasping, we have directly $\dot{\mathbf{X}} = \mathbf{J}_1 \dot{\Theta}_1 = \mathbf{J}_2 \dot{\Theta}_2 = \cdots = \mathbf{J}_n \dot{\Theta}_n$, and the previous expressions can

be much simplified. When there is slipping at the contact point, we can include the slipping component into a "joint rate" vector, and the inverse of the Jacobian matrix J_i becomes a generalized inverse. If a desired sliding velocity is specified, such inverses are deterministic.

5.7 Number of force unknowns at one contact

In dealing with multiple contacts, we encounter the problem of force sensing. We now consider how many force unknowns are present for one point contact, line contact or planar contact, when certain pre-conditions have been given. This is useful in the selection of force sensors.

For a point contact the contact force must lie on the friction cone, with tangential component opposite to the sliding direction. Given the contact point position, if we know the coefficient of friction μ there is 1 unknown associated with the magnitude of the force; otherwise there are 2 unknowns, the extra one is for μ . When there is no sliding the axis of the contact force must lie within the friction cone, so there are 3 unknowns for the force vector acting at the given point. When the contact point is simply confined on a line, or a plane, we need to add 1 or 2 extra unknowns for the location of the contact point. If the frictional torque about the contact normal is also significant, one more unknown needs to be added.

For a line contact between two cylindrical surfaces without rotation about the normal at the contact, when given μ there are 2 unknowns (one for the location of the resultant force and the other for the force magnitude), otherwise there are 3 unknowns. For general developable ruled surfaces we have 5 unknowns if there is no sliding along the line of contact, since we know only that the resultant wrench will pass through the line of contact. If there is frictional torque about the line of contact, we need to add one more unknown.

The planar contact can be treated in a similar manner. For a pure translation, when μ is given there are 3 unknowns associated with the acting point of the resultant force in the plane and the magnitude of the force, otherwise there are

4 unknowns. If there is rotation as well, then there will be 6 unknowns if the pressure distribution is an unknown.

When no conditions are specified there will be 6 unknowns associated with the force and moment at a point contact, line contact and planar contact.

5.8 Contact force manipulability

Relative to static force application, we consider force manipulability for a non-redundant and a redundant spatial manipulator, and discuss the "optimal" arm configuration based on force manipulability in all or some directions.

When a manipulator performs operations where the force application at the end-effector becomes significant, we need to consider its force manipulability as opposed to its kinematic manipulability [Yoshikawa, '85].

For a non-redundant manipulator, from $\dot{X} = J\dot{\Theta}$ we have

$$\dot{X}^T \dot{X} = \dot{\Theta}^T J^T J \dot{\Theta}. \quad (8.1)$$

We define $U = \dot{\Theta} / \sqrt{\dot{X}^T \dot{X} / \dot{\Theta}^T \dot{\Theta}}$ which represents an ellipsoid in variable U . The volume index of the ellipsoid, $|J|$, has been referred to as the measure for kinematic manipulability [Yoshikawa, '85]. On the other hand, from $\tau = J^T F$ we have

$$\tau^T \tau = F^T J J^T F. \quad (8.2)$$

If we define $U = F / \sqrt{F^T F / \tau^T \tau}$, it also represents an ellipsoid in variable U . Since the eigenvalues of $J J^T$ and $J^T J$ are the same – both ellipsoids are of the same shape, hence we can also regard $|J|$ as the measure for force manipulability.

For a 2-joint planar manipulator, the differential area $\delta\theta_1 \delta\theta_2$ in joint space will be mapped to $\delta x \delta y = |J| \delta\theta_1 \delta\theta_2$ at the end effector. At the same time, if there are forces f_x and f_y exerted at the end-effector, the $f_x f_y$ area in force space will be mapped to $\tau_1 \tau_2 = |J| f_x f_y$ in joint torque space. The analogous result is true for an n-degrees-of-freedom manipulator if we consider the n-dimensional volume in force and motion spaces.

In terms of arbitrary directions, the maximum $|J|$ corresponds to the most flexible motion; at the same time it also corresponds to the maximum product of the required joint torques needed to resist the forces at the end-effector. Assuming the available end-effector force for an arm with tight limitation on joint torques is important for an application, maximum $|J|$ is not a desirable solution. At the position with maximum $|J|$, the manipulator also maximizes the absolute position error. The criterion for the best posture of an arm really depends on the task, and on its motion, force or error requirements.

The $\sqrt{JJ^T}$ has been defined as the measure for kinematic manipulability of a redundant manipulator [Yoshikawa, '85]. The same can be used for considering force manipulability, and all the comments above can be extended to a redundant manipulator. To show this, we explain how the kinematic and force study of a redundant manipulator can be performed on an equivalent non-redundant pseudo manipulator.

For a redundant manipulator we replace $J_{n \times n}$ by $J_{r \times n}$, where $n > r$ and $J_{r \times n}$ is of rank r . Since $J^T J$ is symmetric, we can always get an orthogonal transformation matrix C , which makes $C^T J^T J C$ a diagonal matrix and transforms from a pseudo joint rate vector $\dot{\Phi}$ to $\dot{\Theta}$: $\dot{\Theta} = C \dot{\Phi}$. As $J^T J$ is a semi positive definite matrix of rank r , there will be $n - r$ zero eigenvalues. We partition $C = [C_1, C_2]$ and $\dot{\Phi} = [\dot{\Phi}_1^T, \dot{\Phi}_2^T]^T$, where C_1 corresponds to the non-zero eigenvalues and C_2 to the zero eigenvalues, then we have $J C_2 = 0$ since $[J C_2]^T [J C_2]$ is a null sub-matrix. From $\dot{X} = J \dot{\Theta} = (J C_1 \ J C_2) \dot{\Phi} = (J C_1 \ 0) \dot{\Phi}$ we have $\dot{X} = J_1^* \dot{\Phi}_1$, where $J_1^* = J_1 C_1$. So $\dot{X}^T \dot{X} = \dot{\Phi}_1^T J_1^{*T} J_1^* \dot{\Phi}_1$.

For the force part we define a pseudo torque vector Γ which satisfies $\dot{\Theta}^T \tau = \dot{\Phi}_1^T \Gamma$, then $\Gamma = C^T \tau = [\gamma_1, \gamma_2]^T$. It also satisfies

$$\Gamma = (J C)^T F = [J_1^*, 0]^T F = J_1^{*T} F. \quad (8.3)$$

So $\gamma_1 = J_1^{*T} F$ (and $\gamma_2 = 0$). At this step we have built up a statically equivalent pseudo non-redundant manipulator, with effective pseudo joint rates $\dot{\Phi}_1$ and effective pseudo torques γ_1 . The relations here are quite simple,

$$\delta x_1 \delta x_2 \dots \delta x_r = |J_1^*| \delta \phi_1 \delta \phi_2 \dots \delta \phi_r, \quad (8.4)$$

$$\gamma_1 \gamma_2 \dots \gamma_r = |J_1^*| f_1 f_2 \dots f_r. \quad (8.5)$$

Using $|J_1^*|$ as a measure for kinematic and force manipulability, means we consider the motion and force mechanical advantage with the effective joint rates and effective torques as input. For effective joint rates, $\dot{\Phi}_1^T \dot{\Phi}_1^T$ is the minimum norm of $\dot{\Theta}^T \dot{\Theta}$. For effective torques, $\gamma_1^T \gamma_1 \equiv \tau^T \tau$. Since $|JJ^T| = |JCC^T J^T| = |J_1^{*T} J_1^*| = |J_1^* J_1^{*T}|$, so $\sqrt{JJ^T}$ gives the measure for force manipulability as well.

Sometimes we need to consider the directional mechanical advantages. The optimal configuration of an arm corresponding to the appropriate manipulability then needs to be based on both the indices $\sqrt{J_c J_c^T}$ and $\sqrt{J_m J_m^T}$ or some other partition of the Jacobian matrix. For example, it is beneficial for a 2-link planar manipulator to be in a nearly stretched out position if the motion direction corresponds to the eigenvector due to the maximum eigenvalue and the force direction corresponds to the eigenvector due to the minimum eigenvalue (The singularity direction where the contact force is uncontrollable should always be avoided). The directional measure is also useful in the selection of optimal arm configurations based on dynamic manipulability, because in certain directions we need to have less inertia while in the others we may need to have larger inertias.

Chapter 6

AL LANGUAGE SPECIFICATIONS FOR CONTACT

Using the task-frame specifications discussed in the previous chapter, we now describe extensions to the AL robot language which facilitates the high-level programming of direct contact motions.

A robot language is an interface between a human operator and a robot; a good language can accommodate a wide range of applications. Generality and simplicity are vital attributes of robot languages. Language statements directing the end-effector of a robot to contact or roll-slide on a fixed surface or a workpiece require special programming considerations. Free motion of a manipulator is much simpler to specify than direct contact motion. A user of a robot language should be able to specify a general trajectory for a moving body to maintain contact with a curved surface. In each position, the task frames are important for motion or force control. One problem for a high-level language is how to calculate such task frames. The other problem is how to specify the instantaneous motion requirements with respect to such frames.

We develop the necessary high level statements by modifying the AL robot language to include direct contact statements. AL has been under development at Stanford University for about fifteen years. Its operation commands are syntactically structured as follows:

<i>operation statement</i> <i>with clauses</i>

condition monitor clauses

The *operation statement* specifies the moving object and its destination and via positions; *with clauses* specify the parameters of the trajectory, motion speed, stiffness, etc.; *condition monitor clauses* specify the action under certain run-time conditions. In the following, we use AL to denote the new version of the AL robot language which now contains all the statements discussed in this chapter.

6.1 Geometry of a moving object

As a supplement to the frame data type (which uniquely specifies the spatial position and orientation of a frame on the moving body), an object data type with geometric information has been added to AL as a control identity. Such geometric information is necessary for determining task frames and normal accelerations when the object moves with direct contact between curved surfaces (or is going to be re-positioned in a three-finger-hand).

AL can now define an object in a data declaration statement,

```
object(shape (circular_cylinder, r, l), frame)
```

shape (circular_cylinder, r, l) gives the radius and height of the circular cylinder, and *frame* defines the current position of the object.

For an object moving with point or line contact, only the geometry of its contacting surface is interesting to us, and in many cases it can be represented in an analytic form. We can similarly define analytically simple surfaces such as a sphere, an ellipsoid, a cylinder with rectangular or curved cross sections, and a simple ruled surface. Complex surface geometry can be specified by a sequence of surface points, and be approximated locally by a plane (three points) or a second order algebraic surface (nine points).

A compound object composed of simple blocks can be defined by the affixment statement.

```
affix object1 to object2 by [frame ]
```

6.2 Cartesian trajectory of a moving object

An object's trajectory can be characterized by an interpolation trajectory, a function trajectory, a run-time trajectory, etc.. The interpolation trajectory is the most important during planning. The position trajectory (of a reference point) and rotation trajectory (of the object about the reference point) will be discussed separately.

Position trajectory interpolating through via-points

The position trajectory for contact must satisfy surface constraint. However, determining a contact trajectory from a surface's equation is computationally expensive, we partition the position trajectory under contact into two vectors $X = X_F + \delta X$, where X_F an interpolation trajectory as if the reference point were moving in free space and δX an error-correction trajectory.

In AL we have included three types of trajectories for X_F . The first is composed of a sequence of line segments with sharp corners, where a manipulator has to stop momentarily before switching direction (except when two consecutive segments are aligned). The second is composed of line segments with rounded junctions, whose radii can be determined from centripetal acceleration or geometric constraints. And the third is a smooth planar or spatial curve required for a complex geometric environment or operation. Some spline, say a natural spline (with approximate minimum total curvature), will be used. A user can specify a trajectory by selecting

with position in linear path
with position in curved path

The default is set as the linear trajectory with rounded junctions.

If some velocity is also specified at a via point, the trajectory segment is usually not a line, but a planar or spatial curve

where velocity = vector

When position control is performed on the tangential plane at contact, and force control is performed on the contact normal, δX is automatically corrected by

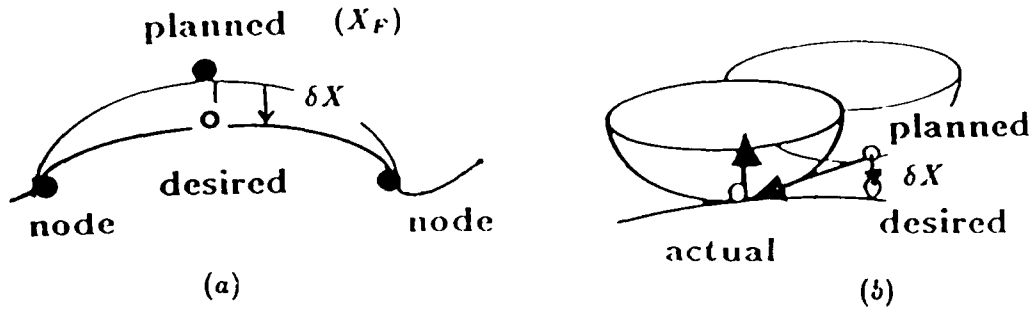


Figure 6.1 *Position-error correction trajectory*

force control. We can calculate δX explicitly in order to obtain the normal acceleration (if there are no sensors available from which to calculate the normal acceleration as described in the last chapter). δX will be a null vector when the object is at either node of a segment (assuming the node points are accurate). For intermediate position δX can be the projection, onto the instantaneous contact normal, of a vector between the planned and actual reference points (under the assumption that the object maintains its contact) (Fig. 6.1(a) (b)).

Rotation trajectory interpolating through via-orientations

When an object moves under point contact, the rotation trajectory can be regarded as though the motion is in free space. When an object moves under line contact, we can partition the rotation trajectory into a free space trajectory and an error-correction trajectory, in a manner similar to that used for position trajectories under point contact.

In free space, the interpolation of rotation trajectories can be calculated using a quaternion representation, for the orientation of a reference line (in an object) and the object's rotation about the line.

Commonly, an orientation A with respect to a reference orientation O can be represented by a quaternion Q_{AO} : a rotation from orientation O to that of A . Similarly, for an orientation B we can have a quaternion representation Q_{BO} . By quaternion calculus we have $Q_{BO} = Q_{BA}Q_{AO}$, where Q_{BA} is a quaternion which

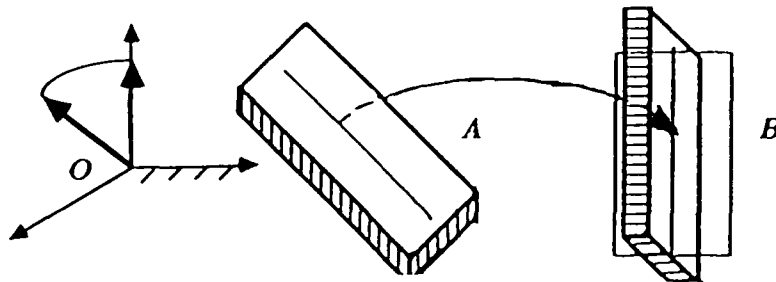


Figure 6.2 *Rotation with a line trajectory specified*

represents a rotation from A to B [Bottema and Roth, '79].

Unfortunately, the interpolation of quaternions does not yield a quaternion which satisfies the rotation requirements. For many rotations, people are interested in the orientation trajectory of a reference line and the object's rotation about the line. Most objects have a meaningful axis (the spinning axis of a screw driver, the symmetric axis of a circular peg, the nozzle axis of a spray gun, etc.), which can be considered as a reference line. In some cases this line is our only concern and we may pay no attention to the object rotation about the line (this is the case for symmetric motions such as inserting a circular peg).

A reference line rotation trajectory commonly can take two patterns. One pattern, as shown in Fig. 6.3(a), occurs when the spherical image curve of a reference line stays in a plane and there is object rotation about the line as well. The actual orientation trajectory of the object is the superposition of a simple rotation of the reference line and the object rotation about the line. We assume that l_1 and l_2 are the initial and goal positions for a reference line, $\bar{\Omega}$ is a vector perpendicular to both of them, and a line R fixed in the moving body initially takes the position of R_1 which is coincident to $\bar{\Omega}$, and R_2 in the goal position. Let θ_2 be a rotation angle about the reference line measured between R_2 and $\bar{\Omega}$. If it is not specified otherwise, the reference line will rotate with a constant angular velocity. In some intermediate position, β_m , the line R moves to an intermediate position R_m , and we can calculate the angle θ_m between R_m and $\bar{\Omega}$ such that $\theta_m = \theta_2 \beta_m / \beta_2$, a proportional rotation about the reference line.

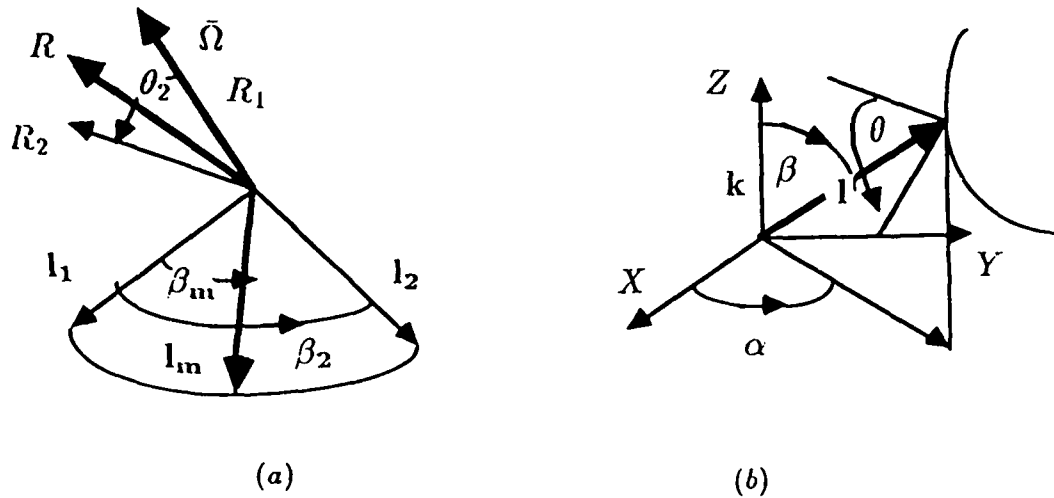


Figure 6.3 *Types of reference-line trajectories*

We adopt the conventions that the rotation angle of the reference line is $\beta_2 \leq 180$ degrees, and that the positive rotation direction around the reference line corresponds to a right-hand screw. If there is no rotation around the reference line, the trajectory is reduced to a simple rotation of the reference line.

The same concept can be extended for several intermediate or via orientations, and the spherical image of the reference line will consist of several planar segments.

The second trajectory pattern follows if we consider that the reference line traces a smooth cone in the spherical image space (a plane is a special case of a cone). A unit vector \mathbf{l} (parallel to the reference line) from the origin is uniquely determined by two angles α, β , where α is the angle rotating about a unit vector \mathbf{k} along the z axis (Fig. 6.3(b)). We can interpolate a natural spline representation of α and β so that α and β are continuous to second order at the end points of each segment. The same continuity will be present in the corresponding spherical image curve. If we add one rotation angle θ about the reference line, then the angular velocity of the body is $\Omega = \dot{\alpha}\mathbf{k} + \dot{\theta}\mathbf{l} + \dot{\beta}\mathbf{k} \times \mathbf{l}/|\mathbf{k} \times \mathbf{l}|$, and its component perpendicular to \mathbf{l} is $\bar{\Omega} = \Omega - \Omega \cdot \mathbf{l} \mathbf{l} = \dot{\alpha}(\mathbf{k} - (\mathbf{k} \cdot \mathbf{l})\mathbf{l}) + \dot{\beta}(\mathbf{k} \times \mathbf{l})/|\mathbf{k} \times \mathbf{l}|$, which

must be parallel to the normal of the spherical image cone. As an alternative to the selection of α and β in determining \mathbf{l} and $\bar{\Omega}$, we can project the end-points of the controlling vectors of the spherical image (starting direction, via directions, and goal direction) onto a plane (for example, a plane tangential to the image sphere), interpolate a curve through those projected points on the plane, and then map each point of the planar curve back to the spherical image. For general motion of a reference line, $\bar{\Omega}$ varies. However, we can still determine θ angle. Assume that a certain line R (fixed in the moving body and perpendicular to the reference line) initially takes position R_1 , which is coincident with the initial $\bar{\Omega}$, and then takes position R_2 at the goal orientation, also assume that θ_2 is an angle measured between the R_2 and the final $\bar{\Omega}$, then the intermediate rotation θ measured between R and Ω , with range 0 to θ_2 , can be interpolated.

For such rotational trajectories, besides via and goal orientations, the user is additionally required to specify a vector parallel to the reference line at the initial position. From such information the system can calculate the via and the goal directions for the reference line and the required rotation angle about the line. The calculation frame, consisting of three mutually perpendicular vectors $R_1, l_1, R_1 \times l_1$, has a fixed orientation with respect to an object frame (they may be coincident). If we have determined the trajectory of the calculation frame, at the same time we know the trajectory of the object frame. Likewise, from the orientation of the object frame we can determine the calculation frame.

In AL one can now specify an orientation trajectory by saying,

with *reference-vector* in planar path
with *reference-vector* in conic path

For the rotation trajectory error correction, if the object is under control of moment or force, the rotation error will be automatically corrected. If there is no accurate force sensor which can determine the angular acceleration along the force-controlled direction, we can explicitly calculate the trajectory. The error-correction trajectory has null values at the beginning and end of a trajectory segment; elsewhere it depends on an error angle measured between the projections of the desired and actual positions of a reference line on a plane which

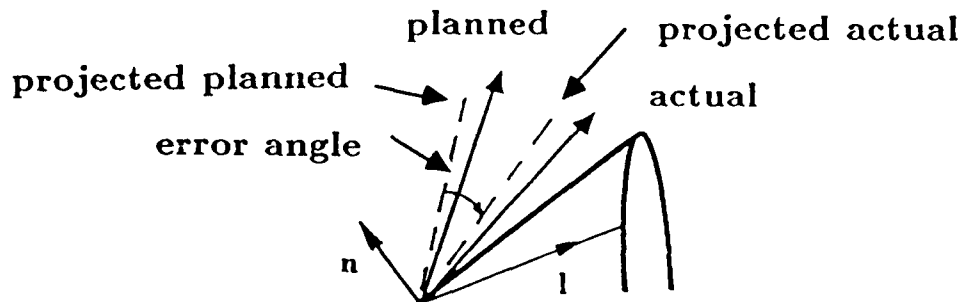


Figure 6.4 Rotation-error correction trajectory

passes through the contact line and the contact normal (Fig. 6.4). Here we assume that the object maintains its line contact.

Function trajectories

AL provides a general helicoidal motion, for which the circular motion is a special case. This can be useful since in assembly most workpieces have either planar or cylindrical surfaces.

move frame by s about *rot_vector* at *pos_vector*
with pitch = s

where the *rot_vector* and *pos_vector* uniquely specify the rotation screw axis, and the pitch is the ratio of the translation along the axis over the rotation angle. Some other function trajectories can be obtained by calculating one of many AL pre-defined functions within a loop structure.

Motion monitored for run-time conditions

Sometimes a motion is monitored for run-time conditions on force, velocity, position, time, etc.: a force condition is sensitive to contact and is useful in locating an obstacle, Fig. 6.5(a); a velocity component (along the sliding surface normal) determines when a tilted peg slides down into a hole, Fig. 6.5(b); position boundary information may provide the limit to stop a motion. AL now lets the user specify

on force *rel s* along *vector* do *action*

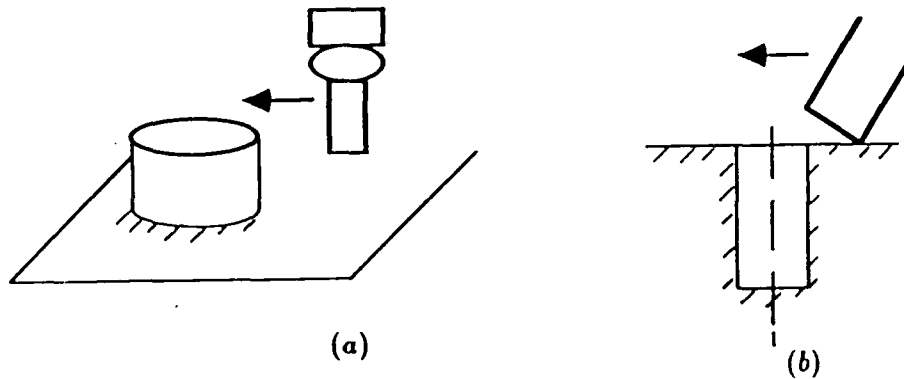


Figure 6.5 Condition-monitored motions

on velocity *rel s* along *vector* do *action*
 on position *rel s* along *vector* do *action*
 on time *rel s* do *action*

where *rel* can be $>$, $<$, \geq , \leq .

Once condition monitors are specified, it is then possible to specify a directional motion using the new move statements

move *frame* along *vector*
 move *frame* about *rotation_vector* at *position_vector*

Similarly, an object-centering strategy (which is sometimes necessary to satisfy assembly clearance requirements or to reduce friction) is also possible. It is performed by having the manipulator make touches at two extreme ends first, then move to the center position. This operation can be performed either along one direction, or two symmetrical directions about a specified axis.

center *object* along (about) *vector*

It is also possible to let a local trajectory, surface contacting or non-contacting, be determined from sensory information. We can build a reflexive strategy into the control system; for example, the local moving direction can be made perpendicular to the surface normal.

The condition monitor can be used for spiral searching as well. Sometimes the exact desired position is not known in advance, but it can be located by match-

ing several run-time conditions, such as force or velocity conditions. When no searching direction is superior to another, the nominal approach is to move in a spiral.

slide *frame* around *vector*
with step = *s*

6.3 Calculation of contact-task frames

Since an object trajectory is partitioned into a position and a rotation trajectory, there is a corresponding positional task frame and a rotational task frame.

AL allows the introduction of a moving object with predefined geometry.

slide [move] *object* [*more specifications*]

From such specifications we know the moving body's geometry and trajectory. We assume there is a force sensor mounted on a robot arm, and consider the kinematics and force sensing aspects for determining the contact task frames, whose origins are usually associated with the contact points.

Positional task frame

As an object moves with surface contact between two planes, a positional task frame can be determined from the trajectory's geometry. The frame's origin is the reference point and its axes are mutually perpendicular unit vectors $\mathbf{i}, \mathbf{j}, \mathbf{k}$, respectively,

$$\mathbf{i} = \frac{\mathbf{v}}{|\mathbf{v}|}, \mathbf{j} = \pm \frac{\mathbf{a} - (\mathbf{a} \cdot \mathbf{i})\mathbf{i}}{|\mathbf{a} - (\mathbf{a} \cdot \mathbf{i})\mathbf{i}|}, \mathbf{k} = \mathbf{i} \times \mathbf{j},$$

where \mathbf{v} and \mathbf{a} are the velocity and acceleration of the reference point, and \mathbf{k} is the trajectory plane's normal. We assign the x axis along the trajectory's tangent, and z axis along the trajectory normal.

When a reference point moves in a straight line, the principal normal and bi-normal are undefined. For an axially symmetrical motion (for example, inserting a circular peg), the explicit determination of one axis may not be necessary; in many other cases (for example, sliding an object on a plane) we may need

to specify one axis, corresponding to the plane normal, for the positional task frame.

with pos_frame $y(z) = vector$

For some cases of planar motion with point contact between two curves, the positional task frame can be determined from the trajectory alone with the appropriate choice of a reference point. For a planar motion with point contact, the trajectory of a generic point on a moving curve does not necessarily trace the fixed curve; however, if the contact point is invariant with respect to the moving curve, its motion trajectory should follow the fixed curve. At any instant, all points on a line moving to coincide with the curve normals (except points coinciding with the curvature center point of the fixed curve) have the same tangent and normal directions as those of the fixed curve. If there is a point fixed in the object such that it always lies on the contact normal, then the tangent and normal of its trajectory are parallel to those of the fixed curve at the contact point. One common example is when a contact point is fixed with respect to a moving curve. When a moving curve is reduced to a circle, although the contact point varies with respect to the circle, the center point is fixed in the moving circle, and can be chosen as a reference point.

Other than in the special cases above, we usually require additional knowledge of a moving body's geometry or motion kinematics in order to determine the positional task frame for a general planar motion with point contact between two curves. For pure rolling the contact point is at the intersection of the normal of the reference point's trajectory and the moving curve. For pure translation, the contact point is at the intersection of the moving curve and a tangent line parallel to the velocity. For general motion, we need to find a point on the moving curve with null normal velocity (given the contact point at the last instant, the current point will be in its vicinity). After the contact point has been located, the contact normal can be determined from the moving curve.

One exception for pure translation is when the moving curve reduces to a line. In this case, the exact contact point is not obvious from only the moving curve information, but the contact normal direction is certainly known.

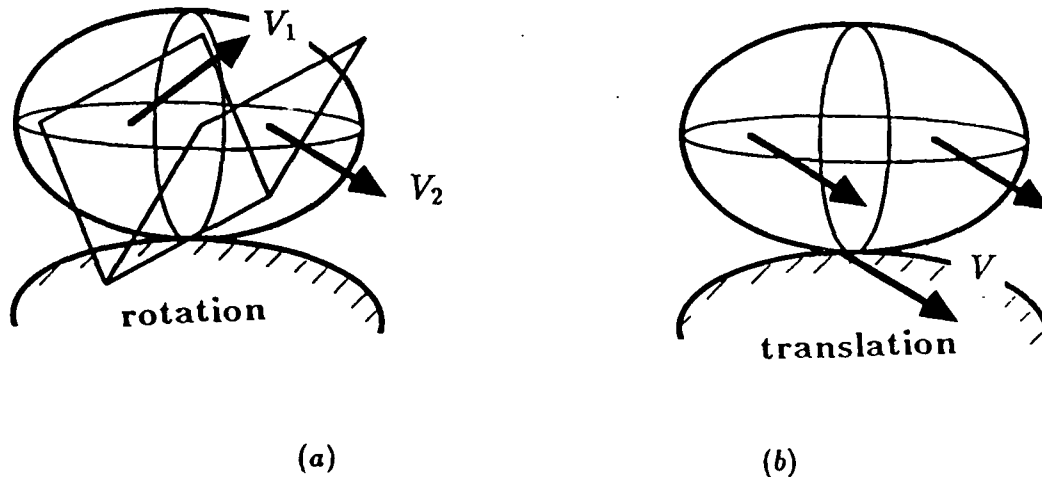


Figure 6.6 *Spatial motion with point contact*

For the spatial motion of a rigid object with point contact (and no frictional torques at the contact point), the velocity field provides only a partial guide in determining the contact point. For pure rolling (Fig. 6.6(a)), we can pick two arbitrary points in the moving body, and find the intersection line of the normal planes of their point trajectories, this line intersects the moving surface at the contact point. However, for pure translation (Fig. 6.6(b)), the normal planes are all parallel and we cannot use the velocity to determine the contact point. Obviously, for a general motion the control frame can not be completely determined just from the motion trajectory and moving surface geometry.

The alternative, which is actually simple and fast, is to determine the contact point from force sensors. Under the constraint of no frictional torque at the contact point, we can generally find a force wrench axis which intersects the moving surface at the contact point, regardless of whether the moving body undergoes a pure rolling, a pure sliding or a general motion, and regardless of whether there are frictional forces at the contact or not.

Rotational task frame

When the rotation trajectory is obtained by quaternion interpolation, we can have one axis of the rotational task frame parallel to either the angular velocity,

or a finite displacement screw axis, or one axis of the world frame. However we prefer to have the rotation trajectory associated with a reference line, in which case the spherical image of the reference line yields a cone. We take the x axis of the rotational task frame parallel to the reference line, and the z axis parallel to the contact normal of the cone ($\tilde{\Omega}$ as mentioned in the last section). This task frame is justifiable since we are interested in the motion of a reference line and the object rotation about the line.

For a simple rotation, although a reference line is usually not explicitly specified, the rotation axis quite often has a clear operational meaning and we can regard it as a reference line; in addition, we need to explicitly specify one axis to complete the definition of the task frame. It seems convenient to specify the axis with respect to an object frame or a frame affixed to it (a hand frame if the object is grasped by a simple gripper). The following statements will now accomplish this.

with rot_frame $y(z) = \text{vector}$
 with rot_frame $y(z) = \text{vector wrt world}.$

When an object is under line contact, the x axis is the contact line, and the z axis is parallel to the contact normal. The positional task frame and rotational task frame have one axis (contact normal) in common.

The kinematic condition for line contact on a ruled surface is that there is no angular velocity component in the direction which is perpendicular to both the contact line and contact normal. From the force condition, the force wrench axis always passes through the contact line if the friction torque about the contact line is negligible. If there is sliding at the contact line, the force wrench becomes a pure force.

6.4 Motion constraints with respect to task frames

In order to have satisfactory relative motion of the end-effector under contact, the error-tolerances, stiffnesses, forces and directional wobble are important parameters which need to be specified with respect to the task frames.

Error tolerance is necessary for obstacle avoidance as well as in operations requiring precision. By the appropriate choice of error tolerances, we can make an operation more efficient and economical. Especially when a redundant manipulator is used, bigger tolerances allow for turning off fine motion, and driving only the coarse motion.

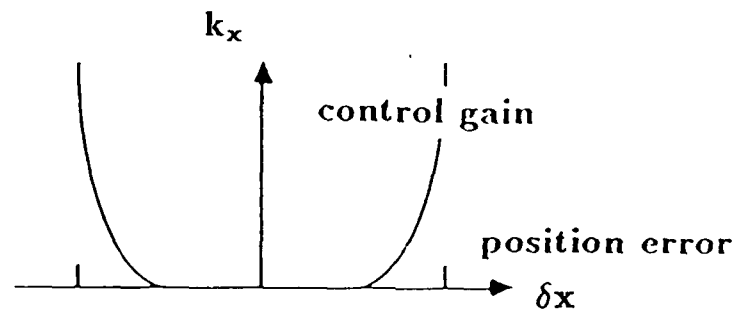


Figure 6.7 A corresponding control gain for an error tolerance

To the run-time control system, an error tolerance is seen as a variable control gain or stiffness. Take the x direction as an example: we can pick $k_x = 1/|(\delta x + a)(\delta x - a)|$, where a is the error tolerance in the x direction and δx a measured error (Fig. 6.7).

In AL one can now specify the error tolerance by simply saying

with tolerance = (s, s, s) with tolerance = (s, s, s, s, s, s)

Instead of error tolerance, we sometimes specify constant stiffness coefficients, and in the contact direction AL interprets the stiffness as directly associated with the contact surface. Normally the stiffness coefficients are regarded as the position gains for a robot, or the stiffness between the robot and an object. In certain situations, e.g. polishing or grinding, we require the force applied by the tool to a workpiece to be proportional to the position error, in these cases the tool's inertia and elasticity should be taken into account.

When the contact surface is elastic with stiffness coefficient k_s , the effective stiffness coefficient for the direct contact will be equal to or less than k_s . If k_s is

zero, as in free space, no force is applied between the object and the environment. AL can do automatic mode selection: when noting a hard contact it uses force control, otherwise it uses pure position control.

For most cases, a force trajectory is not independent of the motion trajectory. For a force guarded motion, the desired force is usually a constant along one or two axes of the positional task frame. Similarly, with respect to the rotational task frame, moments of force are normally specified on one or two axes.

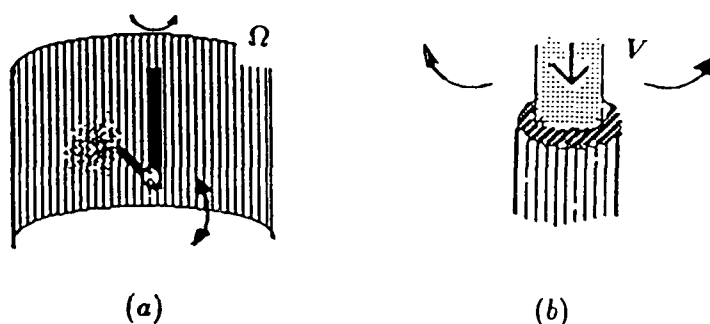


Figure 6.8 Examples of directional wobble

Directional wobble was added to AL in order to expand the types of built-in motion trajectories and for reducing friction. In operations such as erasing a line of pencil writing, or using a piece of cloth to clean a long narrow area: one traces a zigzag trajectory, this is a wobble motion perpendicular to the main direction of motion. Accurate straight line motion is not desirable because dirt will be accumulated along the moving direction. Other examples are the use of rotational wobble for a spray gun's motion in order to have an up and down wobble rotation to cover more area, Fig. 6.8(a), and the use of positional wobble to break friction along a motion trajectory. (It is also used in welding to get a good bead.)

The directional wobble should be specified with respect to the task frame. The translational wobble motion is desired to be perpendicular to, or axially symmetrical about the trajectory. It is most appropriately specified with respect to

the positional task frame. A similar relation holds between the rotational wobble motion and the rotational task frame. The wobble rotation can be specified with respect to one axis of the rotational task frame. We have implemented in the 3- and 6-axes statements:

with wobble = (s, s, s) with wobble = (s, s, s, s, s, s)

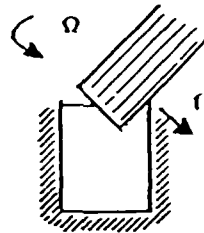


Figure 6.9 A peg rotation

For the application of error tolerances, stiffnesses, forces and wobble constraints, in certain situations the positional task frame and rotational task frame are coincident. For example, in Fig. 6.9, the exact contacting point will be hard to predict. Since we are interested in having constant contact force along the contacting surface normal regardless of contact point, the positional task frame becomes exactly the same as the rotational task frame. Another example occurs when a peg is to be inserted into a cylindrical hole, since no orientation trajectory is defined. If we have the peg axis parallel to that of the hole, we may need to apply a wobble rotation about the axis in order to reduce friction (Fig. 6.8(b)). The rotational task frame is equivalent to the positional task frame in this case.

Another common example of a rotational task frame being coincident to a positional task frame is when one planar surface is sliding on another. In this case there will be some orientation discrepancy between the two surfaces due to trajectory error. To maintain the planar contact, we need to specify either null rotational stiffness coefficients or null moments on the tangential surface; the tangential surfaces are spanned by the two axes of the positional task frame.

In AL we can now characterize these situations by saying,

with path_frame $y(z) = vector$

Chapter 7

IMPACT IMPULSE AND LINK-MASS DISTRIBUTION

All the previous chapters deal with one object already in direct contact another. In this chapter we consider the instant when two objects are making contact. If a high speed motion is underway, or a large mass is being moved, a fairly strong collision may occur at contact. At the instant of collision, the manipulator's control system can do little to mitigate the impact's impulse. In this chapter we analyze the relationships between the impact impulse and the mass distribution of a revolute-jointed planar manipulator. This provides a guide to the proper design and motion planning for parallel axes revolute-joint manipulators working under impact conditions.

This chapter starts with a discussion of what we call the link-space representation, then analyzes the factors associated with the impact impulse at the point of contact. These include the optimum pivot location for a general link, the mass distribution among different links, the influence of the last link, and the change of angular velocity and reaction impulse at each joint.

Fig. 7.1 shows a revolute-joint planar manipulator with n moving links. For the i^{th} link, m_i , I_i are respectively the link mass and the moment of inertia about its joint with the $i - 1$ link, l_i is the distance between its two joints, l_i^* is the distance from its joint with the $i - 1$ link to the link-mass center, and β_i is the angle between the lines along which we measure l_i and l_i^* . We also assume each joint is frictionless, and there is one impact contact point with the environment,

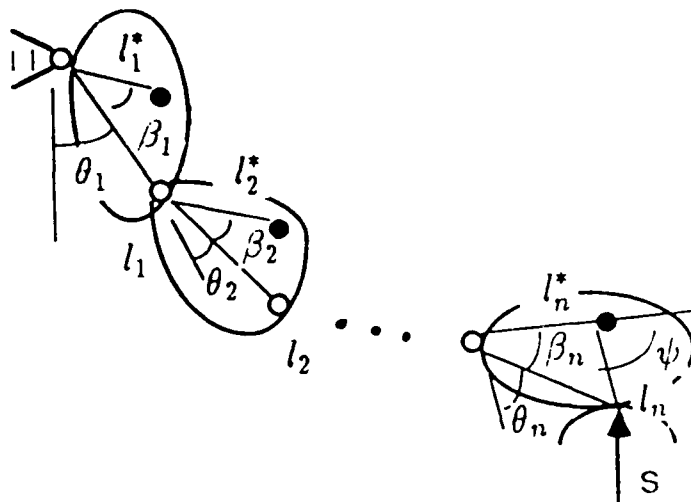


Figure 7.1 A planar manipulator

which is fixed on the end-effector. The base reference coordinate frame will be chosen so that its y-axis is parallel to the instantaneous contact normal.

7.1 Representation in link space

In this chapter we use a link-space representation. The link-space coordinates are the rotation angles of the links with respect to the same fixed line, and the torques on links relative to the base system. The Jacobian matrix, which relates the velocity of the contact point to the joint velocity rates, and the inertia matrix will take simpler forms in link-space than those in joint-space coordinates. Furthermore, in link-space coordinates, the link torques are related to the contact force by the transpose of this same simpler Jacobian matrix.

To illustrate the link-space simplification, we take a 3-link chain as an example. If we follow the usual joint-space convention and use the relative rotations between neighboring links, we have $\dot{\Theta}^* = [\dot{\theta}_1, \dot{\theta}_2, \dot{\theta}_3]^T$. The velocity, \dot{X} , at the contact point satisfies $\dot{X} = J^* \dot{\Theta}^*$, where

$$J^* = \begin{pmatrix} l_1 \cos \theta_1 + l_2 \cos \theta_{12} + l_3 \cos \theta_{13} & l_2 \cos \theta_{12} + l_3 \cos \theta_{13} & l_3 \cos \theta_{13} \\ l_1 \sin \theta_1 + l_2 \sin \theta_{12} + l_3 \sin \theta_{13} & l_2 \sin \theta_{12} + l_3 \sin \theta_{13} & l_3 \sin \theta_{13} \end{pmatrix}; \quad (1.1)$$

the inertia matrix in joint space is

$$M^* = \begin{pmatrix} I_1 + m_{23}l_1^2 + m_2l_{12}^* + m_3l_{13}^* & m_2l_{12}^* + m_3l_{12} + m_3l_{13}^* & m_3l_{13}^* \\ m_2l_{12}^* + m_3l_{12} + m_3l_{13}^* & I_2 + m_3l_2^2 + m_3l_{23}^* & m_3l_{23}^* \\ m_3l_{13}^* & m_3l_{23}^* & I_3 \end{pmatrix}. \quad (1.2)$$

Here, $\theta_{12} = \theta_1 + \theta_2$, $\theta_{13} = \theta_1 + \theta_2 + \theta_3$, $m_{23} = m_2 + m_3$, $l_{12} = l_1l_2\cos\theta_2$, $l_{12}^* = l_1l_2^*\cos(\theta_2 + \beta_2)$, $l_{13} = l_1l_3\cos(\theta_2 + \theta_3)$, $l_{13}^* = l_1l_3^*\cos(\theta_2 + \theta_3 + \beta_3)$, $l_{23} = l_2l_3\cos\theta_3$, and $l_{23}^* = l_2l_3^*\cos(\theta_3 + \beta_3)$.

Noticing that there are many overlaps in expressions (1) and (2), we instead use the links' absolute angular velocity vector, $\dot{\Theta}$, as a base; $\dot{\Theta} = [\dot{\theta}_1, \dot{\theta}_1 + \dot{\theta}_2, \dot{\theta}_1 + \dot{\theta}_2 + \dot{\theta}_3]^T$. We let the velocity at the contact point satisfy $\dot{X} = J\dot{\Theta}$. Then, the Jacobian matrix, J , becomes

$$J = \begin{pmatrix} l_1 \cos \theta_1 & l_2 \cos \theta_{12} & l_3 \cos \theta_{13} \\ l_1 \sin \theta_1 & l_2 \sin \theta_{12} & l_3 \sin \theta_{13} \end{pmatrix}, \quad (1.3)$$

and the corresponding inertia matrix, M , becomes

$$M = \begin{pmatrix} I_1 + m_{23}l_1^2 & m_2l_{12}^* + m_3l_{12} & m_3l_{13}^* \\ m_2l_{12}^* + m_3l_{12} & I_2 + m_3l_2^2 & m_3l_{23}^* \\ m_3l_{13}^* & m_3l_{23}^* & I_3 \end{pmatrix}. \quad (1.4)$$

The expressions (3) and (4) are simpler and hence more efficient for computation than (1) and (2).

The same concept can be extended to an n -link chain. We define $\dot{\Theta} = [\dot{\theta}_1, \dot{\theta}_{12}, \dots, \dot{\theta}_{1n}]^T$. θ_{1i} is the orientation angle, of the i^{th} link, relative to the base; $\theta_{1i} = \theta_1 + \theta_2 + \dots + \theta_i$. Below we use the notations $l_{ij} = l_i l_j \cos(\theta_{i+1} + \theta_{i+2} + \dots + \theta_j)$, $l_{ij}^* = l_i l_j^* \cos(\theta_{i+1} + \theta_{i+2} + \dots + \theta_j + \beta_j)$, and $m_{ij} = m_i + m_{i+1} + \dots + m_j$. The Jacobian matrix now is:

$$J = \begin{pmatrix} J_T \\ J_N \end{pmatrix} = \begin{pmatrix} l_1 \cos \theta_1 & l_2 \cos \theta_{12} & \dots & l_n \cos \theta_{1n} \\ l_1 \sin \theta_1 & l_2 \sin \theta_{12} & \dots & l_n \sin \theta_{1n} \end{pmatrix}. \quad (1.5)$$

The corresponding inertia matrix is:

$$M(n \times n) = \begin{pmatrix} I_1 + m_{2n}l_1^2 & m_2l_{12}^* + m_{3n}l_{12} & \dots & m_nl_{1n}^* \\ m_2l_{12}^* + m_{3n}l_{12} & I_2 + m_{3n}l_2^2 & \dots & m_nl_{(n-1)n}^* \\ \vdots & \vdots & \ddots & \vdots \\ m_nl_{1n}^* & m_nl_{(n-1)n}^* & \dots & I_n \end{pmatrix}. \quad (1.6)$$

In the case of a slender-rod linkage, the mass center of each link is at its geometric center. Hence, $l_i^* = l/2$ and $\beta_i = 0$. The moment of inertia, of the i^{th} link about either of its joint axes, is $I_i = 1/3 m_i l_i^2$. m_i is the mass and l_i is the length of the i^{th} link. (6) becomes

$$M(n \times n) = \begin{pmatrix} (\frac{1}{3}m_1 + m_{2n})l_1^2 & (\frac{1}{2}m_2 + m_{3n})l_{12} & \cdots & \frac{1}{2}m_n l_{1n} \\ (\frac{1}{2}m_2 + m_{3n})l_{12} & (\frac{1}{3}m_2 + m_{3n})l_2^2 & \cdots & \frac{1}{2}m_n l_{(n-1)n} \\ \vdots & \vdots & \ddots & \vdots \\ \frac{1}{2}m_n l_{1n} & \frac{1}{2}m_n l_{(n-1)n} & \cdots & \frac{1}{3}m_n l_n^2 \end{pmatrix}. \quad (1.7)$$

In link space, a link torque vector, Γ , is related to the contact force at the contact point, F , by the transpose of the Jacobian matrix, J^T . We assume the joint torque vector, τ , has components τ_i ; $i = 1, 2, \dots, n$. The link torque vector, $\Gamma = [\gamma_1, \gamma_2, \dots, \gamma_n]^T$, should satisfy

$$\dot{\Theta}^T \Gamma = \dot{\Theta}^{*T} \tau = \tau_1 \dot{\theta}_1 + \tau_2 \dot{\theta}_2 + \dots + \tau_n \dot{\theta}_n. \quad (1.8)$$

This is equivalent to

$$\begin{pmatrix} \gamma_1 + \gamma_2 + \gamma_3 + \dots + \gamma_n \\ \gamma_2 + \gamma_3 + \dots + \gamma_n \\ \vdots \\ \gamma_n \end{pmatrix} = \begin{pmatrix} \tau_1 \\ \tau_2 \\ \vdots \\ \tau_n \end{pmatrix};$$

$$\Gamma = [(\tau_1 - \tau_2), (\tau_2 - \tau_3), \dots, \tau_n]^T. \quad (1.9)$$

On link i , τ_i is the active torque applied by joint i , and τ_{i+1} is the reaction torque applied from joint $i + 1$, so $\gamma_i = \tau_i - \tau_{i+1}$ is the resultant applied torque. Since $\dot{\Theta}^{*T} \tau$ in (8) is equal to $\dot{X}^T F$, and since $\dot{X} = J\dot{\Theta}$, the contact force at the contact point, F , is mapped to Γ by J^T :

$$\Gamma = J^T F. \quad (1.10)$$

The idea of link space can also be applied to spatial linkages. For either planar or spatial linkages with several series and several in-parallel connected links, we can combine a partial link space and a partial joint space.

7.2 Impact impulse at point of contact

Based on link-space representations, we now obtain the impact impulse at the point of contact, as a function of approach velocity and linkage configuration. The derived expressions consider general situations and one particular case: perfectly elastic collision and no surface friction.

We assume that all conventional external forces, such as gravitational forces and applied torques are approximately constant during the impact interval (which is much shorter than the usual controller's sampling period), and that their resultants are negligible compared to the impact's impulse. Hence, from (1.10), the environment acts on the manipulator with a generalized impulse vector $\mathcal{I} = J^T \int F dt$. Since Θ is a generalized coordinate vector, the manipulator's generalized momentum vector is $P = \partial K / \partial \dot{\Theta} = M \dot{\Theta}$. From the principle that the generalized impulse applied to a system equals its change in generalized momentum [Kane and Levinson, '85], $P(t_2) - P(t_1) = \mathcal{I}$:

$$\dot{\Theta} - \dot{\Theta}^\circ = M^{-1} J^T S. \quad (2.1)$$

S is the impact impulse vector which is transmitted to the manipulator at the contact point; $S = \int F dt = [S_T, S_N]^T$. The subscripts T and N denote the tangential and normal components, respectively. We take N as always pointing toward manipulator's contact point along the common contact surface normal and T such that according to the right-hand rule, $T \times N$ yields a vector pointing out of the paper. $\dot{\Theta}^\circ$ and $\dot{\Theta}$ are the links' angular velocity vectors before and after collision, respectively; $\dot{\Theta}^\circ = [\dot{\theta}_1^\circ, \dot{\theta}_{12}^\circ, \dots, \dot{\theta}_{1n}^\circ]^T$. If by joint angle sensing we can determine the velocities in both states, then the impact impulse S can be calculated from

$$S = [J J^T]^{-1} J M (\dot{\Theta} - \dot{\Theta}^\circ). \quad (2.2)$$

By virtue of the constraints on the normal and tangential velocity components after collision, S can be represented as a function of $\dot{\Theta}^\circ$. Using the coefficient of restitution e [Kane and Levinson, '85], we relate the normal contact velocity after collision to its value before collision: $J_N \dot{\Theta} = -e J_N \dot{\Theta}^\circ$.

The constraints on the tangential velocity component are related to friction. If $|S_T| \leq \mu|S_N|$, where μ is the coefficient of friction, there will be no sliding after collision. That is $v_x(t_2) = 0$ or $J_T \dot{\Theta} = 0$, and from (1) the impact impulse becomes

$$S = -[JM^{-1}J^T]^{-1} \begin{pmatrix} J_T \\ (1+e)J_N \end{pmatrix} \dot{\Theta}^o. \quad (2.3)$$

If $|S_T| = \mu|S_N|$ or $S_T = \pm\mu S_N$, there will be sliding after collision, and from (1) the normal impact impulse becomes instead

$$S_N = -(1+e)[J_N M^{-1} J^T \begin{pmatrix} \pm\mu \\ 1 \end{pmatrix}]^{-1} J_N \dot{\Theta}^o. \quad (2.4)$$

The sign is determined from the condition $S_T v_T = S_T (J_T \dot{\Theta}) < 0$.

For our study we assume a perfectly elastic collision, $e = 1$, and a frictionless contact, $\mu = 0$. Then, the impact impulse has only a normal component. These assumptions will not affect our basic conclusions, because e 's value only affects the magnitude of S_N , while μ is almost always relatively small. (4) now becomes

$$S_N = -\frac{2J_N \dot{\Theta}^o}{[J_N M^{-1} J_N^T]} = -\frac{2v_N^o}{[J_N M^{-1} J_N^T]}, \quad (2.5)$$

where v_N^o is the normal component of the approach velocity at the contact point.

7.3 Effect on S_N of the last link's mass distribution

We consider the effect of the mass distribution of the last link on the impact impulse. The result shows that given the mass distribution and the orientation, there exists an optimal pivot location which minimizes the impact impulse; the corresponding S_N is equivalent to that obtained when the link is free from joint constraint.

To see the influence of the last link's inertia distribution on S_N , we first obtain the impact impulse on a single planar link while rotating about a fixed support, as in Fig. 7.2. Applying (2.5) to this configuration yields

$$S_N = -2mv_N^o \left(\frac{\rho}{d}\right)^2. \quad (3.1)$$

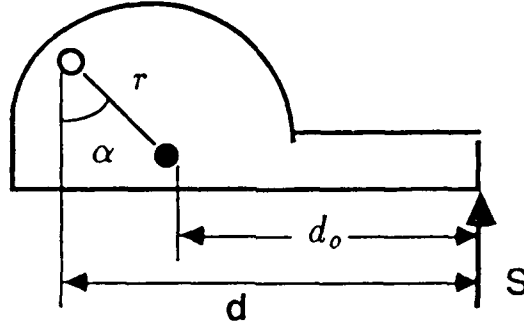


Figure 7.2 Configuration of the last link

ρ is the radius of gyration about its joint, and d is the distance between the joint pivot and the line of the contact normal. Given the mass and the approach velocity, in order to reduce the impact impulse, we need to reduce ρ^2/d^2 ; $\theta_1 = 90$ degrees corresponds to maximum d .

There exists an optimal solution for pivot location. We assume that the radius of gyration about the mass center is ρ_o , the distance between the mass center and line of action of the contact normal is d_o , and that a general pivot position is characterized by variables r and α . Then,

$$S_N = -\frac{(\rho_o^2 + r^2)}{(d_o + r \sin \alpha)^2} 2mv_N^o. \quad (3.2)$$

From $\partial S_N / \partial \alpha = 0$ and $\partial S_N / \partial r = 0$, we obtain the optimal conditions α^* , r^* :

$$\alpha^* = \frac{\pi}{2}, \quad (3.3)$$

$$r^* = \frac{\rho_o^2}{d_o}. \quad (3.4)$$

Substituting α^* , r^* into (2), we obtain minimum S_N :

$$S_N = -\frac{\rho_o^2}{(d_o^2 + \rho_o^2)} 2mv_N^o. \quad (3.5)$$

We can verify that this is equivalent to the formula obtained when the link is free from joint constraint. In other words, there will be no reaction to the impact

impulse at the joint. This is the well-known result that if the impact load is at the center of percussion there are no pivot reaction forces.

Based on this optimal pivot location, we can also compare the effect of a link's geometric shape on S_N . For example, for a slender rod of length l with uniformly distributed mass and perpendicular contact at the end, $r^* = l/6$ —the optimal pivot is at $l/3$; $S_N = -mv_N^o/2$. For a disk with diameter D and uniformly distributed mass, if we assume $d_o = D/2$, then $r^* = D/4$; $S_N = -2mv_N^o/3$.

7.4 Mass proportions of links for reducing S_N

Except in the case when the last joint is an instantaneous optimal pivot for the last link, the supporting links affect the impact impulse on the manipulator. In this section and in sections 6 and 7, we consider the relationships between the impact impulse and the mass distribution among the links.

In this section we analyze how to distribute mass among links in order to reduce S_N . The value of S_N in (2.5) is a function of mass distribution and link orientation, but independent of each link's length. We will show that in order to reduce S_N , generally the mass of the last link should be less than that of its supporting link. Similarly, the mass of that supporting link should be less than its own supporting link's. Although this will also be true for all the rest of the links, we will show later that the other links have little influence on S_N .

For members with uniformly distributed mass, $[J_N M^{-1} J_N^T]$ is independent of each link's dimensions. This can be seen if we express the inverse of the inertia matrix in (1.7) as

$$M^{-1} = \frac{[\bar{m}_{ij}]_{n \times n}}{|M|}, \quad |M| = A \prod_{i=1}^n l_i^2, \quad \bar{m}_{ij} = \frac{B_{ij} \prod_{i=1}^n l_i^2}{l_i l_j}.$$

A and B_{ij} are coefficients independent of l_i . Then,

$$[J_N M^{-1} J_N^T] = \frac{1}{|M|} \sum_{i,j} l_i l_j \sin \theta_{i1} \sin \theta_{j1} \frac{B_{ij} \prod_{i=1}^n l_i^2}{l_i l_j} = \frac{1}{A} \sum_{i,j} \sin \theta_{i1} \sin \theta_{j1} B_{ij}.$$

In cases where links are other than slender-rods, we can take $l^* = g.l_i$, and a similar link-length independence follows.

If we wish to reduce S_N , the last link's mass should be less than that of its supporting link. For example for a slender-rod 2-link chain of total mass M , $m_1 = \lambda M$, and $m_2 = (1 - \lambda)M$, when the chain is in a straight out position

$$S_N = -\frac{1}{2}\left(\frac{\lambda}{3} + 1\right)(1 - \lambda) \frac{M v_N^o}{\sin^2 \theta_1} = -\frac{f_2(\lambda) M v_N^o}{\sin^2 \theta_1}. \quad (4.1)$$

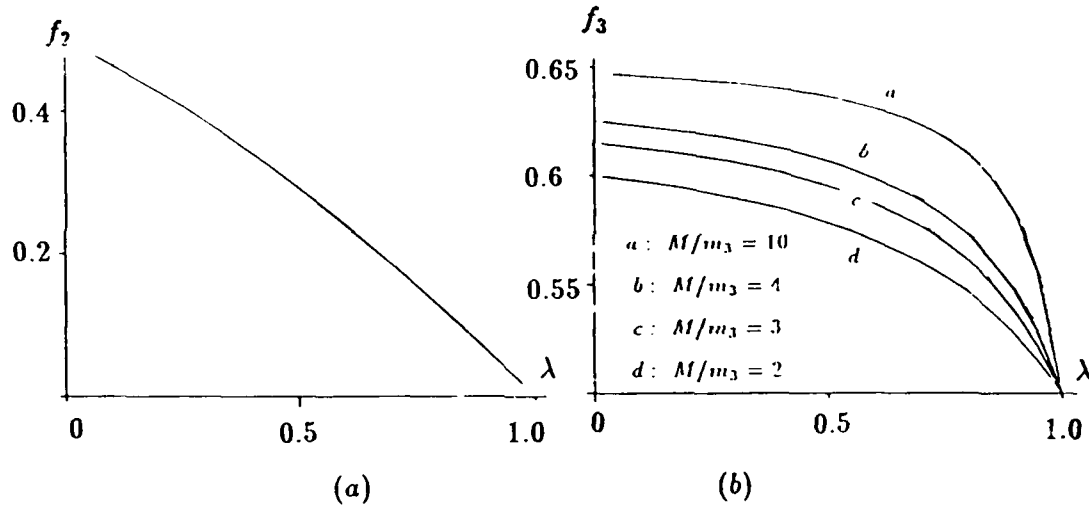


Figure 7.3 Influence on S_N of mass proportions of 2- or 3-link chain

In Fig. 7.3(a) a plot of $f_2(\lambda)$ shows that $f_2(\lambda)$ drops almost linearly with respect to λ . When $\lambda = 1$, i.e., when the mass of the last link is negligible, F_2 , hence S_N , becomes 0.

For the same reason, the mass of the link next to the last should also be less than that of its supporting link. This can be illustrated with an example of a slender-rod 3-link chain in a straight out position. We assume that the last link is of mass m_3 , the first two links have total mass M , $m_1 = \lambda M$, $m_2 = (1 - \lambda)M$,

and $M/m_3 = x$. Then

$$S_N = -\frac{2}{3} \left[\frac{x(1-\lambda)(\lambda+3)+3}{x(1-\lambda)(\lambda+3)+4} \right] \frac{m_3 v_N^o}{\sin^2 \theta_1} = -\frac{f_3(\lambda, x) m_3 v_N^o}{\sin^2 \theta_1}. \quad (4.2)$$

In Fig. 7.3(b) we plot $f_3(\lambda, x)$ as a family of curves with different fixed values of x . From these we notice that when $\lambda = 1$, i.e., the last link is connected to a massless link, S_N has the smallest coefficient 0.5; when $\lambda = 0$, i.e., the second link has all the mass M , the coefficient of S_N has the largest value.

When links are other than slender rods, the functions $f_2(\lambda)$ and $f_3(x, \lambda)$ will have different numerical values, but the same tendency of change is to be expected.

7.5 Dominant influence of last link on S_N

Comparing Fig. 7.3(a) and Fig. 7.3(b), we notice that f_2 drops faster than f_3 as λ increases; this is because S_N is most sensitive to the mass of the last link. Actually, S_N is approximately proportional to the mass of the last link, and inversely proportional to the square of the sine of its orientation angle.

The approximate proportionality to the last link's mass can be seen from the expression for S_N . For a 2-link chain of slender rods,

$$\begin{aligned} S_N &= - \left[\frac{m_1 + 3m_2(1 - 3/4 \cos^2 \theta_2)}{m_2 \sin^2 \theta_1 / \sin^2 \theta_{12} - 3m_2 \cos \theta_2 \sin \theta_1 / \sin \theta_{12} + m_1 + 3m_2} \right] \frac{2m_2 v_N^o}{3 \sin^2 \theta_{12}} \\ &= -F_2 m_2 v_N^o \end{aligned} \quad (5.1)$$

The S_N for a 3-link chain of slender rods can be similarly expressed as

$$S_N = -F_3 m_3 v_N^o. \quad (5.2)$$

Both F_2 and F_3 are dimensionless.

For any link shape, we can partition each moment of inertia I_i in (1.6) as a product of mass and radius of gyration. The general expression for S_N for a 2 or 3-link chain will show, that there is approximately an m_n factor in its numerator.

When the mass of the last link, within a slender-rod linkage, is much less than the mass of the rest of the links, the impact impulse at contact simply takes the form

$$S_N = -\frac{2m_n v_N^o}{3\sin^2\theta_{1n}}. \quad (5.3)$$

For a general link shape, the formula for the case where the last link's mass is comparatively very small is as shown in (3.1). This solution is equivalent to the one for a link attached to a moving base with relatively huge inertia.

As we have seen, S_N is approximately inverse to $\sin^2\theta_{1n}$ for a slender-rod linkage. Regardless of θ_1 for such a 2-link chain, the θ_{12} , which minimizes F_2 , is around 90 degrees –the link is parallel to the contact tangent; the θ_{12} , which maximizes F_2 , is around zero degrees –the link is parallel to the contact normal.

The angles 0° and 90° for a slender-rod linkage actually satisfy the global optimization conditions: $\partial S_N / \partial \theta_{1j} = 0; j = 1, 2, \dots, n$. For a general shape of the last link, on which the impact point is assumed invariant, we define the orientations of the last link which minimize S_N and maximize S_N to be γ_{min} and γ_{max} , respectively. Although γ_{min} should be determined from the global optimization conditions above, we can specify its range from the results of Section 3. When the last link is supported by a fixed base we know that $\theta_{1n} = 90^\circ$, and when the last link is free from constraint we notice from (3.5) that d_o becomes a maximum when a line through the contact point and mass center is parallel to the contact tangent. From Fig. 7.1 the last link's angle should be $\theta_{1n} = 90 + \psi - \beta_n$. So, γ_{min} is in the range $[90, 90 + \psi - \beta_n]$; $\gamma_{max} = \gamma_{min} - 90$. When the mass center is collinear with the contact point and the joint, then $\gamma_{min} = 90$, and $\gamma_{max} = 0$.

7.6 Influence of other links on S_N

The influences of links other than the last one on S_N are affected by the orientation of the last link and their nearness, in terms of sequence, to the last link. It turns out that when the last link gradually rotates from γ_{max} (the link is or nearly is parallel to the contact normal) to γ_{min} (the last link is or nearly is parallel to the contact tangent), the influence on S_N of the two links immediately before the

last decreases, though at the start the influence is significant. It becomes very small once the last link is nearly at γ_{min} . The influence on S_N decreases as one moves backwards link by link toward the fixed end of the chain.

When the last link is at γ_{max} , all its mass is moving in the impact direction, and its supporting link now dominates any variation in S_N . For example, taking $\theta_{12} = 0$ in (5.1) yields

$$S_N = -\frac{2m_1 v_N^o}{3\sin^2\theta_1} \left[1 + \frac{3m_2}{m_1} \left(1 - \frac{3}{4}\sin^2\theta_2 \right) \right]. \quad (6.1)$$

We see S_N is now approximately proportional to m_1 , and inversely proportional to $\sin^2\theta_1$. The last link in this case increases S_N so that when $\theta_2 = 90$ degrees, and $m_1/m_2 = 1$, the S_N is 1.75 times as large as it would be without the last link.

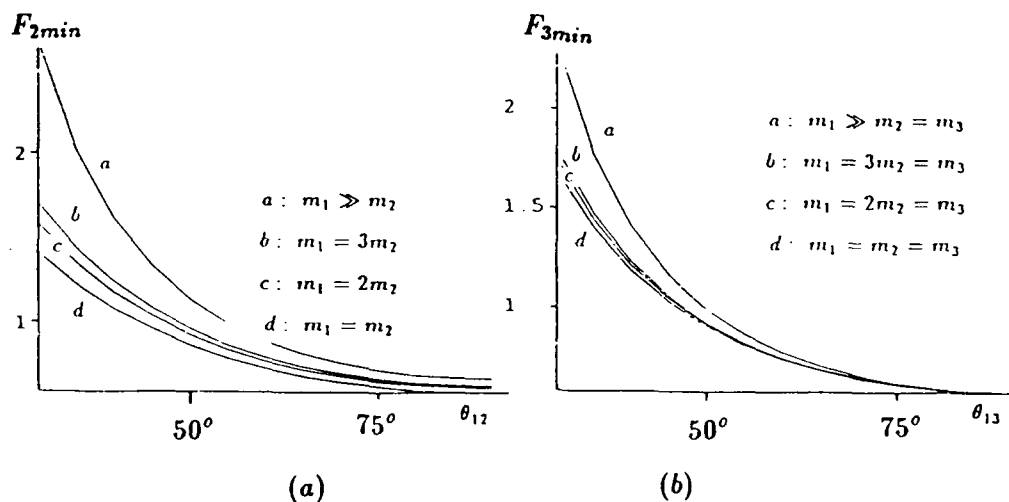


Figure 7.4 Influence on S_N of the first link of 2- or 3-link chain

While the last link rotates away from γ_{max} , the other links still have a relatively big influence within a large range of its orientation. Substituting an orientation for the last link in (5.1) and (5.2), there are for θ_1 two angles which minimize and maximize S_N , respectively. Fig. 7.4(a) shows a family of curves of minimum

F_2 in (5.1) versus θ_{12} , for different link-mass ratios in a 2-link chain of slender rods. The corresponding curve family of maximum F_2 , however, all collapse to one curve which is the same as when $m_1 \gg m_2$. Fig. 4(b) shows similar curves of F_3 in (5.2) versus θ_{13} for a 3-link chain, with the last two links collinear. Clearly, before the last link reaches the contact tangential direction, there are still big differences between extreme values of F_2 and F_3 ; the two links nearest to the last link still have a big influence. As the last link's angle approaches γ_{min} , such influence is dramatically reduced. The influence of the first link of the 3-link chain is seen to be negligible, no matter how much mass it possesses.

Fig. 4(a) and Fig. 7.4(b) also show that the influence on S_N , of the mass and orientation of the first link in a 3-link chain, is much less than in a 2-link chain. As the number of links increase over 3, the additional proximal links have little effect on S_N . We can see this from a comparison of coefficients of S_N . For example, for slender-rod chains with equal mass at each link in straight out configuration, we have: for a single link,

$$S_N = -\frac{2m_1 v_N^o}{3\sin^2\theta_1} = -0.67 \frac{m_1 v_N^o}{\sin^2\theta_1}; \quad (6.2)$$

for a 2-link chain,

$$S_N = -\frac{7m_2 v_N^o}{12\sin^2\theta_1} = -0.58 \frac{m_2 v_N^o}{\sin^2\theta_1}; \quad (6.3)$$

for a 3-link chain,

$$S_N = -\frac{26m_3 v_N^o}{45\sin^2\theta_1} = -0.578 \frac{m_3 v_N^o}{\sin^2\theta_1}. \quad (6.4)$$

The tendency of coefficient convergence is clear: adding additional links causes the coefficient to converge to a value close to 0.578, as can be verified by further calculations.

We point out that, the influence of other links on S_N is lower bounded if we treat the last link as supported on a fixed base, and upper bounded if we treat the last link as free from joint constraint. For a slender-rod link, (5.3) gives its lower bound; its upper bound is,

$$S_N = -\frac{2m_n v_N^o}{3\sin^2\theta_{1n} + 1}.$$

Such lower and upper bounds for a general link are obtainable from (3.1) and (3.5).

7.7 Change of angular velocity and reaction impulse at joint

We have studied different influences on the impact impulse at the point of contact. In this section we show that the change of link angular velocity, and reaction impulse at each joint are proportional to the contact impact impulse. Furthermore, the coefficients of their magnitudes decrease link by link as we move toward the base, if the linkage is near a straight-out position.

The proportionality to S_N of the change in joint angular velocity can be seen directly from (2.1). The change of link angular velocity is

$$\dot{\Theta} = \dot{\Theta}^o + K S_N, \quad (7.1)$$

where $K = M^{-1} J_N^T = [k_1, k_2, \dots, k_n]^T$. The corresponding change of joint rate is $\dot{\theta}_i = \dot{\theta}_i^o + (k_i - k_{i+1})S$.

The diagonal $(n-i)^{th}$ element of the inertia matrix is a significant factor in the denominator of the k_i . Take a 2-link chain composed of slender rods as an example,

$$k_1 = \frac{[\frac{1}{3} \sin \theta_1 - \frac{1}{2} \cos \theta_2 \sin \theta_{12}]}{I_1 [(\frac{m_1}{3} + m_2) \frac{1}{3} - \frac{1}{4} m_2 \cos^2 \theta_2]}, \quad (7.2)$$

$$k_2 = \frac{[(\frac{m_1}{3} + m_2) \sin \theta_{12} - \frac{1}{2} m_2 \cos \theta_2 \sin \theta_1]}{m_2 I_2 [(\frac{m_1}{3} + m_2) \frac{1}{3} - \frac{1}{4} m_2 \cos^2 \theta_2]}. \quad (7.3)$$

When $m_1 > m_2 > \dots > m_n$, and each mass difference is significant, k_i is approximately inversely proportional to the $(n-i)_{th}$ element of inertia matrix. For a 2-link chain of slender rods, $k_1 \sim \frac{1}{(m_1/3 + m_2)l_1}$ and $k_2 \sim \frac{1}{(m_2/3)l_2}$; for a 3-link chain of slender rods, $k_1 \sim \frac{1}{(m_1/3 + m_2 + m_3)l_1}$, $k_2 \sim \frac{1}{(m_2/3 + m_3)l_2}$ and $k_3 \sim \frac{1}{m_3 l_3}$. From the structure of the inertia matrix in (1.7), we can expect the same to be true for an n-link chain of slender rods.

Due to the structure of k_i , when a chain of rods is in a straight out position, the magnitudes of k_i decrease from the last link to the first link. When $m_1 = m_2$ in

a 2-link chain of slender rods,

$$k_1 = -\frac{6 \sin \theta_1}{7m_2 l_1}, k_2 = \frac{30 \sin \theta_1}{7m_2 l_2}. \quad (7.4)$$

When $m_1 = m_2 = m_3$ in a 3-link chain of slender rods,

$$k_1 = \frac{3 \sin \theta_1}{13m_3 l_1}, k_2 = -\frac{15 \sin \theta_1}{13m_3 l_2}, k_3 = \frac{57 \sin \theta_1}{13m_3 l_3}. \quad (7.5)$$

Similarly, when all m_i are equal in an n -link chain, we can expect that $|k_1| < |k_2| < \dots < |k_n|$ and the sign of k_i changes alternatively as we go from 1 to $n-1$; the sign of k_n is positive.

The reaction impulse at each joint is also proportional to the impact impulse at the point of contact. Let J_i^* be the transformation matrix which relates the velocity of the mass center of the i_{th} link to the manipulator's angular velocity vector; $\dot{X}_i^* = J_i^* \dot{\Theta}$:

$$J_i^* = \begin{pmatrix} l_1 \cos \theta_1 & l_2 \cos \theta_{12} & \dots & l_j \cos(\theta_{1j} + \beta_j) & 0 & \dots & 0 \\ l_1 \sin \theta_1 & l_2 \sin \theta_{12} & \dots & l_j \sin(\theta_{1j} + \beta_j) & 0 & \dots & 0 \end{pmatrix}. \quad (7.6)$$

Let R_i be the reaction impulse at the i_{th} joint; $R_i = [R_{ix}, R_{iy}]^T$. Then,

$$\begin{aligned} R_1 &= R_2 - m_1 J_1^* K S_N \\ R_2 &= R_3 - m_2 J_2^* K S_N \\ R_3 &= R_4 - m_3 J_3^* K S_N \\ &\dots \end{aligned} \quad (7.7)$$

This reduces to the equations below for a slender-rod linkage:

$$\begin{aligned} \begin{pmatrix} R_{1x} \\ R_{1y} \end{pmatrix} &= \begin{pmatrix} 0 \\ S_N \end{pmatrix} - (m_{1n}^* k_1 \begin{pmatrix} l_1 \cos \theta_1 \\ l_1 \sin \theta_1 \end{pmatrix} + m_{2n}^* k_2 \begin{pmatrix} l_2 \cos \theta_{12} \\ l_2 \sin \theta_{12} \end{pmatrix} + \dots \\ &\quad + \frac{m_n}{2} k_n \begin{pmatrix} l_n \cos \theta_{1n} \\ l_n \sin \theta_{1n} \end{pmatrix}) S_N; \end{aligned} \quad (7.8)$$

$$\begin{aligned} \begin{pmatrix} R_{jx} \\ R_{jy} \end{pmatrix} &= \begin{pmatrix} 0 \\ S_N \end{pmatrix} - (m_{jn}^* k_j \begin{pmatrix} l_j \cos \theta_{1j} \\ l_j \sin \theta_{1j} \end{pmatrix} + m_{(j+1)n}^* k_{j+1} \begin{pmatrix} l_{j+1} \cos \theta_{1(j+1)} \\ l_{j+1} \sin \theta_{1(j+1)} \end{pmatrix} + \dots \\ &\quad + \frac{m_n}{2} k_n \begin{pmatrix} l_n \cos \theta_{1n} \\ l_n \sin \theta_{1n} \end{pmatrix}) S_N \end{aligned} \quad (7.9)$$

$m_{j_n}^* = \frac{1}{2}m_j + m_{j+1} + \dots + m_n$; $m_{j_n}^* k_j$ is not too sensitive to mass distribution since k_j has a comparable term in its denominator.

When a linkage is in a straight-out position, the impact impulse at each joint reduces from the last link to the first link. We can look at a slender-rod linkage parallel to the contact tangent. For a 2-link chain

$$R_{1y} = -\frac{1}{12}m_2 v_N^o; R_{2y} = \frac{2}{3}m_2 v_N^o. \quad (7.10)$$

For a 3-link chain

$$R_{1y} = \frac{1}{45}m_3 v_N^o, R_{2y} = -\frac{14}{45}m_3 v_N^o, R_{3y} = \frac{31}{45}m_3 v_N^o. \quad (7.11)$$

Obviously, all $R_{ix} = 0$ in this configuration.

7.8 On the extension to spatial linkages

The above analysis helps us in understanding spatial motion as well. The idea of link space can be directly applied to a spatial linkage. The normal impact impulse is still given by expression (2.5), as long as we keep the same assumptions, though the Jacobian matrix and the inertia matrix need to be associated with spatial configurations. When the reference z axis is not parallel to the contact normal, \mathbf{n} , the denominator in (2.5) simply becomes $[\mathbf{n}^T \mathbf{J}^T \mathbf{M}^{-1} \mathbf{J} \mathbf{n}]$.

For spatial linkages, the influences of link-mass distribution on the impact impulse are further complicated by the orientations of the joint axes. If there exists a wrist point and it can be modeled as a spherical joint (we assume the moments of inertia of the grasped object is dominant and the link inertias can be neglected), the lower bound of the influence of the other links on the impact impulse can be obtained when we assume the wrist point is fixed:

$$S_N = -\frac{2v_N^o}{(l_2 n_3 - l_3 n_2)^2 / I_1 + (l_3 n_1 - l_1 n_3)^2 / I_2 + (l_1 n_2 - l_2 n_1)^2 / I_3}. \quad (8.1)$$

Here, the reference axes are parallel to the principal axes of inertia, I_i are the principal moments of inertia about the wrist point, and l_i, n_i are, respectively,

the components of a vector from the joint to the contact point and a unit vector parallel to the contact normal. Similarly, the upper bound can be obtained when we assume the object is free from joint constraints. The expression is the same as (8.1) except we need to add $1/M$ to the denominator and all quantities are now associated with the mass center.

By the same procedure as for planar linkages, we can obtain the optimal spherical joint location for an end-link (including the grasped object) mass. Let $\mathbf{w} = \mathbf{1} \times \mathbf{n}$. For a general reference frame at the mass center, the denominator of (8.1) becomes $\mathbf{w}^T \mathbf{M}_o^{-1} \mathbf{w}$, where \mathbf{M}_o is a matrix of moments of inertia. Assigning a position vector to the wrist point, calculating moments of inertia using the parallel axis transfer theorem, and taking derivatives with respect to the wrist point position vector, we can obtain the optimal joint location solution.

In a similar manner all our analyses for planar chains can be extended to spatial configurations. Although the techniques are essentially the same, the details for spatial linkages are of course much more complex than for the simpler planar devices.

This completes our study of the influences of the linkage design and configuration parameters on the impact impulse which occurs at the beginning of a direct contact motion.

Chapter 8

CONCLUSIONS

For robot motion with environmental contact, we have studied the contact kinematics, a model based control formulation and extensions of the AL robot programming language. We have also studied design rules for the reduction of the impact impulse at the onset of contact.

The contact kinematics we studied was for rigid bodies moving under planar motions with point contacts (between curves), spatial motions with point contacts (between surfaces) and spatial motions with line contacts (between developable ruled surfaces). For point contact, we studied the instantaneous contact point fixed on the moving body and its trajectory, the moving point trajectory. We also studied the moving and fixed contact trajectories for a pair of imaginary points which do not belong to either body, but are always coincident with the instantaneous contact points. For line contact we studied a moving reference point on the instantaneous contact line, and the moving and fixed contact trajectories for a pair of imaginary points. In each case we have obtained the velocity, acceleration, and jerk for the moving contact point, and the velocity and acceleration for the pair of imaginary points. Constraints on the motion to maintain point or line contacts have also been obtained. All these are expressed as functions of surface geometry and the roll-slide motion parameters at the contact.

The forms of these basic relationships for special motions and special geometries have also been included. The special motions for point contact are pure rolling and pure sliding; those for line contact are motions with no rotation about the

contact line and no sliding at the moving point. The special geometries treat cases where either moving or fixed surface is a point, a line or a plane.

The expressions obtained for the contact trajectories are directly useful for automatic trajectory planning and actual motion sensing. By specifying the contact trajectories, and the moving bodies instantaneous orientation and sliding, the moving point's trajectory is partially or completely determinable from the expressions derived in this thesis. The same relationships can also be useful for detecting an object motion from tactile sensor reading, since the contact trajectories become determinable quantities. It has been shown that when the moving body is undergoing special motion, one force or tactile sensor is sufficient for determining the angular velocity or the sliding velocity of the moving body. We have also extended the expressions for a single contact to analogous ones for two or three contacts; from these we can determine a moving body's general roll-slide motion.

The analytical expressions are also useful for estimating a moving object's position from touch sensor information. For point contact between two planar curves, the reading of the tactile sensor can be used to locate the contact point on the moving curve. The constraint that the rotation angle of the moving body is the sum of the angles turned through by the two contact normals (measured with respect to the corresponding curves) provides a useful guide to locate the contact position on the moving body. For spatial point contact, we introduce an approximate integration to determine the position of the point of contact.

The derived relationships governing the instantaneous properties of the moving point's trajectory can be used for both position and force control. We have extended the operational space control formulation so that the controller error equations are decoupled in task coordinates. This new formulation is valid even when the contact point varies with respect to the moving surface or there are multiple contacts. The control variables can be directly associated with contact constraints, and force control in these directions will not affect the decoupling of the motion-error equations as long as friction is negligible.

In designing a motion compatibility filter, we include the normal acceleration in the control law and simply set the stiffness coefficients corresponding to the force control directions to zeroes. For a spatial manipulator we also derived a first order motion compatibility filter using the contact normals. The dynamics parameters for task coordinate formulations can be simply calculated from those for the usual operational space. When there are only orientation differences between a task frame and an operational reference frame, the control in "operational space" and in task space are equivalent. The model-based control can be extended to grasping, where both the moving body and the supporting fingers need to be considered as a single system.

It is useful for a control formulation to be specified in a high-level language. We have extended the AL robot language to incorporate direct contact. We let AL accept information about the moving surface's geometry, and provide means to generate general position-interpolation trajectories, general orientation-interpolation trajectories (particularly when a reference line of an object is specified), and certain function and run-time condition monitored trajectories. We have also discussed the kinematic and force conditions for determining the positional and rotational task frames, and introduced ways to specify position-error tolerances, directional wobbles and several other practically useful motion characteristics.

In considering the instant of making contact, we have analyzed the sensitivity of impact impulse to the mass distribution of a planar manipulator. We have shown that for a revolute-joint planar manipulator, the Jacobian and inertia matrix can be simplified if they are expressed in link-space coordinates. For the last link there exists an optimal location of the joint pivot. We have also shown that: 1) The mass should decrease link by link as one moves toward to the end-effector, in order to reduce the impact impulse. 2) The last link dominates the impact impulse. 3) Its neighboring links' masses and orientations have a big influence when the last link is not nearly parallel to the contact tangent. 4) The change of the angular velocity and reaction impulse at a joint are proportional to the impact impulse at the point of contact. The results of

this analysis imply that it is worthwhile to consider light-weight end-effectors and micro-manipulator attachments in order to reduce the impacts associated with environmental contacts.

In this work we have given an extensive development of the instantaneous kinematics of direct contact. This is the heart of this dissertation, and has received most of our attention. The control system and AL language extensions have been less developed in this work, and these are the areas that could profit most from further study and extensions. In order to broaden the practical implementations of the developed theory, it would be useful to have a corresponding AL run-time system connected to the AL language system through message passing. Finally, the results of this thesis should be implemented with a hardware system consisting of a force controlled manipulator, and a gripper with a pair of force fingers capable of sensing all six force components.

Appendix A – Curvatures of the Contacting Curves

It is well known from elementary calculus that for a planar curve, given in the explicit form $y = h(x)$, the curvature can be expressed as

$$k = \frac{h_2}{(1 + h_1^2)^{\frac{3}{2}}} \quad (A1)$$

At the zero position, using equations (2.2.3) (equation 2.3 of Chapter 2) we have

$$k_m = h_{m,2}, \quad k_f = h_{f,2} \quad (A2)$$

The derivative of the curvature with respect to the arc length can be obtained using the chain rule, $dk/ds = (dk/dx)(dx/ds)$. From (A1) $dk/dx = h_3(1 + h_1^2)^{-\frac{3}{2}} - 3h_2^2h_1(1 + h_1^2)^{-\frac{5}{2}}$ and as is well known $dx/ds = (1 + h_1^2)^{-\frac{1}{2}}$. Substituting into the dk/dx expression for the initial position from equations (2.2.3) yields $dk_m/dx = h_{m,3}$ and $dk_f/dx = h_{f,3}$. Similarly from the dx/ds expression we obtain $dx_m/ds_m = 1$ and $dx_f/ds_f = 1$. Substituting into the chain rule we have

$$k'_m = \frac{dk_m}{ds_m} = h_{m,3}, \quad k'_f = \frac{dk_f}{ds_f} = h_{f,3} \quad (A3)$$

where s_m and s_f are the arc length variables with respect to the moving and the fixed curves respectively.

Higher order derivatives of the curvature can be derived in a similar manner.

Appendix B – Compound Planar Motion at a Point of Contact

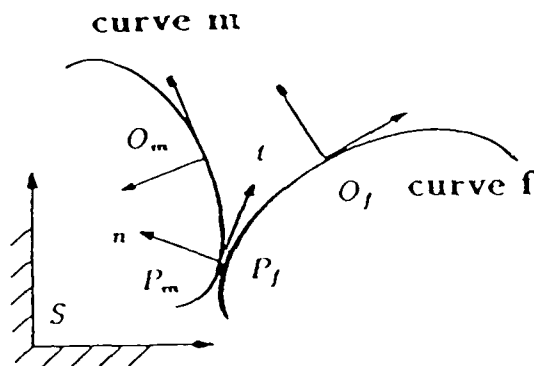


Figure B.1 Two moving curves

When both contacting bodies are in motion, we introduce a third frame S , which is stationary (see Figure B.1). There is now a motion of body f , defined by the O_f frame, with respect to the S frame, and a motion of the body m , with frame O_m , with respect to both body f and frame S .

We define $\bar{\omega}$, $\bar{\epsilon}$, $\bar{\mathbf{v}}$, $\bar{\mathbf{a}}$ to be, respectively, the angular velocity, angular acceleration, and the contact point's velocity and acceleration, for the motion of body m relative to f ; and ω_m , ϵ_m , \mathbf{v}_m , \mathbf{a}_m to be the same variables for the motion of body m with respect to S , while ω_f , ϵ_f , \mathbf{v}_f , \mathbf{a}_f are the variables for the motion of body f with respect to S . The linear velocities and accelerations defined here are for the points coincident at P , the first two cases deal with P_m and the third case is for point P_f .

For body m the angular velocity and acceleration satisfy the simple linear superpositions:

$$\omega_m = \omega_f + \bar{\omega}, \quad \epsilon_m = \epsilon_f + \bar{\epsilon} \quad (B1)$$

Similarly for point P_m on body m we have $\mathbf{v}_m = \mathbf{v}_f + \bar{\mathbf{v}}$. The contact condition requires that in the direction of the contact tangent, \mathbf{t} ,

$$\mathbf{v}_m \cdot \mathbf{t} = \mathbf{v}_f \cdot \mathbf{t} + \bar{\mathbf{v}} \cdot \mathbf{t} \quad (B2)$$

and in the direction of the contact normal \mathbf{n}

$$\mathbf{v}_m \cdot \mathbf{n} = \mathbf{v}_j \cdot \mathbf{n} \quad (B3)$$

Similarly for the acceleration of point P_m on body m , we have $\mathbf{a}_m = \mathbf{a}_j + \bar{\mathbf{a}} + 2\omega_j \times \bar{\mathbf{v}}$ and in the tangential direction this yields

$$\mathbf{a}_m \cdot \mathbf{t} = \mathbf{a}_j \cdot \mathbf{t} + \bar{\mathbf{a}} \cdot \mathbf{t} \quad (B4)$$

while the normal component must be

$$\mathbf{a}_m \cdot \mathbf{n} = \mathbf{a}_j \cdot \mathbf{n} + 2\omega_j v_x + \bar{\mathbf{a}} \cdot \mathbf{n} \quad (B5)$$

where $\bar{\mathbf{a}} \cdot \mathbf{n}$ is the same as in (2.2.12) or (2.2.13), except that the velocities and angular velocities are replaced by their respective relative velocities.

Appendix C – Derivatives of $h(x, y)$ from a General Surface Representation

A general analytic expression for a surface can be in either the form $\mathbf{r}(u, v)$ (u and v are two parameters) or $F(X, Y, Z) = 0$. Here \mathbf{r} is a position vector and F is a scalar function, they are associated with a frame which has an arbitrary point as the origin and three arbitrary perpendicular lines as the X, Y and Z coordinate axes. We first assume the $\mathbf{r}(u, v)$ expression. Let $\mathbf{r}(u_o, v_o)$ denote the position vector to the point of contact. We define a new reference frame which has its origin at the point of contact, and its z axis parallel to the inwardly directed surface normal * ($z = h(x, y)$, the x and y axes are in the tangent plane). We denote $\mathbf{i}, \mathbf{j}, \mathbf{k}$ as three unit vectors parallel to the x, y and z axes respectively, x, y and h satisfy the relations

$$x = [\mathbf{r}(u, v) - \mathbf{r}(u_o, v_o)] \cdot \mathbf{i} \quad (C1)$$

$$y = [\mathbf{r}(u, v) - \mathbf{r}(u_o, v_o)] \cdot \mathbf{j} \quad (C2)$$

$$h = [\mathbf{r}(u, v) - \mathbf{r}(u_o, v_o)] \cdot \mathbf{k} \quad (C3)$$

From (C1) and (C2), if the surface is continuous and differentiable at the point of contact, and the x - y pair has one to one correspondence to the u - v pair, there exist the inverse relations

$$u = u(x, y), \quad v = v(x, y) \quad (C4)$$

To show how to determine the partial derivatives of h , we take an example. The partial derivative of h with respect to x is (from (C3)),

$$f_x = [\mathbf{r}_u u_x + \mathbf{r}_v v_x] \cdot \mathbf{k} \quad (C5)$$

To obtain u_x, v_x we take the partial derivative with respect to x of (C1) and (C2):

$$1 = (\mathbf{r}_u u_x + \mathbf{r}_v v_x) \cdot \mathbf{i}, \quad 0 = (\mathbf{r}_u u_x + \mathbf{r}_v v_x) \cdot \mathbf{j} \quad (C6)$$

* For the outwardly directed normal, instead of h we use $-h$, and every step in the following remains unaltered.

From this we can obtain u_x, v_x ,

$$u_x = \mathbf{r}_v \cdot \mathbf{j} [\mathbf{r}_u \cdot \mathbf{i} \mathbf{r}_v \cdot \mathbf{j} - \mathbf{r}_u \cdot \mathbf{j} \mathbf{r}_v \cdot \mathbf{i}]^{-1}, \quad v_x = -\mathbf{r}_u \cdot \mathbf{j} [\mathbf{r}_u \cdot \mathbf{i} \mathbf{r}_v \cdot \mathbf{j} - \mathbf{r}_u \cdot \mathbf{j} \mathbf{r}_v \cdot \mathbf{i}]^{-1} \quad (C7)$$

The partial derivatives of h with respect to x and y up to an arbitrary order can be obtained from (C3). The partial derivatives of u and v with respect to either x or y can be obtained by taking the partial derivatives simultaneously over equations (C1) and (C2), and then inverting the resulting equations.

When a surface is of the form $F(X, Y, Z) = 0$, by the rule of implicit partial derivatives, if we regard Z as a function of x and y :

$$Z_X = -\frac{F_X}{F_Z}, \quad Z_Y = -\frac{F_Y}{F_Z} \quad (C8)$$

If we define $u = X$ and $v = Y$, although we do not have the explicit expression $\mathbf{r}(u, v)$, we can obtain all its partial derivatives from (C8). We notice in the foregoing context, the partial derivatives of h are related to only the partial derivatives of $\mathbf{r}(u, v)$. So from a general analytic expression for a surface, we can in general obtain the partial derivatives of $h(x, y)$.

Appendix D – Curvature Expressions from $h(x, y)$

It is well known that the curvature of a curve which is on the surface $z = h(x, y)$ and in a plane parallel to the x-z plane is

$$k_x = \frac{h_{xx}}{(1 + h_x^2)^{\frac{3}{2}}}$$

If instead the curve is in a plane parallel to the y-z plane the curvature is

$$k_y = \frac{h_{yy}}{(1 + h_y^2)^{\frac{3}{2}}}$$

Substituting (3.1.3) for the initial position,

$$k_x = h_{xx}, \quad k_y = h_{yy} \quad (D1)$$

Taking the partial derivatives of the above curvatures, and substituting (3.1.3) for the initial position, we have

$$k_{xx} = h_{xxx}, \quad k_{xy} = h_{xxy}, \quad k_{yx} = h_{xyy}, \quad k_{yy} = h_{yyy} \quad (D2)$$

To measure the parallelism of tangents of a family of curves which are either in planes parallel to the x-z plane or in planes parallel to the y-z plane, we only need to observe one component (since it is a unit vector). The x component of a tangent of a curve parallel to the x-z plane and the y component of a tangent of a curve parallel to y-z plane are respectively,

$$t_x = \frac{f_x}{\sqrt{1 + f_x^2}}, \quad t_y = \frac{f_y}{\sqrt{1 + f_y^2}}$$

The partial derivative of t_x with respect to y (or the partial derivative of t_y with respect to x) at the initial position is

$$g = f_{xy} \quad (D3)$$

Appendix E – Compound Spatial Motion at a Point of Contact

Assuming there are three frames, S , m and f , attached to a fixed space, a moving body and a finger respectively. We denote Ω_m , \mathcal{E}_m , V_m and \mathbf{a}_m to be respectively the angular velocity, angular acceleration, and the velocity and acceleration of the point of contact for the motion of the moving body relative to S . We denote Ω_f , \mathcal{E}_f , V_f and \mathbf{a}_f as the same variables for the motion of the finger relative to S , and $\bar{\Omega}$, $\bar{\mathcal{E}}$, \bar{V} and $\bar{\mathbf{a}}$ to be the variables for the motion of the moving body relative to f . For the angular velocity, it is well known that $\Omega_m = \Omega_f + \bar{\Omega}$, or

$$\begin{pmatrix} \omega_{m,1} \\ \omega_{m,2} \\ \omega_{m,3} \end{pmatrix} = \begin{pmatrix} \omega_{f,1} \\ \omega_{f,2} \\ \omega_{f,3} \end{pmatrix} + \begin{pmatrix} \bar{\omega}_1 \\ \bar{\omega}_2 \\ \bar{\omega}_3 \end{pmatrix} \quad (E1)$$

For the angular acceleration $\mathcal{E}_m = \mathcal{E}_f + \bar{\mathcal{E}} + \Omega_f \times \bar{\Omega}$, in matrix form

$$\begin{pmatrix} \epsilon_1 \\ \epsilon_2 \\ \epsilon_3 \end{pmatrix} = \begin{pmatrix} \epsilon_{f,1} \\ \epsilon_{f,2} \\ \epsilon_{f,3} \end{pmatrix} + \begin{pmatrix} \bar{\epsilon}_1 \\ \bar{\epsilon}_2 \\ \bar{\epsilon}_3 \end{pmatrix} + \begin{pmatrix} \omega_{f,2}\bar{\omega}_3 - \omega_{f,3}\bar{\omega}_2 \\ \omega_{f,3}\bar{\omega}_1 - \omega_{f,1}\bar{\omega}_3 \\ \omega_{f,1}\bar{\omega}_2 - \omega_{f,2}\bar{\omega}_1 \end{pmatrix} \quad (E2)$$

The velocity of the point of contact is $V_m = V_f + \bar{V}$, or

$$\begin{pmatrix} v_{m,1} \\ v_{m,2} \\ v_{m,3} \end{pmatrix} = \begin{pmatrix} v_{f,1} \\ v_{f,2} \\ v_{f,3} \end{pmatrix} + \begin{pmatrix} \bar{v}_1 \\ \bar{v}_2 \\ 0 \end{pmatrix} \quad (E3)$$

For acceleration of the point of contact, it is also well known that $\mathbf{a}_m = \mathbf{a}_f + \bar{\mathbf{a}} + 2\Omega_f \times \bar{V}$, in matrix form

$$\begin{pmatrix} a_{m,1} \\ a_{m,2} \\ a_{m,3} \end{pmatrix} = \begin{pmatrix} a_{f,1} \\ a_{f,2} \\ a_{f,3} \end{pmatrix} + \begin{pmatrix} \bar{a}_1 \\ \bar{a}_2 \\ \bar{a}_3 \end{pmatrix} + 2 \begin{pmatrix} -\bar{v}_2\omega_{f,3} \\ \bar{v}_1\omega_{f,3} \\ \bar{v}_2\omega_{f,1} - \bar{v}_1\omega_{f,2} \end{pmatrix} \quad (E4)$$

Appendix F - Finding an Orthogonal Curve on a Ruled Surface

In this appendix we prove that we can always find curves \mathbf{r}_i which are normal to the directions L_i .

A developable ruled surface can be described by

$$\bar{R} = \bar{\mathbf{r}} + d\bar{L}, \quad (F1)$$

where $\bar{\mathbf{r}}$ is an arbitrary curve on the surface. We can always obtain a curve \mathbf{r} which passes through a given reference point \bar{d} and is perpendicular to the corresponding \bar{L} . Using a superscript prime to denote each derivative with respect to an arbitrary parameter u , we have,

$$\bar{R}' = \bar{\mathbf{r}}' + \bar{d}'\bar{L} + \bar{d}\bar{L}', \quad \bar{R}'' = \bar{\mathbf{r}}'' + \bar{d}''\bar{L} + 2\bar{d}'\bar{L}' + \bar{d}\bar{L}''. \quad (F2)$$

By varying \bar{d} we can let the locus of \bar{R} be the required curve \mathbf{r} . To first order, the orthogonality condition requires that $R' \cdot L = 0$, from which we obtain $\bar{d}' = -\bar{\mathbf{r}}' \cdot \bar{L}$. To second order the orthogonality condition requires that $R'' \cdot L + R' \cdot L' = 0$, so we obtain $d'' = -R' \cdot L' - \alpha'' L' - dL'' \cdot L$. In this way we can construct \bar{R} , \bar{R}' and \bar{R}'' to be respectively the position vector and the first two derivatives of our desired curve \mathbf{r} . In order to obtain the derivatives with respect to the arc-length of \mathbf{r} , we have the relations,

$$\frac{dR'}{ds} = \frac{dR'}{du} \frac{du}{ds} = T, \quad \frac{d^2 R}{ds^2} = \frac{d^2 R}{du^2} \left(\frac{du}{ds} \right)^2 + \frac{dR}{du} \frac{d^2 u}{ds^2}, \quad (F3)$$

where $du/ds = 1/(R' \cdot T)$, and $d^2 u/ds^2 = -(d^2 R/du^2)(du/ds)^3$. Thus we have justified our statement.

Bibliography

- H. Asada and K. Ogawa, "On the Dynamic Analysis of a Manipulator and Its End Effector Interacting with the Environment," **Proceedings 1987 IEEE International conference on Robotics and Automation**, pp. 751-756
- A. Ben-Israel and T. N. E. Greville, **Generalized Inverses: Theory and Applications**, Wiley, New York, 1974
- W. Blaschke and H. R. Müller, **Ebene Kinematic**, R. Oldenbourg, München, 1956.
- O. Bottema, "Zur Kinematik des Rollgleitens," **Arch. Math.** 6, pp. 25-28, 1955
- O. Bottema, "The λ -Pairs of Curves for a Cycloidal Motions," **Mechanism and Machine Theory**, 10, pp. 189-196, 1975
- O. Bottema and B. Roth, **Theoretical Kinematics**, Elsevier, Amsterdam, 1979
- D. Brock and S. Chiu, "Environment Perception of an Articulated Robot Hand Using Contact Sensors," **Robotic and Manufacturing Automation**, pp. 89-96, ASME Winter Annual Meeting, Miami. 1985
- C. Cai and T. Binford, "Operational Space Motion Specification in AL Robot Language," **Proceedings, 1987 IEEE International Conference on Robotics and Automation**, pp. 1307-1313
- C. Cai and B. Roth, "On the Planar Motion of a Rigid Body with Point Contact," **Journal of Mechanism and Machine theory**, V. 21, No. 6, pp. 453-466, 1986
- C. Cai and B. Roth, "On the Spatial Motion of a Rigid Body with Point Contact," **Proceedings, 1987 IEEE International Conference on Robotics and Automation**, pp. 686-695

- C. Cai and B. Roth, "Impact Sensitivity to Mass Distribution of a Planar Manipulator," **Proceedings, '87 ICAR: Third International Conference on Advanced Robotics**, France, October, 1987
- M. R. Cutkosky, **Robotic Grasping and Fine Manipulation**, Kluwer Academic Publishers, 1985
- R. S. Fearing, "Some Experiments with Tactile Sensing during Grasping," **Proceedings, 1987 IEEE International Conference on Robotics and Automation**, pp.1637-1643
- R. Garnier, **Cours de Cinématique**, Gauthier -Villars, Paris, 1954
- R. Goldman, "Design of an Interactive Manipulator Programming Environment." Report No. STAN-CS-82-955, Stanford University, CA, 1982
- R. M. Goor, "A New Approach to Minimum Time Robot Control," **Robotic and Manufacturing Automation**, pp. 1-12, ASME Winter Annual Meeting, Miami. 1985
- G. Grüss, "Zur Kinematik des Rollgleitens," **Z. Angw. Math. Mech.**, **31**, pp. 97-103, 1951
- K. H. Hunt, "**Kinematic Geometry of Mechanisms**," Oxford University Press, 1978
- Z. Ji, **Dexterous Hands: Optimizing Grasp by Design and Planning** Ph. D. thesis. Stanford University Dept. of Mechanical Engineering, 1987
- T. Kailath, **Linear System**, Prentice-Hall, Inc., 1980
- T. Kane and D. Levinson, **Dynamics: Theory and Applications**, McGraw-Hill Book Company, New York, 1985
- J. Kerr, **An analysis of multi-fingered hands**. Ph. D. thesis. Stanford University Dept. of Mechanical Engineering, 1984
- O. Khatib, **Commande Dynamique dans L'Espace Opérationnel des Robots Manipulateurs en Présence d'Obstacles**. Thèse de Doteur-Ingénieur. École Nationale Supérieure de l'Aéronautique et de l'Espace, Toulouse, France, 1980
- Khatib,O., "Dynamic Control of Manipulators in Operational Space," **Sixth CISM-IFTToMM Congress on Theory of Machines and Mechanisms**,

pp.1128-1131, 1983

- O. Khatib and J. Burdick "Motion and Force Control of Robot Manipulators," **Proceedings 1986 IEEE International conference on Robotics and Automation**, pp. 1381-1386
- H. Lipkin and J. Duffy, "Hybrid Twist and Wrench Control for a robotic manipulator," **Journal of Mechanisms, Transmissions and Automation in Design, Trans ASME**, 1987
- M. Mason, "Compliance and Force Control for Computer Controlled Manipulators," **IEEE Trans. on Systems, Man, and Cybernetics**, Vol. SMC-11, No.6, June, pp.418-432, 1981.
- David J. Montana, **Tactile Sensing and the Kinematics of Contact**, Ph.D. thesis, The Division of Applied Sciences, Harvard University, 1986
- S. Mujtaba and R. Goldman, "AL Users' Manual." STAN-CS-81-889, Stanford University, CA 1981
- H. R. Müller, "Zur Kinematik des Rollgleitens," **Arch. Math**, Part 1, 4, pp. 239-246, 1953
- H. R. Muller, "Zur Kinematik des Rollgleitens II," **Arch Math**, Vol. V1, pp. 471-480, 1955
- H. R. Müller, "Zur Ermittlung von Hüllflächen in der räumlichen Kinematik." **Monh. f. Math.** 63, pp. 231-240, 1959
- H. R. Müller, **Kinematik**, Sammlung Göschel, Band 584/584a, Walter De Gruyter & Co., Berlin, 1963
- M. Raibert and J. Craig, "Hybrid position/force control of manipulators," **ASME Journal of dynamic systems, measurement and control**, Vol. 105, pp. 126-133, 1981.
- B. Roth and A. T. Yang, "Application of Instantaneous Invariants to the Analysis and Synthesis of Mechanisms," **Journal of Engineering for Industry, Trans. ASME**, 99, pp. 97-103, 1977
- J. K. Salisbury and B. Roth, "Kinematic and Force Analysis of Articulated Mechanical Hands," **Journal of Mechanisms, Transmissions and Automation in Design, Trans. ASME**, 105, pp. 35-41, 1983

- G. R. Veldkamp, **Curvature Theory in Plane Kinematics**, doctoral dissertation, Groningen, 1963
- M. Vukobratović and V. Potkonjak, **Applied Dynamics and CAD of Manipulation Robots**, Springer Verlag, Berlin, 1985
- Y. Wang and M. Mason, "Modeling Impact Dynamics of a Rigid Body with Point Contact," **Proceedings 1987 IEEE International conference on Robotics and Automation**, pp. 678-685
- W. West and H. Asada, "Kinematic and Mechanical Advantage of Manipulators Constrained by Contact with the Environment," **Robotic and Manufacturing Automation**, ASME Winter Annual Meeting, Miami. pp. 175-186, 1985
- T. Yoshikawa, "Manipulability of Robotic Mechanism," **The International Journal of Robotics Research**, Vol.4, No.2, pp. 3-9, 1985.
- T. Yoshikawa, "Dynamic Manipulability of Robot Manipulators," **Proc. 1985 IEEE Int. Conf. on Robotics and Automation**, pp. 1033-1038